IOWA STATE UNIVERSITY
Digital Repository

Retrospective Theses and Dissertations

Iowa State University Capstones, Theses and Dissertations

1971

Error analysis of an integrated inertial/Doppler-satellite navigation system with continuous and multiple satellite coverage

Donley James Winger
Iowa State University

Follow this and additional works at: https://lib.dr.iastate.edu/rtd

 Part of the Electrical and Electronics Commons

Recommended Citation
Winger, Donley James, "Error analysis of an integrated inertial/Doppler-satellite navigation system with continuous and multiple satellite coverage " (1971). *Retrospective Theses and Dissertations*. 4864.
https://lib.dr.iastate.edu/rtd/4864

This Dissertation is brought to you for free and open access by the Iowa State University Capstones, Theses and Dissertations at Iowa State University Digital Repository. It has been accepted for inclusion in Retrospective Theses and Dissertations by an authorized administrator of Iowa State University Digital Repository. For more information, please contact digirep@iastate.edu.

www.manaraa.com

71-21,982

WINGER, Donley James, 1938-
ERROR ANALYSIS OF AN INTEGRATED
INERTIAL/DOPPLER-SATELLITE NAVIGATION SYSTEM
WITH CONTINUOUS AND MULTIPLE SATELLITE COVERAGE.

Iowa State University, Ph.D., 1971
Engineering, electrical

University Microfilms, A XEROX Company, Ann Arbor, Michigan

THIS DISSERTATION HAS BEEN MICROFILMED EXACTLY AS RECEIVED

Error analysis of an integrated inertial/Doppler-satellite navigation system with continuous and multiple satellite coverage

by

Donley James Winger

A Dissertation Submitted to the
Graduate Faculty in Partial Fulfillment of
The Requirements for the Degree of
DOCTOR OF PHILOSOPHY

Major Subject: Electrical Engineering

Approved:

Signature was redacted for privacy.

In Charge of Major Work

Signature was redacted for privacy.

Head of Major Department

Signature was redacted for privacy.

Dean of Graduate College

Iowa State University
Ames, Iowa

1971

TABLE OF CONTENTS

I. INTRODUCTION

This dissertation presents the results of a study of an integrated inertial/Doppler-satellite navigation system which uses a Kalman filter method of integration. Measurements of the Doppler effect on signals transmitted from orbiting satellites are used to provide measurement information to the filter and the Kalman filter is modeled to estimate the inertial system errors.

The purpose of the study was to investigate the performance of a hypothetical integrated system when sufficient satellite coverage is provided to enable continuous Doppler measurements from two satellites to be used for the filter input. The availability of continuous dual satellite coverage, which can be termed the "two-in-view" condition, provides several specific areas for investigation. These are:

(a) a performance comparison of the "two-in-view" and "one-in-view" systems,

(b) a performance comparison of the "two-in-view" system when measurements are processed from satellite pairs whose trajectories are nearly parallel and nearly orthogonal,

(c) a performance comparison for satellite configurations at different altitudes,

(d) a performance comparison for different quality inertial systems.

Also, two new problems of theoretical interest arise in the Kalman filter model for the "two-in-view" system. These two problems deal with the sequential processing of two (or more) simultaneous satellite measurements and the processing of two (or more) satellite measurements which are not in time coincidence. A treatment of these two problems is included in this dissertation.

The motivation for this study stems from the results of some previous studies of integrated inertial/Doppler-satellite systems in which infrequent single satellite measurements were used to update the error estimates. This dissertation then represents an extension of these previous studies. The remaining portion of this chapter presents a brief review of these studies with an elaboration on the results which provided motivation for this "two-in-view" study, and the chapter concludes with a description of the method in which the benefits of the "two-in-view" systems were analyzed.

Consider a situation in which a navigator has a measurement of his position from each of several instruments. The question he faces is, "How do I determine the best estimate of my position?" A simple approach would be to use the reading from the instrument he feels is the most accurate and reset the readings of the other instruments accordingly. This could be termed a simple "reset" method. A more sophisticated method of integration would be to obtain the position

fix from a blend of the data from all the instruments, giving the data of each instrument some statistical weight. The two "instruments" in this study are an inertial navigation system and a Doppler-satellite system.

An inertial navigation system is comprised of accelerometers which are mounted on a gyro-stabilized platform. The sensed accelerations are resolved into an appropriate coordinate frame and integrated to yield velocity and position information. Though conceptually simple, the inertial system is subject to errors caused by initial misalignment of the platform and imperfect instrumentation (accelerometers and gyros). Error analysis of an inertial system reveals that accelerometer and gyro errors cause the quality of the system's position estimates to degrade with time.

The Doppler-satellite system provides a high quality estimate of one's position by observing the Doppler effect on a signal transmitted from a passing satellite whose orbital parameters are precisely known. This is possible because the Doppler shift profile is unique to the observer's position on the earth. A disadvantage of this system for many applications is that position information is available only at discrete times during the satellite's pass.

Thus, in many respects the two navigation systems are complementary and well suited for an integration scheme. In a loose sense, the inertial system then will act as a

continuous interpolator for the discrete-time Doppler-satellite system. The simple "reset" approach to the integration of the two systems would be to reset the position readout of the inertial system to the Doppler-satellite position fix every time a satellite position fix is obtained. The problem with this technique is that no attempt is made to estimate other inertial system errors nor to follow the error dynamics after a satellite pass. Conceivably, this approach could often lead to inertial system performance which is poorer than without the reset technique. A statistical "blending" of the two systems is achieved by modeling the inertial errors as random processes in a state-variable format and using a Kalman filter to estimate these errors from the satellite measurements.

In 1965, Bona and Hutchinson (1) first presented a model in which the two systems are integrated using a Kalman filter. In this study, they assumed the inertial system was mounted in a slow-moving marine vehicle and modeled the difference between the satellite position fix and the inertial position as the basic observable.

Hagerman (7) points out that the state of the system and the measurement noise are correlated in Bona and Hutchinson's model. This violates a basic assumption in the derivation of the recursive Kalman filter equations. He then presents a model in which the difference between

the instantaneous computed and measured Doppler shift frequencies is treated as the observable and presents a variance analysis for a marine vehicle computer simulation.

A subsequent paper by Brown and Hagerman (3) presents a model in which the integral of the difference between the computed and measured Doppler shift frequency is treated as the observable. This Doppler "count" model represents a more appropriate model since instantaneous frequency is not a measurable quantity.

In the preceding studies, the performance of the integrated systems were evaluated by conducting variance analyses on computer simulated applications. The results of these studies are based on a priori assumptions which cannot be tested. The results of the first application of Kalman filtering techniques to actual flight test data are presented in a report by Brown and Winger (5). In this series of flights, the inertial and Doppler-satellite systems were operated independently and data from each were recorded on magnetic tape. These data were "reflown" on a computer employing a Kalman filter to estimate inertial system errors. In that study, the basic observable was the Doppler count and the Kalman filter integration technique was shown to be an effective method of system integration. The position estimates at the end of a satellite pass were better than the "nonintegrated" satellite position fixes, and the position

estimates of the Kalman integrated system were superior to those of both the pure inertial system and the inertial system aided by a satellite position fix in a simple "reset" manner.

The flight test processing and the previous simulation studies by Hagerman used a single satellite observation from one of a limited number of satellites, so measurement data were available for approximately 12-minute intervals once every 90 to 120 minutes. These studies provided the following results.

(a) Although position estimates are generally quite good during a satellite pass, estimates which are not so tightly coupled to the measurement are not of very high quality.

(b) Low elevation passes (below 15^{o}) are of questionable value since the reliability of the Doppler data is poor, and it is suspected that the Doppler data may contain some uncorrected systematic errors due to refraction effects.

(c) Coverage by a single satellite in a polar orbit results in estimates of latitude errors which are generally of better quality than longitude error estimates.

The results of the flight test processing suggested to this author that one is asking a great deal in expecting to

be able to estimate the sixteen errors modeled in the system on the basis of a few number of scaler measurements. The question that then arises is, "What type of performance can one expect to get out of an integrated inertial/Doppler-satellite system if extensive satellite coverage is provided?"

This study investigates three hypothetical systems of satellites which provide continuous dual satellite coverage to a vehicle at any point on the earth. The benefits of dual satellite coverage is first established by extending an error analysis of the Doppler-satellite position fix from a single satellite case to a two satellite case in which their subtrack intersection angles are a parameter. The effectiveness of the hypothetical system is next demonstrated by conducting variance analyses on a computer simulated aircraft flight.

These studies show the following results.

(a) Continuous satellite coverage provides sufficient measurement information to provide effective estimation of most of the errors in the model.

(b) The dual satellite or "two-in-view" system provides significantly improved estimates of inertial errors over the "one-in-view" system.

(c) The additional information provided by two satellite measurements, rather than a single measure-

ment, is optimized by choosing satellite pairs with orthogonal trajectories.

(d) The quality of the position estimates degrades almost linearly with increased satellite altitude in the range of 1000 to 2200 nautical miles.

(e) A trade-off between satellite altitude and inertial system quality can be made.

The details of the mathematical modeling of the system and the simulation results are presented in the following chapters.

II. THE DOPPLER SATELLITE NAVIGATION SYSTEM

A Doppler satellite navigation system has been operational since 1964 and has been known by two names, TRANSIT and the Navy Navigation Satellite System (NNSS). Originally a military project, TRANSIT was opened to commercial use in 1967. The satellites in this integration study are assumed to be similar to those employed in the TRANSIT system with the major changes being in the orbital configurations and the satellite altitudes. A short review of the conventional operation of TRANSIT and a statistical analysis of the "two-in-view" problem from a simple position-fix viewpoint are presented in this chapter.

A. The TRANSIT System

It has been found that observing the Doppler effect on a continuous-wave (CW) signal transmitted from a passing satellite provides sufficient information to determine the location of the observer (6). This assumes that the satellite orbital parameters are precisely known.

A minimum of three and as many as five operational TRANSIT satellites have been maintained in nearly circular polar orbits at an altitude of about 600 nautical miles, and they provide sufficient coverage to enable an observer to obtain a position fix every 1 1/2 to 2 hours. Each satellite has a very stable oscillator which transmits two harmonically

related CW signals at approximately 400 MHz and 150 MHz. By suitably combining these two harmonically related frequencies, the first order ionospheric refraction errors are corrected in the received 400 MHz signal. This technique is discussed by Guier and Weiffenbach (6).

The satellite also continuously transmits navigation messages of two minutes duration which describe the satellite's orbital parameters at the end of each two-minute interval and interpolation data to enable one to find the satellite's position during the interval. Timing markers are also dispersed throughout each two-minute interval. The navigation message in the satellite is worked out through ground tracking and this message is updated about every twelve hours by a ground injection station.

The transmitted frequency of a satellite is not exactly 400 MHz but rather 398.968 MHz. The ground receiver has a very stable 400 MHz reference frequency which is mixed with the received signal producing a nominal 32 KHz difference frequency. The Doppler effect will cause this difference frequency to vary by as much as $\pm$ 8 KHz during a satellite pass.

If one assumes a location of the ground receiver, a theoretical Doppler curve can be computed for any satellite pass for which the satellite orbital parameters are known. In the general solution of the navigation problem, this

theoretical Doppler curve is compared to the observed Doppler curve and a "best fit" is obtained by an iterative technique. The variables which are adjusted to yield a "best fit" are the navigator's longitude, latitude and a bias term to account for long term drift in the satellite and receiver oscillators.

One method used to obtain a position fix from the Doppler data is a least squares fit of the theoretical Doppler frequency curve to the observed curve. At time t_k, the difference between the theoretical and observed Doppler frequency forms a residual U_k, given by

$$U_k = f_{Tk}(\Theta,\lambda,b) - f_{ok} \tag{2.1}$$

where

f_{ok} is the observed Doppler frequency at t_k,

$f_{Tk}(\Theta,\lambda,b)$ is the theoretical Doppler frequency at t_k,

Θ is latitude,

λ is longitude, and

b is oscillator bias.

An error function is defined as

$$F(\Theta,\lambda,b) = \sum_k U_k^2 \tag{2.2}$$

and the "best fit" is found by adjusting Θ, λ and b to minimize the error function. This minimum condition satisfies

the three equations which result from setting the partial derivatives to zero,

$$F_\theta(\theta,\lambda,b) = 0 \tag{2.3}$$

$$F_\lambda(\theta,\lambda,b) = 0 \tag{2.4}$$

$$F_b(\theta,\lambda,b) = 0 \quad . \tag{2.5}$$

A second method of obtaining a position fix involves dividing the observed Doppler curve into three equal time periods and forming the integral of the frequency for each time interval. These integrals are then "counts" of the number of cycles in each time span and are given by

$$N_{o1} = \int_{t_o}^{t_1} f_o(t)dt \tag{2.6}$$

$$N_{o2} = \int_{t_1}^{t_2} f_o(t)dt \tag{2.7}$$

$$N_{o3} = \int_{t_2}^{t_3} f_o(t)dt \quad . \tag{2.8}$$

Theoretical values of these three counts may be computed based on receiver latitude, longitude and oscillator bias. Equality of the theoretical and observed "counts" for the three intervals, that is,

$$N_{T1}(\theta,\lambda,b) = N_{o1} \tag{2.9}$$

$$N_{T2}(\theta,\lambda,b) = N_{o2} \tag{2.10}$$

$$N_{T3}(\theta,\lambda,b) = N_{o3} \tag{2.11}$$

is achieved only when the true values of receiver latitude, longitude, and oscillator bias are used in the theoretical computation.

In either the frequency measurement method or the count measurement method, approximate values for θ, λ, and b can be obtained by using an iterative technique on Equations 2.3, 2.4, 2.5 or Equations 2.9, 2.10, 2.11 since these are sets of nonlinear equations which cannot be solved explicitly. The iterative algorithm selected would be determined by the desired accuracy and the computational facilities available. It should also be noted that if more than three count intervals are available in the second method, one could not in general obtain equality of the observed and computed counts for all the intervals since there are only three unknown parameters. A technique which minimizes the sum of the squares of the resulting residuals would then be employed.

It should be noted that for a stationary or slowly moving vehicle traveling on the surface of the earth, the preceding simple model is sufficient. However, when considering a fast-moving aircraft, the model should also include

velocities and vertical position. It can be seen that the computational effort in one of these iterative techniques is considerably increased by adding more variables to the model.

Results of error analysis studies (17) show that position error estimates in the along-track direction are generally of better quality than the cross-track error estimates. This is particularly true for high elevation angle passes and should be anticipated intuitively since slant range is less sensitive to changes in cross-track position. The Doppler count is proportional to the change in slant range.

If one uses a high elevation satellite in a polar orbit to determine his position, he would expect the large uncertainty in his cross-track position to be primarily reflected as a large longitude error in the conventional latitude-longitude navigation coordinates. Cross-track and longitude errors are only approximately equal because of earth rotation and vehicle motion.

B. The Effect of Orbital Geometry in the Position-Fix Determination from Two Doppler Satellites

One would expect to be able to obtain a better quality position fix if the Doppler measurements from two satellites are processed and the resulting estimates of position are statistically weighted to achieve an "optimal" estimate. Since the satellite measurement errors do not reflect equally into the cross-track and along-track position errors, the

improvement in position which could be expected by using two satellites instead of one is a function of their orbit geometries. This section extends the results of single satellite error studies to determine the quantitative improvement one might expect from the "two-in-view" condition as a function of their subtrack velocity angular displacements. The results provide substantial justification for providing dual satellite coverage for the integrated inertial/Doppler-satellite system.

Consider a situation in which position fixes are obtained from two satellites simultaneously in view. A coordinate system may be set up such that y is coincident with the subtrack direction of satellite A and forms an angle Θ with the subtrack of satellite B as shown in Figure 2.1. Let α be the interior angle between the receiver and satellite radius vectors at the point of minimum distance between the receiver and the satellite's subtrack. This is illustrated in Figure 2.2.

Let the cross-track error, δm, of each satellite and the along-track error, δn, of each satellite be considered to be approximately normally distributed random variables with zero mean or

$$\delta m \sim N(0, v_m)$$

$$\delta n \sim N(0, v_n)$$

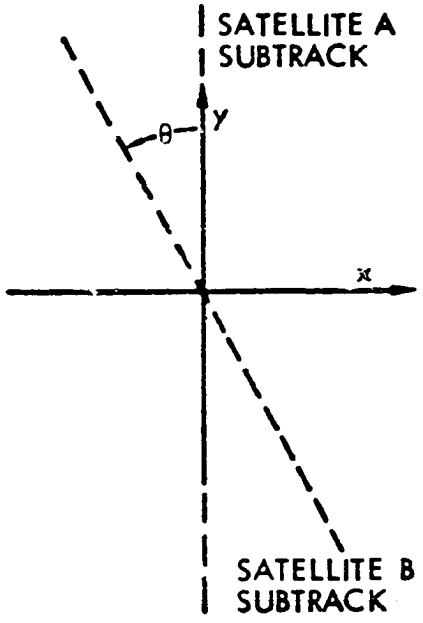

Figure 2.1. Angular orientation of subtracks

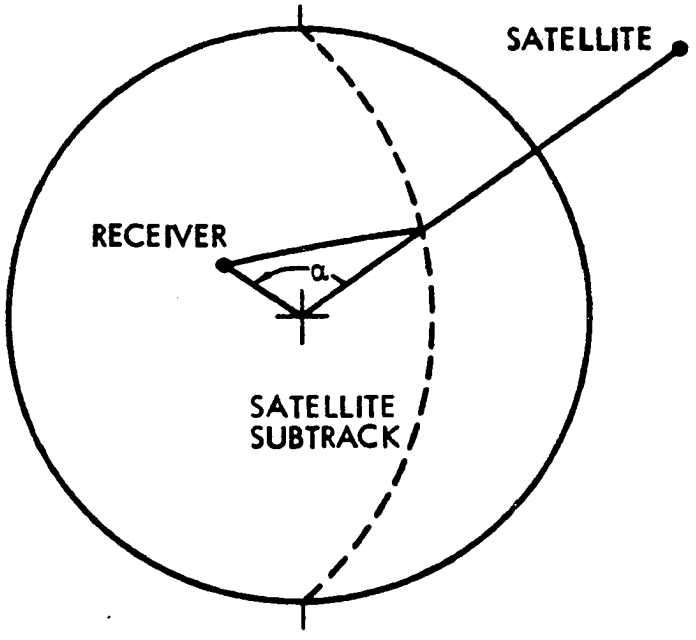

Figure 2.2. Angular orientation of radius vectors

where

$$v_m = f(\alpha)$$

$$v_n = g(\alpha) \quad .$$

These errors reflect into the x, y coordinate system as

$$\delta x_a = \delta m_a \tag{2.12}$$

$$\delta y_a = \delta n_a \tag{2.13}$$

for satellite A and,

$$\delta x_b = \delta m_b \cos \Theta - \delta n_b \sin \Theta \tag{2.14}$$

$$\delta y_b = \delta m_b \sin \Theta + \delta n_b \cos \Theta \tag{2.15}$$

for satellite B.

Assuming δm and δn are uncorrelated,

$$E[\delta x_a^2 | \alpha_a, \Theta] = v_{ma} \tag{2.16}$$

$$E[\delta y_a^2 | \alpha_a, \Theta] = v_{na} \tag{2.17}$$

$$E[\delta x_b^2 | \alpha_b, \Theta] = v_{mb} \cos^2\Theta + v_{nb} \sin^2\Theta \tag{2.18}$$

$$E[\delta y_b^2 | \alpha_b, \Theta] = v_{mb} \sin^2\Theta + v_{nb} \cos^2\Theta \quad . \tag{2.19}$$

When n measurements of a variable z are made with unequally precise instruments, the optimum (in a minimum mean square error sense) estimate of z is a weighted sample mean is

$$\bar{z} = \frac{\sum_{k=1}^{n} \frac{z_k}{v_k}}{\sum_{k=1}^{n} \frac{1}{v_k}} \quad . \tag{2.20}$$

This is discussed in more detail in Appendix A.

For two independent satellite measurements, then the resulting error in the x direction is given by

$$\overline{\delta x} = \frac{v_{xa}v_{xb}}{v_{xa}+v_{xb}} \left[\frac{\delta x_a}{v_{xa}} + \frac{\delta x_b}{v_{xb}}\right] \tag{2.21}$$

and the corresponding error in the y direction is

$$\overline{\delta y} = \frac{v_{ya}v_{yb}}{v_{ya}+v_{yb}} \left[\frac{\delta y_a}{v_{ya}} + \frac{\delta y_b}{v_{yb}}\right] \quad . \tag{2.22}$$

The conditional mean square errors of the weighted means are

$$E[\overline{\delta x}^2 | \alpha_a, \alpha_b, \theta] = \frac{(v_{mb}\cos^2\theta + v_{nb}\sin^2\theta)v_{ma}}{v_{mb}\cos^2\theta + v_{nb}\sin^2\theta + v_{ma}} \tag{2.23}$$

$$E[\overline{\delta y}^2 | \alpha_a, \alpha_b, \theta] = \frac{(v_{mb}\sin^2 + v_{nb}\cos^2)v_{na}}{v_{mb}\sin^2 + v_{nb}\cos^2 + v_{na}} \quad . \tag{2.24}$$

Consider that α_a and α_b are independent discrete random variables taking on N values with equal probability so

$$E[\overline{\delta x}^2 | \theta] = \frac{1}{N^2} \sum_b \sum_a E[\overline{\delta x}^2 | \alpha_a, \alpha_b, \theta] \tag{2.25}$$

$$E[\overline{\delta y}^2 | \theta] = \frac{1}{N^2} \sum_b \sum_a E[\overline{\delta y}^2 | \alpha_a, \alpha_b, \theta] \quad . \tag{2.26}$$

Equations 2.25 and 2.26 give a measure of the quality of the measurements as a function of the angle of intersection of the two subtracts. A commonly used criteria for the overall quality of a position fix is the RMS radial error given by

$$\text{Rad. error}_{RMS} = \{E[\overline{\delta x}^2|\theta] + E[\overline{\delta y}^2|\theta]\}^{1/2} \quad . \qquad (2.27)$$

To get some numerical measure of the effect of θ on the position fix quality, Equations 2.25 and 2.26 were implemented by a computer program using the results of the single satellite error analysis study by Watson (17) to obtain values of v_m and v_n. The two satellites are considered to have identical quality instrumentation and are in 600 nautical mile circular orbits. The received signal is corrupted by uncorrelated noise at the rate of 1 part per 10^8 RMS. The angle α of each satellite is considered to be a discrete random variable ranging from 1 degree to 17 degrees at 1 degree intervals with equal probabilities. This corresponds to a range in the elevation angle from about 85 degrees to 19 degrees, so direct overhead passes and low elevation passes were excluded. The values of v_m and v_n used are tabulated in Table 2.1. The resulting RMS errors for the "two-in-view" condition are plotted in Figure 2.3 as a function of θ.

Note that orthogonal satellites yield an RMS radial error which is only 60 percent of that of the parallel

Table 2.1. Cross-track variance (v_m) and along-track variance (v_n) as functions of interior angle

α (deg.)	v_m $(n.m.)^2$	v_n $(n.m.)^2$	α (deg.)	v_m $(n.m.)^2$	v_n $(n.m.)^2$
1	0.06250	0.00036	10	0.00250	0.00048
2	.01960	.00036	11	.00250	.00048
3	.01082	.00040	12	.00250	.00053
4	.00640	.00040	13	.00250	.00053
5	.00462	.00040	14	.00250	.00058
6	.00360	.00040	15	.00250	.00062
7	.00325	.00040	16	.00250	.00068
8	.00292	.00044	17	.00250	.00073
9	.00250	.00044			

satellites.

Another measure of the overall quality of the position fix is the circular error probable (CEP) which is defined as the radius of a circle which will enclose 50 percent of distribution (12, 13). In the preceding analysis, the error has a bivariate normal distribution with zero correlation in cross-track and along-track errors for $\Theta = 0$ degrees and $\Theta = 90$ degrees. The corresponding radii of the circles about the origin which include 50 percent of the error distribution are

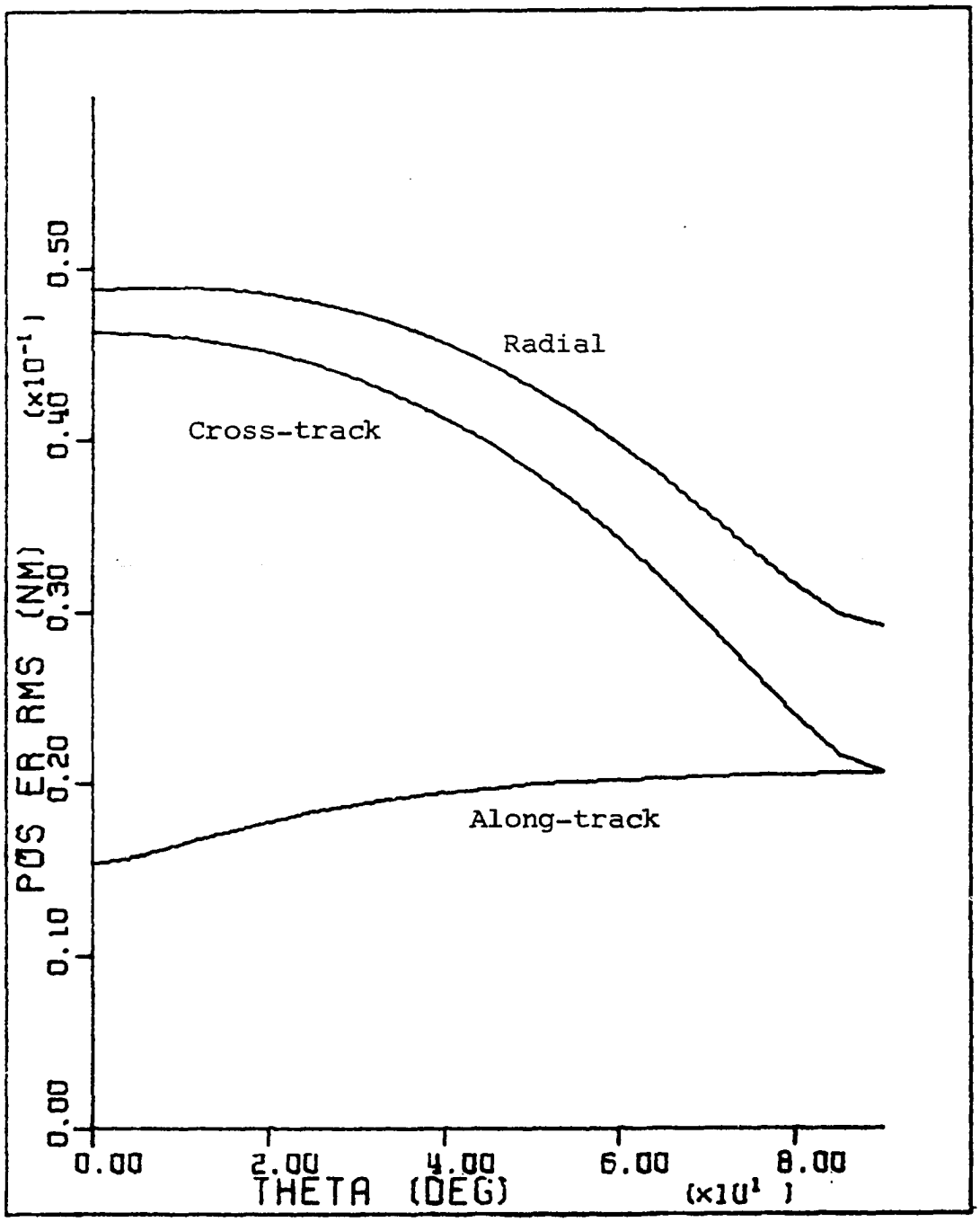

Figure 2.3. Position error using measurements from two satellites (theta = angle between satellite subtracks)

$CEP(\theta = 0^{o})$ = 0.0355 nautical miles and

$CEP(\theta = 90^{o})$ = 0.0242 nautical miles.

The orthogonal satellites' error is only 68 percent of that of the parallel satellites using CEP as the measurement of quality.

A number of assumptions made in the analysis should be noted with comment.

(a) The variances of the cross-track errors and along-track errors are derived from longitude and latitude error curves using a polar orbiting satellite. These are only approximately equal because of earth spin.

(b) The cross-track and along-track measurement errors of each satellite are assumed to be uncorrelated. This is approximately correct only for a stationary receiver.

(c) The interior angle α is considered to be a discrete random variable for computational purposes.

(d) The only source of error is considered to be due to uncorrelated measurement noise.

Therefore, one must view these numerical results only as an indication of the variation in the quality of a dual satellite position fix as a function of the subtrack angles. However, the results certainly suggest that there is considerable advantage in viewing satellites whose subtracks are

nearly orthogonal. This aspect of an expanded satellite configuration is investigated more fully in Chapter IV with a computer simulated integrated inertial/Doppler-satellite navigation system.

III. THE KALMAN FILTER SYSTEM INTEGRATION

The block diagram in Figure 3.1 illustrates the integration technique used to couple the Doppler satellites with the inertial system. This is similar to a technique used by Brown and Hagerman(3) in their single satellite coverage studies. The basic observable is the Doppler count in the interval between sample times and the input to the filter is the difference between this observed count and the predicted count from the inertial system's estimate of vehicle position. It will be shown later that the measurement has a linear connection to the previous state as well as the present state which requires a modified version of the Kalman filter. This will be referred to as the delayed-state filter.

A. The Delayed-State Kalman Filter

A more complete treatment of this modified filter is found in Appendix B as well as other references (3, 4). This section will define the model structure and summarize the set of recursive equations that constitutes the filter.

The random process $\underline{x}(t)$ to be estimated is assumed to satisfy the vector differential equation

$$\dot{\underline{x}}(t) = A(t)\underline{x}(t) + B(t)\underline{f}(t) \qquad (3.1)$$

where

$\underline{x}(t)$ is the $(n \times 1)$ system state vector,

$A(t)$ is the $(n \times n)$ time-varying dynamics matrix,

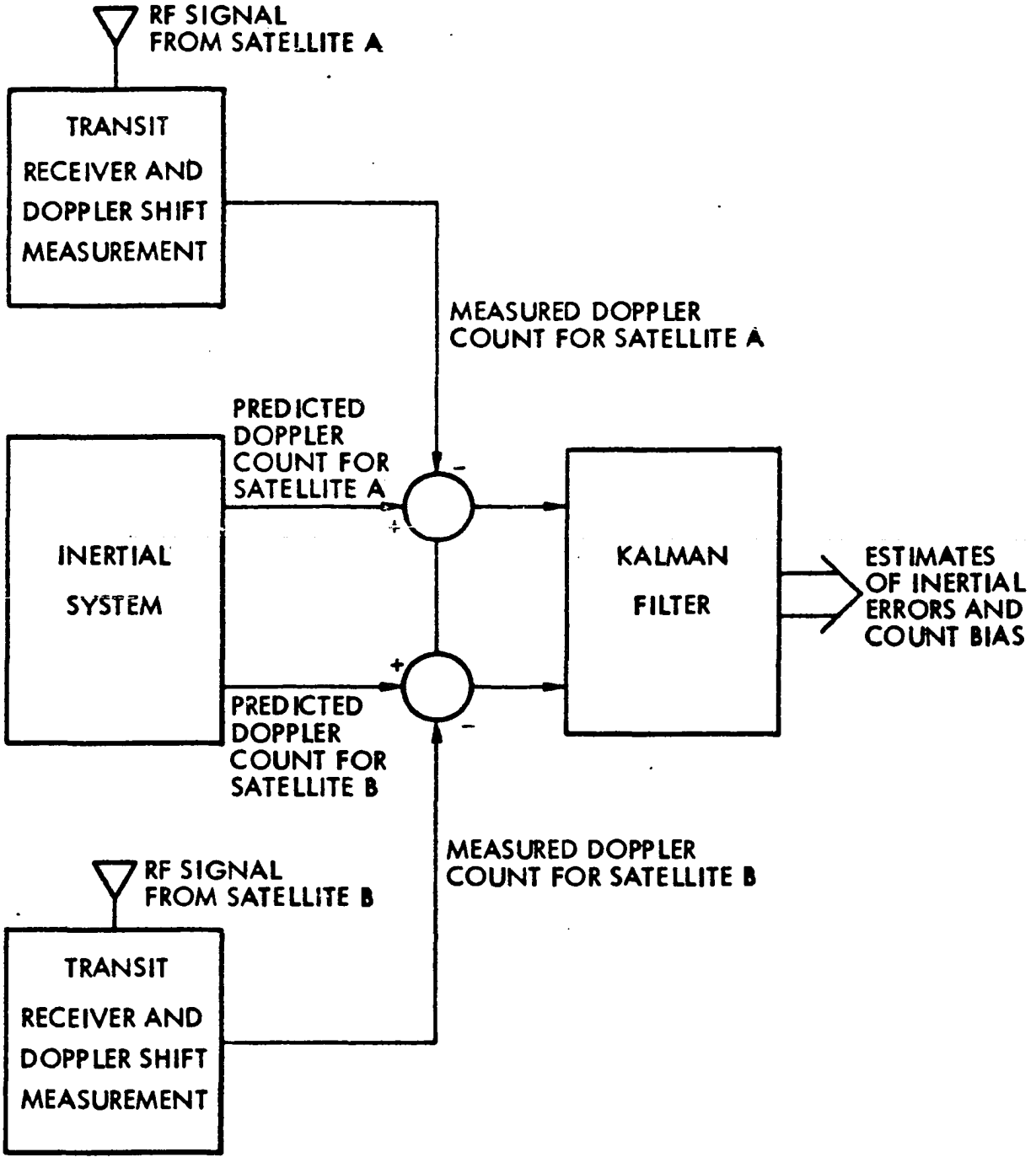

Figure 3.1. Block diagram of integration technique for the "two-in-view" problem

$\underline{f}(t)$ is a $(p \times 1)$ white noise input vector, and

$B(t)$ is the $(n \times p)$ time-varying matrix which connects the input to the state at time t.

For the discrete-time case, the solution of Equation 3.1 results in the vector difference equation

$$\underline{x}(k) = \emptyset(k,k-1)\underline{x}(k-1) + \underline{g}(k-1) \tag{3.2}$$

where

$\underline{x}(k)$ is the state vector at time t_k,

$\emptyset(k,k-1)$ is the state transition matrix from time t_{k-1} to t_k, and

$\underline{g}(k-1)$ is the system response due to the white noise input in the time interval (t_{k-1}, t_k).

The measurement model is represented by a vector equation of the form

$$\underline{y}(k) = M(k)\underline{x}(k) + N(k)\underline{x}(k-1) + \underline{v}(k) \tag{3.3}$$

where

$\underline{y}(k)$ is the $(m \times 1)$ discrete measurement vector at time t_k,

$M(k)$ is a $(m \times n)$ matrix linearly relating the present state to the measurement,

$N(k)$ is a $(m \times n)$ matrix linearly relating the previous state to the measurement, and

$\underline{v}(k)$ is the uncorrelated measurement error.

The recursive Kalman filter equations for the model specified by the state Equation 3.1 and the measurement Equation 3.3 are (4)

$$P(k|k-1) = \Phi(k,k-1)P(k-1|k-1)\Phi'(k,k-1) + H(k-1) \tag{3.4}$$

$$\hat{\underline{x}}(k|k-1) = \Phi(k,k-1)\hat{\underline{x}}(k-1|k-1) \tag{3.5}$$

$$\begin{aligned} Q(k) = {} & M(k)P(k|k-1)M'(k) + V(k) + N(k)P(k-1|k-1)N'(k) \\ & + M(k)\Phi(k,k-1)P(k-1|k-1)N'(k) \\ & + [M(k)\Phi(k,k-1)P(k-1|k-1)N'(k)]' \end{aligned} \tag{3.6}$$

$$K(k) = [P(k|k-1)M'(k) + \Phi(k,k-1)P(k-1|k-1)N'(k)]Q^{-1}k \tag{3.7}$$

$$P(k|k) = P(k|k-1) - K(k)Q(k)K'(k) \tag{3.8}$$

$$\begin{aligned} \hat{\underline{x}}(k|k) = {} & \hat{\underline{x}}(k|k-1) + K(k)[\underline{y}(k) - M(k)\hat{\underline{x}}(k|k-1) \\ & - N(k)\hat{\underline{x}}(k-1|k-1)] \end{aligned} \tag{3.9}$$

where

$\hat{\underline{x}}(k-1|k-1)$ is the optimal estimate of $\underline{x}(k-1)$ given all measurements through t_{k-1},

$P(k-1|k-1)$ is the covariance matrix of the estimation error $[\underline{x}(k-1) - \hat{\underline{x}}(k-1|k-1)]$,

$\hat{\underline{x}}(k|k-1)$ is the optimal estimate of $\underline{x}(k)$ given all measurements through t_{k-1},

$P(k|k-1)$ is the covariance matrix of the estimation

error $[\underline{x}(k) - \hat{\underline{x}}(k|k-1)]$,

$K(k)$ is the gain matrix which optimally "weights" the measurement at t_k into the estimate,

$\hat{\underline{x}}(k|k)$ is the optimal estimate of $\underline{x}(k)$ given all measurements through t_k,

$P(k|k)$ is the covariance matrix of the estimation error $[\underline{x}(k) - \hat{\underline{x}}(k|k)]$,

$H(k-1)$ is the covariance matrix of the state response to the white noise inputs in the time interval (t_{k-1}, t_k), and

$V(k)$ is the covariance matrix of the uncorrelated measurement error at t_k.

Once the models of the state and measurement equations are formulated and the initial state estimate $\hat{\underline{x}}(0|0)$ and covariance $P(0|0)$ are chosen, the recursive Equations 3.4 through 3.9 uniquely specify the optimal estimates for any sequence of measurements.

The next three sections describe the modeling of an integrated inertial/Doppler-satellite system. The first section describes the state equation model, the second describes the measurement equation model and the third describes the initialization.

B. The State Equation Model

The errors in the inertial system which are to be estimated are described by two basic error equations which are derived in Appendix C and Pitman (13),

$$\dot{\underline{\psi}} + \underline{\omega} \times \underline{\psi} = \underline{\varepsilon} \tag{3.10}$$

and

$$\delta\ddot{\underline{R}} + 2\underline{\omega} \times \delta\dot{\underline{R}} + \dot{\underline{\omega}} \times \delta\underline{R} + \underline{\omega} \times (\underline{\omega} \times \delta\underline{R}) = \delta\underline{a} - \underline{\psi} \times \underline{a} - \omega_0^2 \delta R_{tan} \quad . \tag{3.11}$$

where

$\underline{\psi} = \underline{\phi} - \delta\underline{\theta}$,

$\underline{\phi}$ is the platform coordinate frame vector error,

$\delta\underline{\theta}$ is the computer coordinate frame vector error,

$\underline{\omega}$ is the platform angular rate with respect to an inertial reference frame,

$\underline{\varepsilon}$ is the gyro drift rate vector error,

$\delta\underline{R}$ is the radial position vector error,

$\delta\underline{a}$ is the accelerometer vector error,

$\underline{a}$ is the sensed acceleration vector (including both inertial and mass attraction forces),

$\delta\underline{R}_{tan}$ is the component of $\underline{\delta R}$ tangential to the earth,

g_m is the mass attraction acceleration of the earth at a distance R from center of the earth, and

$\omega_0^2 = g_m/R$ is the square of the so-called "Schuler frequency."

At this point, it is necessary to establish the following "ground rules" concerning the choice of coordinate frames and inertial system.

(a) The inertial system operates in a terrestial (near earth) condition.

(b) The inertial system operates in a geocentric latitude-longitude coordinate frame with the platform always maintained with its x axis north, y axis west and z axis up.

(c) The vertical (z) channel is not implemented by the inertial system and is assumed to be independent of the level channels.

Three right-hand cartesian coordinate frames which are used are shown in Figure 3.2. These will be denoted by (x,y,z), (X,Y,Z) and (X',Y',Z') where

(x,y,z) is a geocentric navigation frame with x north, y west, and z up,

(X,Y,Z) is an earth-fixed frame with X through Greenwich meridian at the equator, Z through the north pole and Y mutually orthogonal.

(X',Y',Z') is an inertially fixed frame which is coincident with (X,Y,Z) at an initial reference time $t = 0$,

Θ is geocentric latitude,

λ is longitude, and

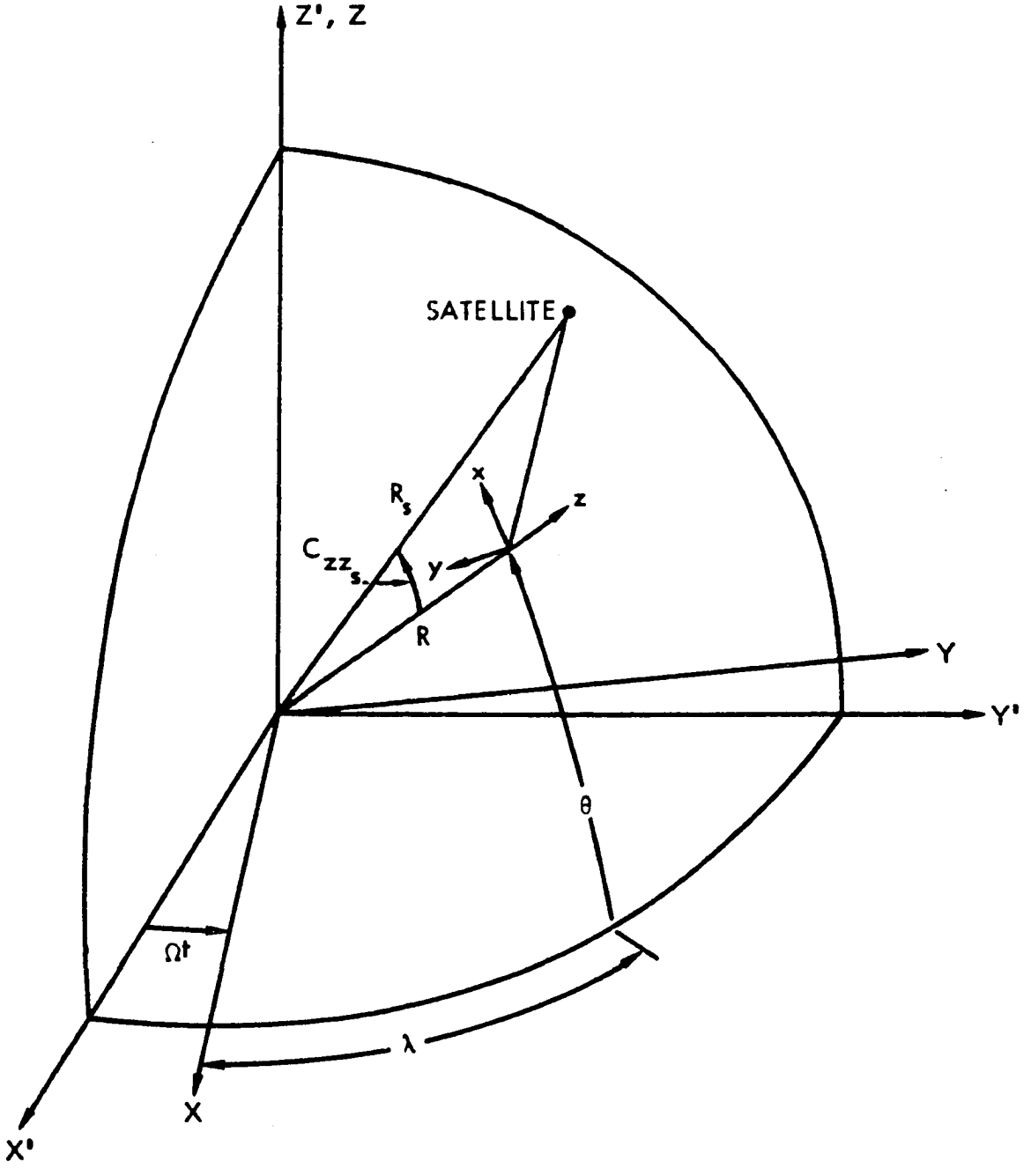

Figure 3.2 Coordinate frames

Ω is earth rotation rate.

The state variables are selected in the (x,y,z) navigation frame.

Equation 3.10 yields ψ_x, ψ_y and ψ_z as state variables and Equation 3.11 yields δR_x, $\delta \dot{R}_x$, δR_y, $\delta \dot{R}_y$, δR_z and $\delta \dot{R}_z$ as state variables. However, the random process driving functions in Equation 3.10 are the gyro drifts, and in Equation 3.11 accerometer errors are driving functions. Physically, these could not be modeled as white noise processes and therefore the form of the state Equation 3.1 is not yet achieved.

The usual method to incorporate gyro drifts and accelerometer errors into the model is to consider them to be first order Markov processes resulting from white noise inputs to a shaping filter. This is illustrated in Figure 3.3 in a conventional s-domain block diagram. These processes then satisfy an equation of the form

$$\dot{x} + \beta x = (2\sigma^2\beta)^{1/2} f(t) \qquad (3.12)$$

where

σ^2 is the variance of the process,

β is the reciprocal time constant, and

$f(t)$ is unity white noise.

By an appropriate choice of β and σ, the process can be used to represent true bias, white noise, random walk and all

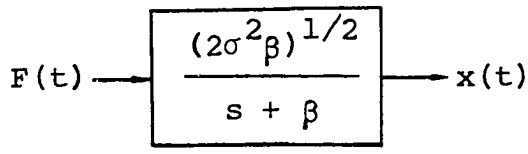

Figure 3.3 Shaping filter for Markov process

shades of grey in between.

Since the vertical channel of the inertial system is decoupled from the horizontal channels, the vertical velocity will also be modeled as a Markov process. Again by proper choice of β and σ, a wide range of situations can be accommodated by this model.

The system or plant model is completed by accounting for drifts in the satellite transmitter and the reference oscillator in the receiver as well as other correlated errors in the count measurement. Since two satellites are viewed, two such Markov processes are included as state variables in the state equation.

A total of 16 state variables are then used in the model. It is convenient to define the state variables to be dimensionless quantities. For example, level position errors are expressed in terms of angular displacements, $\delta\Theta_x = -\delta R_y/R$ and $\delta\Theta_y = \delta R_x/R$. The final state variables are then defined as follows:

$x_1 = \psi_x$
$x_2 = \psi_y$ — psi
$x_3 = \psi_z$

$x_4 = \delta\theta_x$
$x_5 = \delta\dot{\theta}_x/\omega_0$
$x_6 = \delta\theta_y$ — Position and velocity errors
$x_7 = \delta\dot{\theta}_y/\omega_0$
$x_8 = \delta\dot{R}_z/R$

$x_9 = \varepsilon_x/\omega_0$
$x_{10} = \varepsilon_y/\omega_0$ — Gyro drifts
$x_{11} = \varepsilon_z/\omega_0$

$x_{12} = \delta a_x/R\omega_0^2$
$x_{13} = \delta a_y/R\omega_0^2$ — Accelerometer errors

$x_{14} = \delta\dot{R}_z/R\omega_0$ — Vertical velocity error

$x_{15} = N_A$
$x_{16} = N_B$ — Doppler-count errors

The first eight rows of the A matrix in Equation 3.1 are formed (after much algebraic manipulation) from the Equations 3.10 and 3.11. The remaining eight rows are all Markov state variables of the form of Equation 3.12. Assuming level flight, the nonzero terms of the A matrix are then:

$$a_{1,2} = \omega_z$$

$$a_{1,3} = -\omega_y$$

$$a_{1,9} = \omega_0$$

$$a_{2,1} = -\omega_z$$

$$a_{2,3} = \omega_x$$

$$a_{2,10} = \omega_0$$

$$a_{3,1} = \omega_y$$

$$a_{3,2} = -\omega_x$$

$$a_{3,11} = a_{4,5} = a_{6,7} = \omega_0$$

$$a_{5,1} = (\omega_x^2 + \omega_y^2 - \omega_0^2)/\omega_0$$

$$a_{5,3} = (\dot{\omega}_y + \omega_x\omega_z)/\omega_0$$

$$a_{5,4} = (\omega_x^2 + \omega_z^2 - \omega_0^2)/\omega_0$$

$$a_{5,6} = (\dot{\omega}_z + \omega_x\omega_y)/\omega_0$$

$$a_{5,7} = 2\omega_z$$

$$a_{5,8} = (-\dot{\omega}_x + \omega_y\omega_z)/\omega_0$$

$$a_{5,13} = -\omega_0$$

$$a_{5,14} = -2\omega_x$$

$$a_{7,2} = (\omega_x^2 + \omega_y^2 - \omega_0^2)/\omega_0$$

$$a_{7,3} = (-\dot{\omega}_x + \omega_y\omega_z)/\omega_0$$

$$a_{7,4} = (\omega_y\omega_x - \dot{\omega}_z)/\omega_0$$

$$a_{7,5} = -2\omega_z$$

$$a_{7,6} = (w_y^2 + \omega_z^2 - \omega_0^2)/\omega_0$$

$$a_{7,8} = (-\dot{\omega}_y - \omega_z\omega_x)/\omega_0$$

$$a_{7,12} = a_{8,14} = \omega_0$$

$$a_{7,14} = -2\omega_y$$

$$a_{9,9} = -\beta_9$$

$$a_{10,10} = -\beta_{10}$$

$$a_{11,11} = -\beta_{11}$$

$$a_{12,12} = -\beta_{12}$$

$$a_{13,13} = -\beta_{13}$$

$$a_{14,14} = -\beta_{14}$$

$$a_{15,15} = -\beta_{15}$$

$$a_{16,16} = -\beta_{16}$$

If the sample step size is sufficiently small, then the elements of the A matrix describing the dynamics of the system are approximately constant during the sampling interval. The transition matrix for a constant A matrix is determined by the expression

$$\emptyset(k,k-1) = \exp[A\Delta t] \qquad (3.13)$$

where Δt is the sample step size $(t_k - t_{k-1})$. The sample step size in the simulation studies was 20 seconds which is

comparatively "small", so the transition matrix was generated by an eight term series expansion of Equation 3.13 for each step of the process.

The final consideration in the system model is the additional uncertainty in the state estimates arising from the white noise driving functions, $\underline{g}(k-1)$. This uncertainty is denoted by the covariance matrix H(k-1) and defined as

$$H(k-1) = E[\underline{g}(k-1)\underline{g}'(k-1)] \quad .$$

Recall that the Markov process is considered to be derived from passing unity white noise through a shaping filter and satisfies an equation of the form of Equation 3.12. This can be expressed as a difference equation over the Δt interval as

$$x(k) = \exp(-\beta\Delta t)x(k-1) + \int_{o}^{\Delta t} (2\sigma^2\beta)^{1/2}\exp(-\beta u)f(t-u)du \quad . \tag{3.14}$$

The variance of the response of x(k) due to the white noise driving function is then

$$h = E[\int_{o}^{\Delta t} (2\sigma^2\beta)^{1/2}\exp(-\beta u)f(t-u)du$$

$$\int_{o}^{\Delta t} (2\sigma^2\beta)^{1/2}\exp(-\beta v)f(t-v)dv] \quad .$$

Using conventional random process techniques to evaluate this expectation leads to

$$h = \sigma^2[1 - \exp(-2\beta\Delta t)] \quad . \tag{3.15}$$

State variables x_9 through x_{16} will each have a response of the form of Equation 3.15 or

$$h_{i,i} = \sigma_i^2[1 - \exp(-2\beta_i\Delta t)] \ , \quad i = 9,10,\ldots,16 \quad . \tag{3.16}$$

The white noise driving functions also produce a response in state variables x_1 through x_7. However, the error dynamics of the inertial system are comparatively slow and its "smoothing effect" will reduce this white noise response to a negligible amount if the Δt sampling interval is small. This is to say that all of these responses are of second order in Δt, or higher, and may be neglected. The mechanism for random walk in state variables 1 through 7 is diffusion of the Markov responses of state variables 9 through 16 with each step via Equation 3.4.

The vertical position channel is modeled as an integrated Markov process whose time constant is small. Therefore, the response in the vertical position error to the white noise input cannot be neglected. The vertical channel model is shown in a conventional s-domain block diagram form in Figure 3.4. The weighting function corresponding to $C(s) = W_1(s)W_2(s)$ is

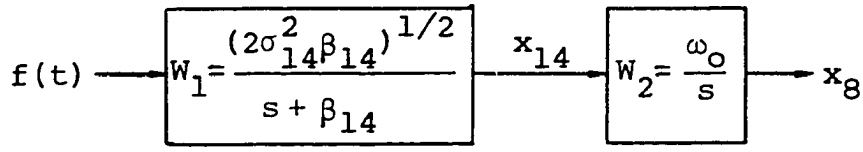

Figure 3.4. Block diagram for vertical channel model

$$c(u) = \omega_o(2\sigma_{14}^2\beta_{14})^{1/2}[1 - \exp(-\beta_{14}u)]/\beta_{14} \tag{3.17}$$

so

$$h_{8,8} = E[\int_o^{\Delta t} c(u)f(t-u)du \int_o^{\Delta t} c(v)f(t-v)dv]$$

$$= \frac{2\omega_o^2\sigma_{14}^2}{\beta_{14}^2}\{\beta_{14}\Delta t - 2[1 - \exp(-\beta_{14}\Delta t)]$$

$$+ 1/2[1 - \exp(-2\beta_{14}\Delta t)]\} \quad . \tag{3.18}$$

The covariance terms, $h_{8,14}$ and $h_{14,8}$, are similarly formed as

$$h_{8,14} = h_{14,8} = E[\int_o^{\Delta t} w_1(u)f(t-u)du \int_o^{\Delta t} c(v)f(t-v)dv]$$

$$= \frac{2\omega_o\sigma_{14}^2}{\beta_{14}}\{[1 - \exp(-\beta_{14}\Delta t)] - 1/2[1 - \exp(-2\beta_{14}\Delta t)]\} \quad . \tag{3.19}$$

The model permits inclusion of uncorrelated components of gyro drift and accelerometer error. These will enter into

states 1, 2, 3, 5 and 7 as approximately constant terms for $h_{1,1}$, $h_{2,2}$, $h_{3,3}$, $h_{5,5}$ and $h_{7,7}$ in the H matrix.

C. The Measurement Equation

The measurement quantity in the model is the difference between the number of cycles received from a satellite and the "expected" number of cycles which is computed from the inertial system's estimates of position. This assumes perfect knowledge of the satellite's orbital parameters.

The modeling problem is then to find a linear connection between the measurement and the state variables in the form of Equation 3.3. If one assumes that the two measurements from dual satellite coverage are in time coincidence and are statistically independent, these measurements may be processed either simultaneously or sequentially. Simultaneous processing of the measurements will be used since the Kalman filter recursive Equations 3.4 through 3.9 are not valid for sequential processing. The problem of sequential processing of the data is discussed in Appendix B. The following model is based on a "conservation of cycles" argument by Stansell (16) and is similar to the model used by Brown (2) in the single satellite coverage studies.

Consider a satellite that transmits a CW signal at a frequency f_T for a time interval (t_{k-1}, t_k) which is determined by the satellite timing markers. Then the number

of cycles transmitted in this interval is

$$N_T(k) = \int_{t_{k-1}}^{t_k} f_T dt \quad . \tag{3.20}$$

At the receiver, the start of the time interval is delayed by δt_{k-1} due to propagation delay; the end of the time interval is also delayed by an amount δt_k. Neglecting refraction effects, the propagation delays are determined by the slant range and the velocity of propagation as given by

$$t_j = \rho_j / c \tag{3.21}$$

where ρ_j is the slant range between the satellite and receiver and c is the velocity of propagation.

The receiver has a reference oscillator operating at a frequency f_o which is mixed with the received satellite transmission and the difference frequency is then integrated to yield a measured Doppler count. This can be expressed as the difference of two integrals

$$N(k) = \int_{t_{k-1}+\delta t_{k-1}}^{t_k+\delta t_k} f_o dt - \int_{t_{k-1}}^{t_k} f_T dt \quad . \tag{3.22}$$

Integrating and rearranging,

$$N(k) = (f_o - f_T)(t_k - t_{k-1}) + f_o(\delta t_k - \delta t_{k-1}) \quad . \tag{3.23}$$

The difference in the propagation delays can be expressed in

terms of the difference in slant range by Equation 3.21 or

$$N(k) = (f_0 - f_T)(t_k - t_{k-1}) + \frac{f_o}{c}[\rho(k) - \rho(k-1)] \quad . \quad (3.24)$$

N(k) is an ideal measured Doppler count which does not include oscillator drift and other measurement errors. These errors can be categorized into correlated and uncorrelated errors. Two state variables, δN_A and δN_B, modeled as Markov processes have already been introduced in section B to account for the correlated errors in the two received Doppler-counts. The uncorrelated error in the counts is denoted by the vector $\underline{v}(k)$. The measured count for either satellite A or B would be of the form

$$N_m(k) = N(k) - \delta N(k) - v(k) \quad . \quad (3.25)$$

The Doppler count can be computed from the inertial system's position estimates using an expression similar to Equation 3.24 with an additional error term to account for errors in the computed range. This computed count is then

$$N_c(k) = N(k) + \frac{f_o}{c}[\delta\rho(k) - \delta\rho(k-1)] \quad (3.26)$$

where $\delta\rho(k)$ is the error in slant range due to position error in the inertial system. Taking the difference between $N_c(k)$ and $N_m(k)$,

$$y(k) = N_c(k) - N_m(k) = \frac{1}{\gamma_o}[\delta\rho(k) - \delta\rho(k-1)] + \delta N + v(k)$$

where γ_o is the wavelength (c/f_o). (3.27)

This is not yet of the form of Equation 3.3 since $\delta\rho$ is not a state variable. A linear connection between $\delta\rho$ and the state variables $\delta\theta_x$, $\delta\theta_y$, and $\delta R/R$ can be obtained using the technique of Brown and Hagerman (3). The slant range between the vehicle and satellite is given by

$$\rho = (R^2 + R_s^2 - 2RR_sC_{zz_s})^{1/2}$$

where

R is the radial distance from the center of the earth to the vehicle,

R_s is the radial distance from the center of the earth to the satellite, and

C_{zz_s} is the cosine of the angle between the navigation z axis and a vector z_s directed from the center of the earth to the satellite.

A small perturbation of R and C_{zz_s} results in a perturbation in the slant range of

$$\delta\rho = \frac{R - R_sC_{zz_s}}{\rho}\,\delta R - \frac{RR_s}{\rho}\,\delta C_{zz_s} \quad . \tag{3.28}$$

The perturbation δC_{zz_s} can be related to the level position errors by considering the problem of computing the change in direction cosines relating two reference frames when there is relative motion between them. Using only first order perturbations, the approximate relationship between δC_{zz_s} and the level position errors is

$$\delta C_{zz_s} = \delta C_{xx_s} \delta\Theta_y - C_{yz_s} \delta\Theta_x \tag{3.29}$$

so

$$\delta\rho = \frac{R - R_s C_{zz_s}}{\rho} \delta R + \frac{RR_s C_{yz_s}}{\rho} \delta\Theta_x - \frac{RR_s C_{xz_s}}{\rho} \delta\Theta_y \; . \tag{3.30}$$

The measurement from satellite A can now be expressed as a linear combination of state variables and the measurement noise or

$$\begin{aligned} y_A(k) = {} & Ra_A(k)x_8(k) + b_A(k)x_4(k) + c_A(k)x_6(k) \\ & - Ra_A(k-1)x_8(k-1) - b_A(k-1)x_4(k-1) \\ & - c_A(k-1)x_6(k-1) + x_{15}(k) + v_A(k) \end{aligned} \tag{3.31}$$

where

$$a_A = \frac{R - R_s C_{zz_s}}{\gamma_o \rho}$$

$$b_A = \frac{RR_s C_{yz_s}}{\gamma_o \rho}$$

and

$$c_A = \frac{-RR_s C_{xz_s}}{\gamma_o \rho} \; .$$

A similar expression for the measurement from satellite B can be formed.

When simultaneous processing of the measurements from

the two satellites is employed the measurement equation becomes

$$\underline{y}(k) = M(k)\underline{x}(k) + N(k)\underline{x}(k-1) + \underline{v}(k) \qquad (3.32)$$

where

$$M(k) = \begin{bmatrix} 0\ 0\ 0\ b_A(k)\ 0\ c_A(k)\ 0\ Ra_A(k)\ 0\ 0\ 0\ 0\ 0\ 0\ 1\ 0 \\ 0\ 0\ 0\ b_B(k)\ 0\ c_B(k)\ 0\ Ra_B(k)\ 0\ 0\ 0\ 0\ 0\ 0\ 0\ 1 \end{bmatrix}$$

$$N(k) = -\begin{bmatrix} 0\ 0\ 0\ b_A(k-1)\ 0\ c_A(k-1)\ 0\ Ra_A(k-1)\ 0\ 0\ 0\ 0\ 0\ 0\ 0\ 0 \\ 0\ 0\ 0\ b_B(k-1)\ 0\ c_B(k-1)\ 0\ Ra_B(k-1)\ 0\ 0\ 0\ 0\ 0\ 0\ 0\ 0 \end{bmatrix}$$

and

$$\underline{v}(k) = \begin{bmatrix} v_A(k) \\ v_B(k) \end{bmatrix} .$$

If the position data of a satellite is given in the earth-fixed (X,Y,Z) reference frame as shown in Figure 3.2, the satellite radial distance is simply

$$R_s = (X_s^2 + Y_s^2 + Z_s^2)^{1/2} .$$

The nine direction cosines relating the earth-fixed (X,Y,Z) and navigation (x,y,z) can be computed from latitude and longitude of the vehicle. They are listed below where Θ is geocentric latitude and λ is longitude. S and C are

used to denote sine and cosine respectively.

$$C_{xX} = -S\theta C\lambda$$

$$C_{xY} = -S\theta S\lambda$$

$$C_{xZ} = C\theta$$

$$C_{yX} = S\lambda$$

$$C_{yY} = -C\lambda$$

$$C_{yZ} = 0$$

$$C_{zX} = C\theta C\lambda$$

$$C_{zY} = C\theta S\lambda$$

$$C_{zZ} = S\theta \quad .$$

The three direction cosines in measurement matrix can now be computed as

$$C_{xz_s} = (X_s C_{xX} + Y_s C_{xY} + Z_s C_{xZ})/R_s \tag{3.33}$$

$$C_{yz_s} = (X_s C_{yX} + Y_s C_{yY} + Z_s C_{yZ})/R_s \tag{3.34}$$

$$C_{zz_s} = (X_s C_{zX} + Y_s C_{zY} + Z_s C_{yZ})/R_s \tag{3.35}$$

The final consideration of the measurement equation model is the formation of V(k), the covariance matrix of the uncorrelated measurement error. For simultaneous processing of the two satellite measurements, the assumption of

independence leads to a diagonal matrix whose terms are simply the variances of the uncorrelated measurement error.

D. The Initial Estimates and Covariance Matrix

All of the state variables are assumed to be zero mean random variables at t = 0, so with no a priori knowledge, the initial value of the state vector would be zero.

Initialization of the covariance matrix is another matter. Though the a priori initial estimates of the state variables are zero, the variances associated with those estimates are nonzero since one would normally not have perfect knowledge of any of the state variables. The method of selecting these initial variances would probably best be categorized in the realm of "engineering judgment". Nonzero covariance terms may also arise depending on the alignment scheme used for the inertial system. The effect of the initial covariance matrix is to determine the relative weight given to the measurements and also the distribution of their "weights" among all the state variables. Fortunately, the sensitivity of the filter's performance to the initial covariance matrix is reduced by having continuous satellite coverage so this aspect of the modeling process is not as influential in the filter's performance as it is when very few measurements are available. At least this can be said with some assurance after the first hour of simulation, and the results presented later support this.

All the parameters of the filter have now been specified, so this completes the discussion of the filter model.

IV. SIMULATION STUDIES

As was pointed out in the introduction, studies of the integration of an inertial navigation system and a limited Doppler-satellite system have shown the scheme to be successful, though not without some problems. One intuitively feels that most of these problems would be greatly reduced with a more extensive satellite system. However, the term "intuitively" does not really answer any questions concerning specific performance improvements. Furthermore, intuition is of questionable value when dealing with a complex system as evidenced by the large number of state variables in this model.

A number of questions arise when one considers an expanded satellite system. For example, "How does the altitude of the satellites affect navigation performance?", "What performance benefits occur from viewing two rather than one satellite?", or "How is the accuracy of the system affected by the choice of satellite pairs?" These questions plus a number of others are investigated in this chapter. Naturally, the best approach to investigate such questions would be to set up the various satellite configurations under study and with an airborne inertial system, perform the Kalman filter integration in real time. Since this is obviously impractical because of the effort and cost involved, the next best

approach is a computer simulation of the various satellite configurations and the vehicle dynamics. One can then analyze the variances of the system error estimates in the mathematical model.

Before presenting the results of the simulation studies, the mathematical model of the satellite kinematics and vehicle dynamics are described in the next two sections.

A. Satellite Kinematics

The satellites move in a force field defined by the earth's gravitational potential U, which in general can be written in the form (9)

$$U = (GM/R_s)[1 - \sum_{n=2}^{\infty} J_n(R_e R_s)^n P_n(\sin\Theta)] \qquad (4.1)$$

where

G is the gravitational constant,

M is the mass of the earth,

R_s is the radial distance to the satellite,

R_e is the equatorial radius of the earth,

J_n are constants, and

$P_n(\sin\Theta)$ is the Legendre polynomial of degree n whose argument is the sine of the geocentric latitude.

A spherical earth was assumed for this study so only the first term of the series was used. The additional terms account for asymmetries in the earth's shape but they are relatively unimportant for error analysis purposes.

The satellites were considered to be in circular orbits since there is no advantage in an elliptical orbit. The angular velocity of a satellite is then

$$\omega_s = (U/R_s^2)^{1/2} \quad . \tag{4.2}$$

Details of the orbital mechanics of satellites are found in several references such as King-Hele (9).

An expression for the three-dimensional description of motion of any satellite can be obtained. Referring to Figure 4.1, the previously defined inertially-fixed (X',Y',Z') coordinate system is shown with a satellite whose orbital motion is in the X''-Y'' plane of an (X'',Y'',Z'') coordinate system. The equations for circular motion of a satellite in the (X'',Y'',Z'') coordinate system are then

$$X_s'' = R_s \cos \alpha \tag{4.3}$$

$$Y_s'' = R_s \sin \alpha \tag{4.4}$$

$$Z_s'' = 0 \tag{4.5}$$

$$\alpha = \omega_s t + q \tag{4.6}$$

where

ω_s is the angular velocity of the satellite,

q is the initial angular displacement, and

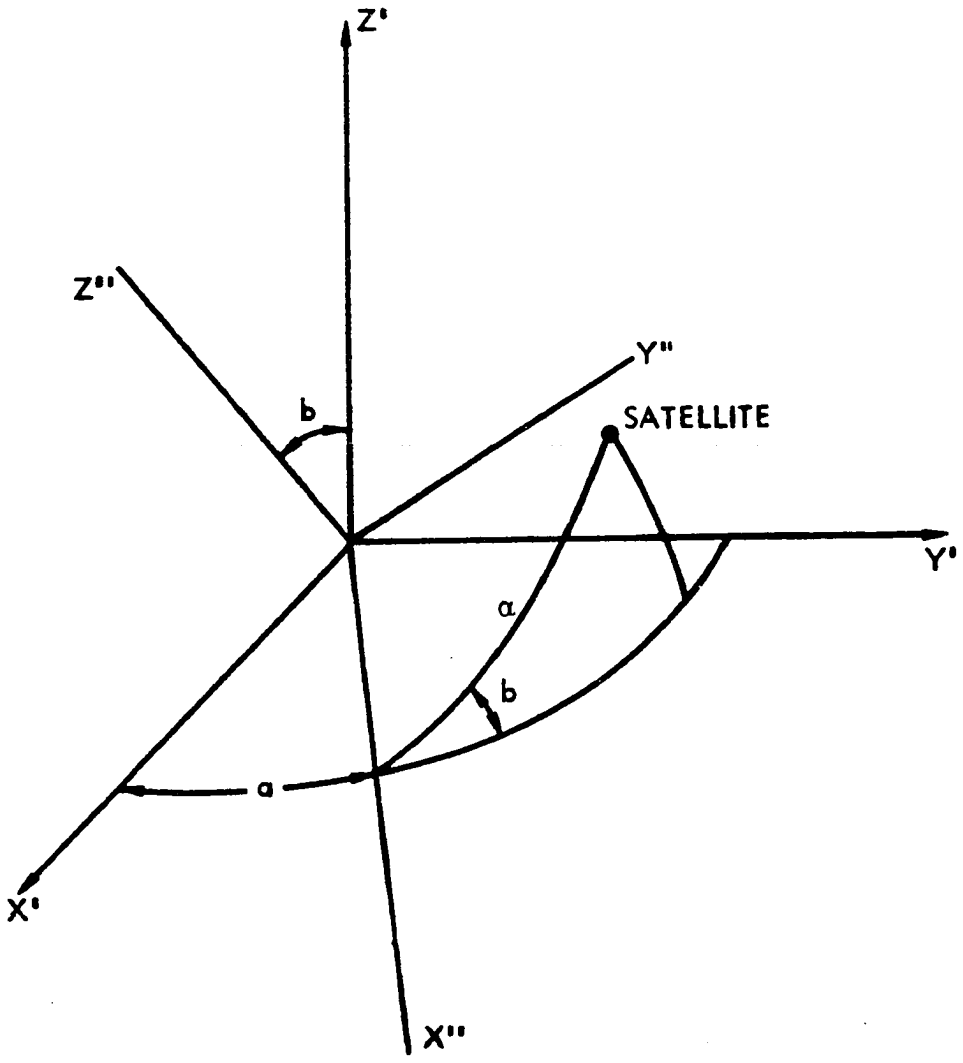

Figure 4.1. Satellite coordinates

t is time.

To transform these equations into the (X',Y',Z') inertially fixed coordinate system, the following transformation applies:

$$\begin{bmatrix} X_s' \\ Y_s' \\ Z_s' \end{bmatrix} = \begin{bmatrix} \cos a & -\sin a \cos b & \sin a \sin b \\ \sin a & \cos a \cos b & -\cos a \sin b \\ 0 & \sin b & \cos b \end{bmatrix} \begin{bmatrix} X_s'' \\ Y_s'' \\ Z_s'' \end{bmatrix} \quad . \quad (4.7)$$

This will accommodate satellites in polar, equatorial and inclined orbits.

For a satellite in a polar orbit, b = 90 degrees, and the transformation in Equation 4.7 simplifies to

$$\begin{bmatrix} X_s' \\ Y_s' \\ Z_s' \end{bmatrix} = \begin{bmatrix} \cos a & 0 & \sin a \\ \sin a & 0 & -\cos a \\ 0 & 1 & 0 \end{bmatrix} \begin{bmatrix} X_s'' \\ Y_s'' \\ Z_s'' \end{bmatrix} \quad . \quad (4.8)$$

For a satellite in an equatorial orbit, b = 0 degrees, and the transformation in Equation 4.7 simplifies to

$$\begin{bmatrix} X_s' \\ Y_s' \\ Z_s' \end{bmatrix} = \begin{bmatrix} \cos a & -\sin a & 0 \\ \sin a & \cos a & 0 \\ 0 & 0 & 1 \end{bmatrix} \begin{bmatrix} X_s'' \\ Y_s'' \\ Z_s'' \end{bmatrix} \quad . \quad (4.9)$$

The measurement equation derived in the previous chapter requires that the position of the satellites be given in the earth-fixed (X,Y,Z) coordinates. To reduce the description of motion given by Equation 4.7 in inertial space to one of position relative to the earth-fixed coordinates requires the following transformation:

$$\begin{bmatrix} X_s \\ Y_s \\ Z_s \end{bmatrix} = \begin{bmatrix} \cos \Omega t & \sin \Omega t & 0 \\ -\sin \Omega t & \cos \Omega t & 0 \\ 0 & 0 & 1 \end{bmatrix} \begin{bmatrix} X_s' \\ Y_s' \\ Z_s' \end{bmatrix} \tag{4.10}$$

where

Ω is the rotational rate of the earth and

t is the time since the X' axis and X axis were coincident.

In these studies it will be assumed that a number of satellites will be equally spaced in the same orbital ring. Mathematically, this simply means that in Equation 4.6 the initial displacement angle q is adjusted to give the proper phasing for each satellite in the ring. The assumption of a ring of satellites is not without some practical justification since such satellites could be placed in orbit by a single booster in a "piggy-back" fashion.

B. Vehicle Dynamics

The dynamics of the vehicle in which the inertial navigation system travels determines terms in the A matrix of Equation 3.1. For a simulated aircraft flight, these terms are related to the vehicle's velocity and direction. The simulation studies which follow will consider aircraft in flights due east and due south.

Consider first an aircraft which travels in level flight due south at a constant velocity V. Then in Equation 3.11,

$$\underline{\omega} = \begin{bmatrix} \Omega \cos \Theta \\ -V/R \\ \Omega \sin \Theta \end{bmatrix} \tag{4.11}$$

where the latitude is $\Theta = \Theta_o - (V/R)t$. Next consider that the aircraft travels in level flight due east at a constant velocity V. Then in Equation 3.11,

$$\underline{\omega} = \begin{bmatrix} \Omega \cos \Theta + V/R \\ 0 \\ \Omega \sin \Theta + (V/R)\tan \Theta \end{bmatrix} \tag{4.12}$$

where Θ is constant.

C. Simulation I

The first computer simulation was primarily designed to determine the effect of choosing satellites from orthogonal

orbital rings rather than more nearly parallel orbital rings for the "two-in-view" condition. Recall that in Chapter II, there is statistical evidence that there should be a better "balance" in the longitude and latitude channel errors with orthogonal rings.

For this part of the study, the aircraft was assumed to be traveling due east with a velocity of 100 knots starting from 80 degrees north latitude and 0 degrees longitude. At this high latitude, the slow speed was necessary so that the measurement geometry would not change appreciably during the flight. The position of the vehicle at any time t during the flight is then given by

$$\theta = (8/9)(\pi/2)$$

$$\lambda = (Vt/R)/\cos\theta \quad .$$

(Unless otherwise indicated, all latitudes and longitudes will be expressed in radians.) The altitude of the aircraft in all simulated flights is 4 nautical miles.

The satellite configuration was chosen to consist of six polar rings of seven satellites per ring at an altitude of 1000 nautical miles. For purposes of identification, let each ring be identified by a ring number and each satellite in a particular ring be identified by a satellite number. Then the position of the i^{th} satellite in the j^{th} ring is given by the following parameters which were defined in section A and illustrated in Figure 4.1,

$$q_{ij} = 2\pi(i-1)/7 + (-1)^j\pi/14$$

$$a_j = \pi(j-1)/6$$

$$b_j = \pi/2$$

where i = 1,2 ... 7, j = 1,2 ... 6.

Two computer runs were made for a flight of 1 hour duration. In the first flight (let this be referred to as flight I-a), satellite A was chosen from ring 1 and satellite B from ring 2. Two high elevation satellites were then always in view and their subtracks intersected at an angle of 30 degrees at the poles. The second flight (I-b) was identical to the first except that satellite B was chosen from ring 4 so the intersection of the subtracks of the two rings used was now 90 degrees.

The numerical values used for the variances and time constants of the Markov processes are listed in Table 4.1, and the initial variances of the error estimates are listed in Table 4.2. The gyros, accelerometers and count errors have large time constants and are essentially modeled as biases. The vertical velocity error has a short time constant associated with it and is essentially modeled as white noise so the vertical position error will be a random walk. The numerical values used for the accelerometer and gyro models are typical of a medium quality inertial system with an error growth of about one nautical mile per hour. The

Table 4.1. Variances and time constants of the Markov processes

variable	$[\text{variance}]^{1/2}(\sigma)$	time constant$(1/\beta)$
x gyro	0.01 deg./hr.	10.0 hr.
y gyro	0.01 deg./hr.	10.0 hr.
z gyro	0.01 deg./hr.	10.0 hr.
x accelerometer	10.0 $\overset{\frown}{\text{sec}}$.	10.0 hr.
y accelerometer	10.0 $\overset{\frown}{\text{sec}}$.	10.0 hr.
vertical velocity	0.50 ft./sec.	5.55 sec.
sat. A count	1000 counts	10^8 sec.
sat. B count	1000 counts	10^8 sec.

measurement noise in the filter was set at 10 counts RMS for each satellite Doppler-count measurement.

The resulting plots of longitude, latitude and radial RMS errors are shown in Figures 4.2 and 4.3. From these plots, it is apparent that there is considerable advantage in viewing two satellites from two orthogonal or nearly orthogonal satellite rings. The last 28 minutes of the flight appears to represent a "quasi steady-state" condition in which the transients due to the initial uncertainty are small. The time averages of the RMS level position errors over this last 28 minute time interval are listed in Table 4.3.

Table 4.2. Initial RMS value of error estimates

variable	RMS value	
ψ_x	14.1	$\widehat{\text{sec}}$.
ψ_y	14.1	$\widehat{\text{sec}}$.
ψ_z	3.0	$\widehat{\text{min}}$.
y (longitude) position	1000.0	ft.
y velocity	4.0	ft./sec.
x (latitude) position	1000.0	ft.
x velocity	4.0	ft./sec.
vertical position	200.0	ft.
x gyro	0.01	deg./hr.
y gyro	0.01	deg./hr.
z gyro	0.01	deg./hr.
x accelerometer	10.0	$\widehat{\text{sec}}$.
y accelerometer	10.0	$\widehat{\text{sec}}$.
vertical velocity	0.50	ft./sec.
satellite A count	1000.0	counts
satellite B count	1000.0	counts

Table 4.3. Average RMS level position errors

Flight	Average latitude error RMS (n.m.)	Average longitude error RMS (n.m.)	Average radial error RMS (n.m.)
I-a	0.037	0.100	0.107
I-b	0.045	0.048	0.067

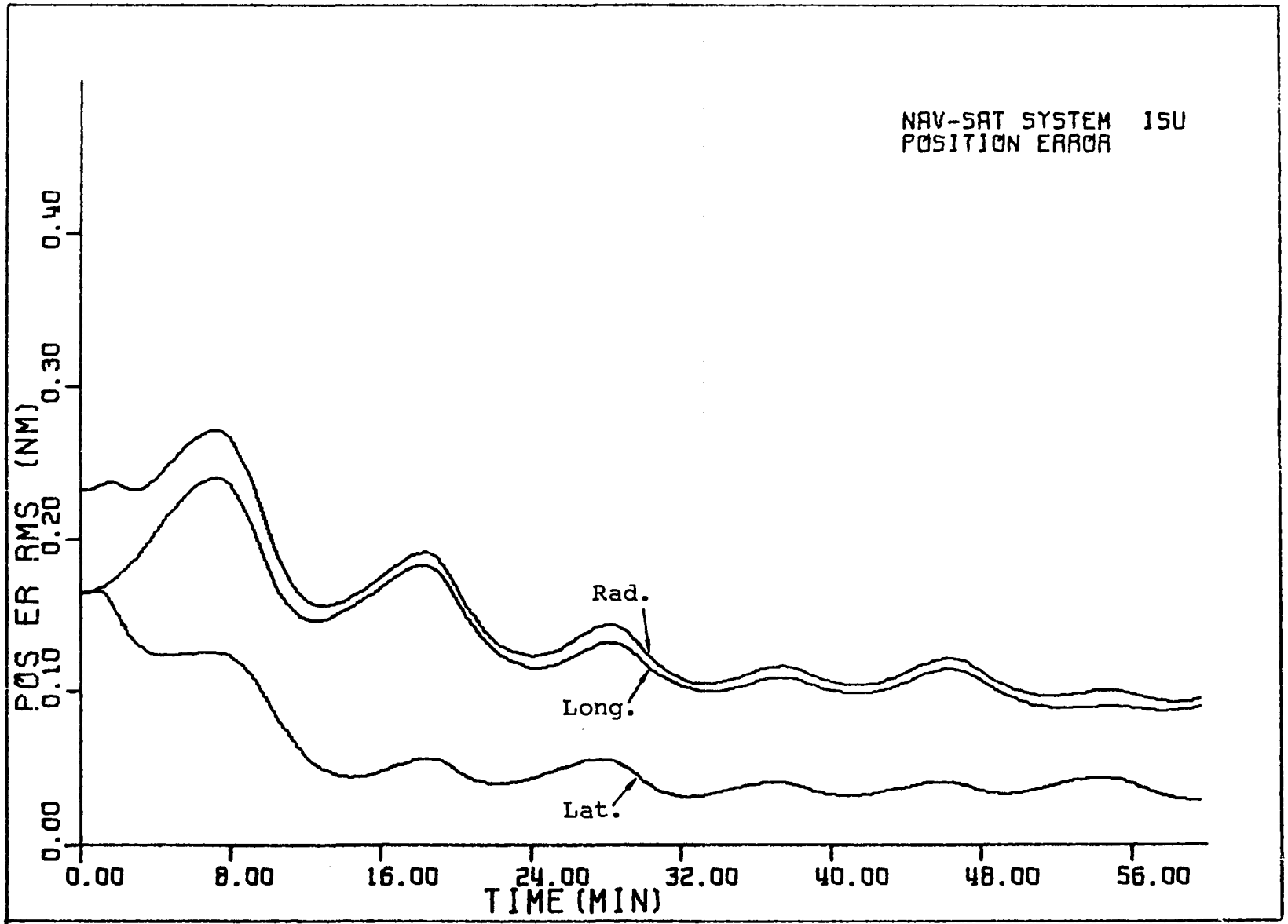

Figure 4.2. Position error for flight I-a (30 degree ring separation)

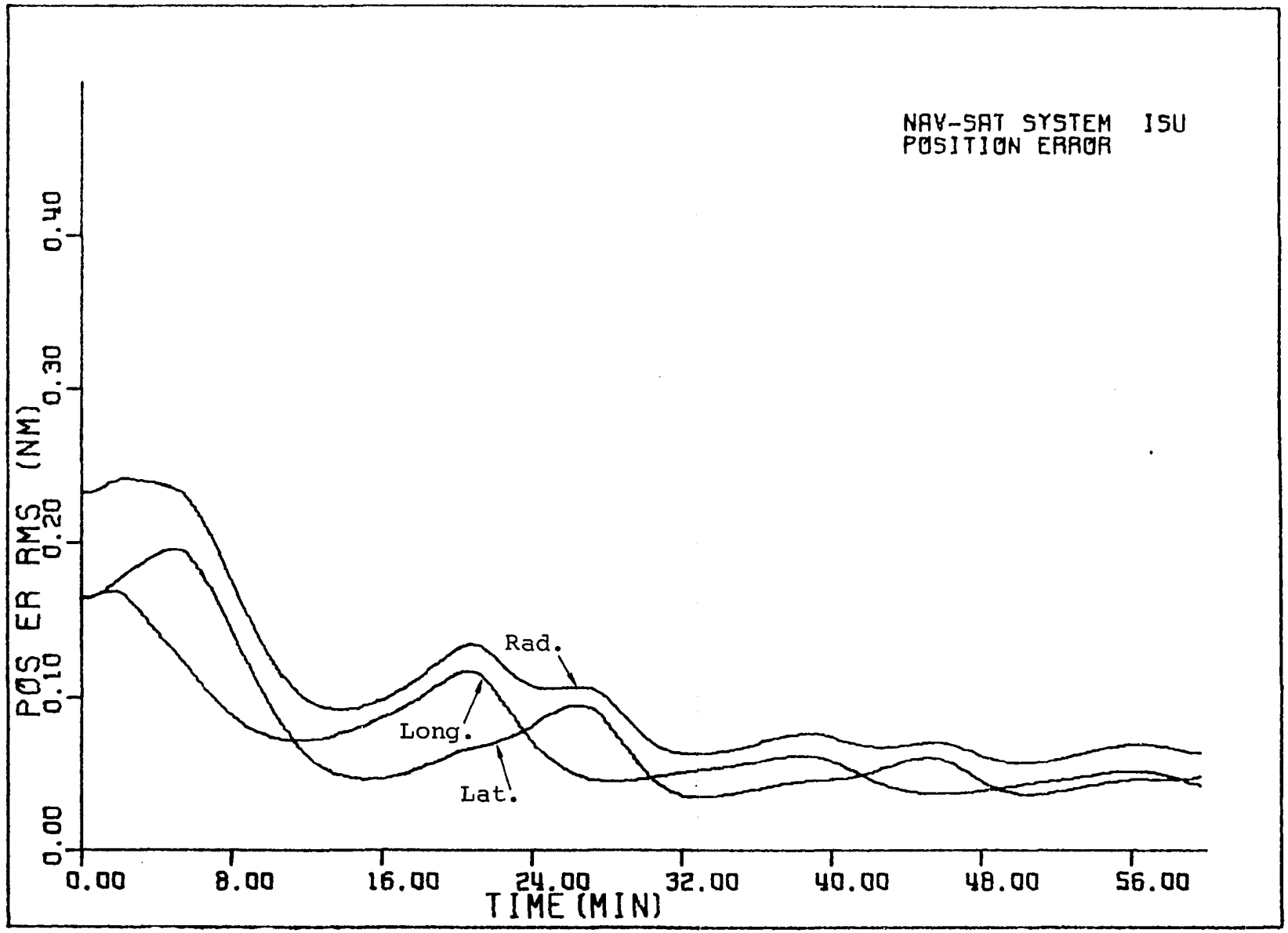

Figure 4.3. Position errors for flight I-b (90 degree ring separation)

In flight I-a, the longitude errors are on the order of 2 to 3 times as large as latitude errors whereas the errors are more nearly equal or "balanced" in I-b. This is in basic agreement with the results in Chapter II. The radial error for I-b is about 63 percent of that of I-a as a result of the better coupling of the measurements into the longitude channel. This result is also in basic agreement with the results in Chapter II.

D. Simulation II

A large number of computer simulation runs were made to investigate various aspects of continuous dual satellite coverage for a longer aircraft flight which covers a larger region of the earth's surface.

The aircraft was assumed to begin its flight at 0 degrees longitude, 45 degrees north latitude and headed due south at a velocity of 500 knots. Five hours into the flight, the aircraft turned due east and maintained the same altitude and velocity for 2 1/2 hours so the entire flight was 7 1/2 hours long and covered a region from the mid-latitudes to the equator. During the last 2 1/2 hours, the aircraft was at about 3.3 degrees north latitude or nearly on the equator. The position of the vehicle for the first 5 hours of the flight is then

$$\theta = \pi/4 - Vt/R$$

$$\lambda = 0.$$

and for the last 2 1/2 hours is

$$\theta = \pi/4 - V(18000)/R \simeq 3.3 \text{ deg.}$$

$$\lambda = V(t - 18000)(\cos\theta)/R$$

where t is in seconds.

Three different satellite configurations were used in this study. All these satellite configurations have at least two satellites available to the aircraft on a continuous basis. The following sections describe these configurations and present some of the results of the computer simulated flights.

1. Satellite configuration A (low-altitude rings)

The satellites were placed at an altitude of 1000 nautical miles in five polar rings and one equatorial ring with seven satellites per ring giving a total of 42 satellites. The position of the i^{th} satellite in the j^{th} ring is then given by

$$q_{ij} = 2\pi(i-1)/7 + (-1)^j\pi/10$$

$$a_j = \pi(j-1)/6$$

$$b_j = \pi/2$$

where $i = 1,2,\ldots,7$ and $j = 1,2,\ldots,5$ and

$$q_{ij} = 2\pi(i-1)/7$$

$$a_j = 0$$

$$b_j = 0$$

where i = 1,2,...,7 and j = 6.

Four simulated flights were processed for this satellite configuration. The first three used measurements from two satellites and were identical except for the quality of the inertial system gyros. Gyro drift rates of 0.005, 0.01 and 0.02 degrees per hour were used and the variances of the initial gyro drift rate estimates were correspondingly changed in the initial covariance matrix. The initial variance of ψ_z was also changed since it is directly proportional to the east-west gyro error in the alignment. Other than the changes noted above, all other parameters in the filter were identical to those given in Tables 4.1 and 4.2. Let these three flights with the 0.005, 0.01 and 0.02 degree per hour gyros be designated as flights A-1, A-2 and A-3 respectively. The fourth flight of the series, A-4, was identical to A-1 except only one satellite measurement is used.

The RMS level position errors are plotted in Figures 4.4, 4.5, 4.6 and 4.7. These plots show a number of interesting results.

(a) For A-1, A-2 and A-3, the first two hours of the flight used measurements from two satellites in

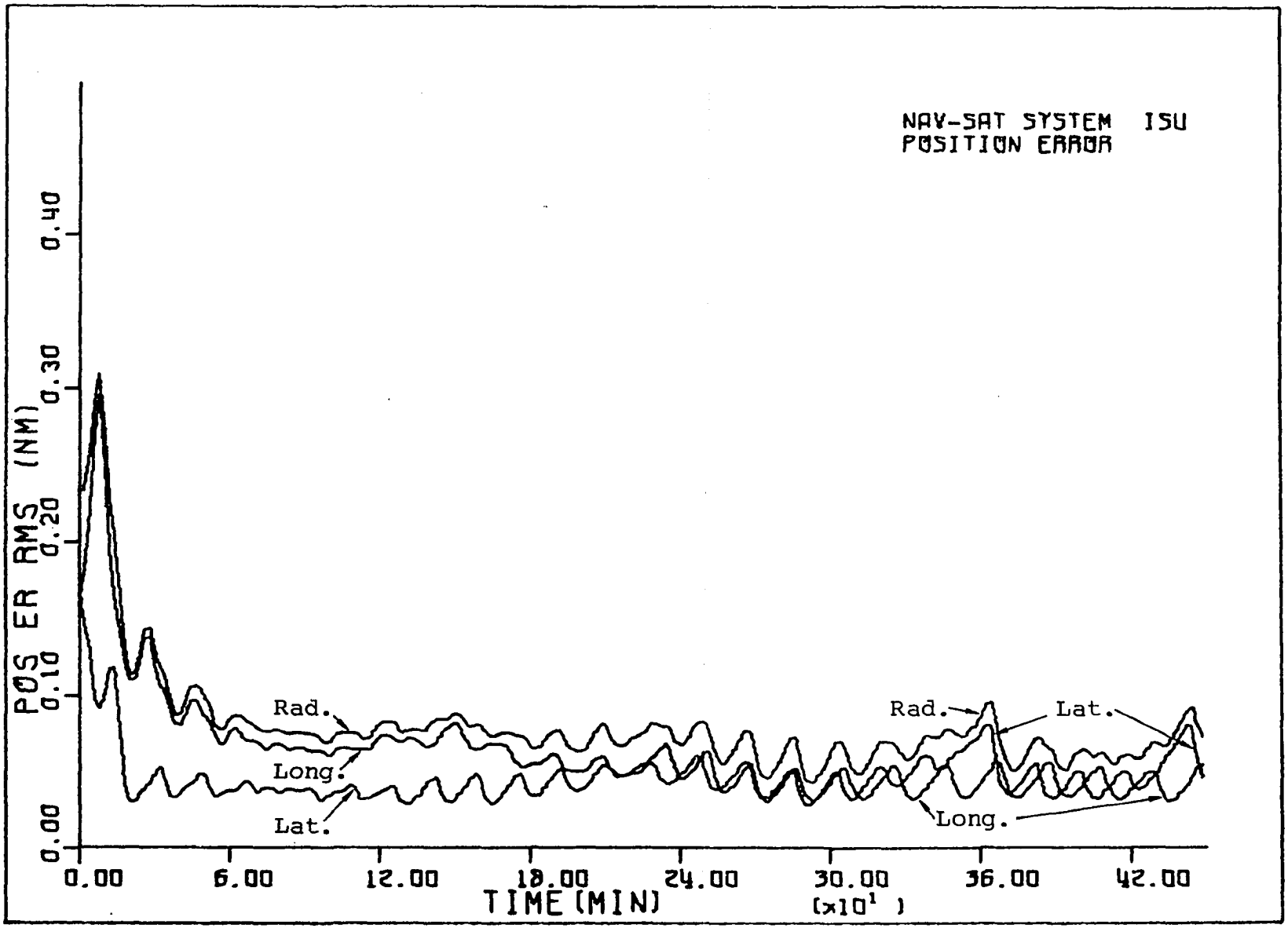

Figure 4.4. Position errors for flight A-1 (0.005 deg./hr. gyros)

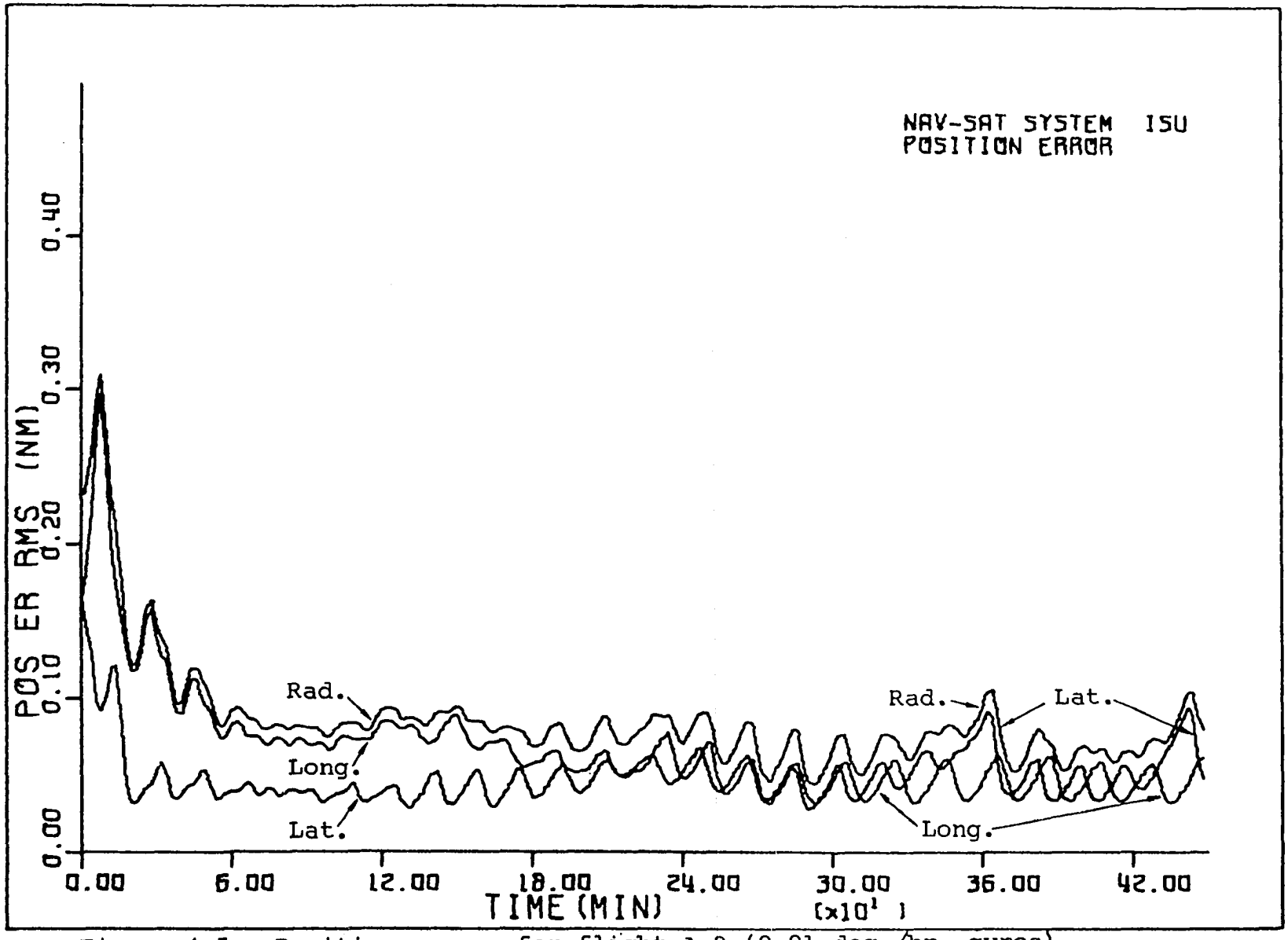

Figure 4.5. Position errors for flight A-2 (0.01 deg./hr. gyros)

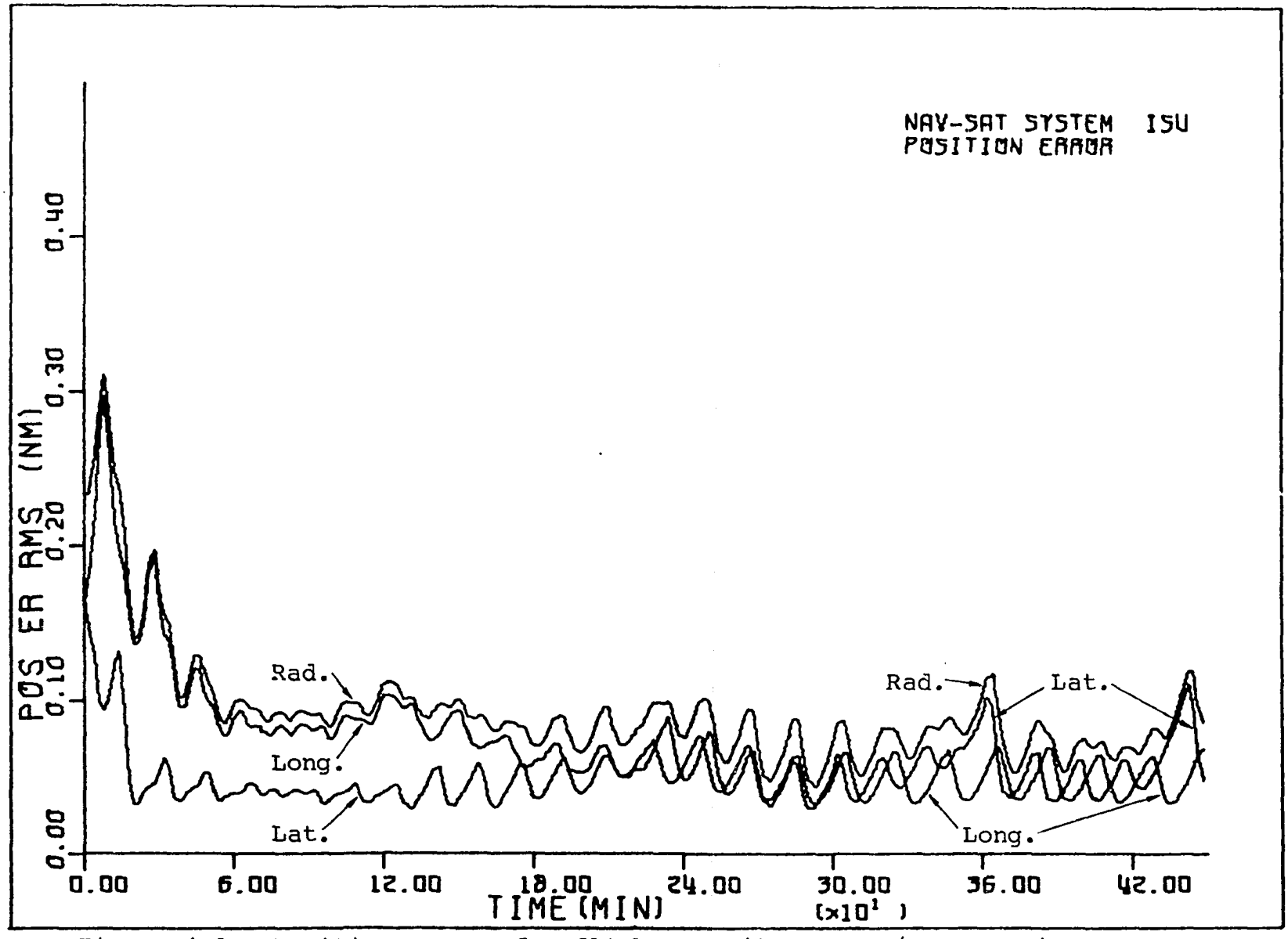

Figure 4.6. Position errors for flight A-3 (0.02 deg./hr. gyros)

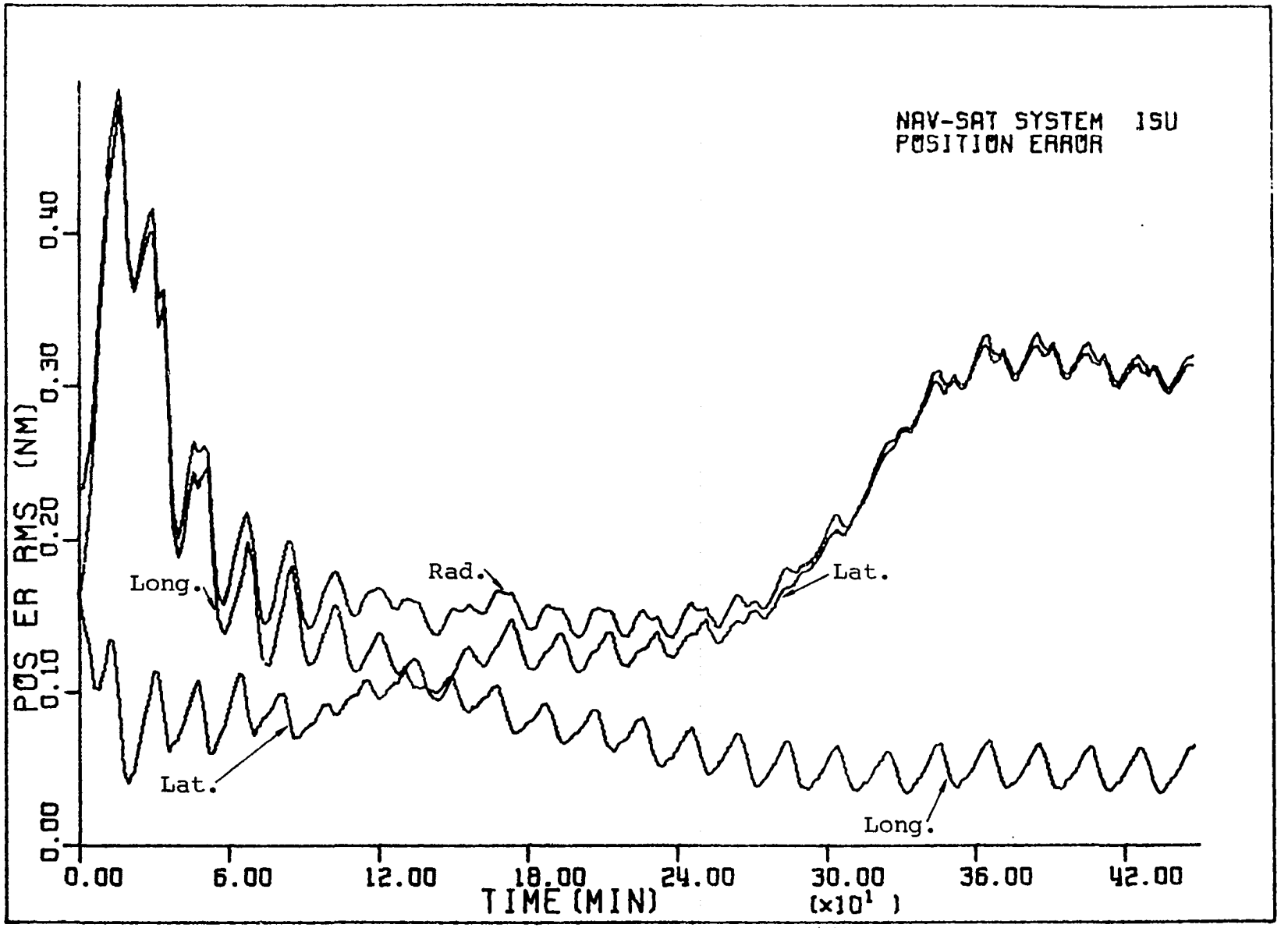

Figure 4.7. Position errors for flight A-4 (0.005 deg./hr. gyros using one satellite)

adjacent polar rings to update the error estimates. In this time interval, large longitude errors are noted. The remaining portion of the flight used measurements from a polar satellite and an equatorial satellite resulting in a better "balance" between the two channel errors. It is noted that about 360 minutes and 440 minutes into the flight, latitude error is higher. This is due to the fact that the aircraft is about midway between two polar rings and the elevation angle to a satellite in these rings is lower than usual. The polar satellites are providing nearly all of the latitude error information to the filter during the last 2 1/2 hours of the flight.

(b) The plot for the "one-in-view" condition of A-4 shows an exchange of the "imbalance" between channels as the switch from a polar to an equatorial satellite is made about 120 minutes into the flight. From 300 minutes until the end of the flight, the aircraft was nearly directly under the equatorial ring and the latitude error increases dramatically. Again, this points out the problem that arises due to the lack of coupling of the measurement into the cross-track channel for high elevation satellites. This run clearly demonstrates the advantage

of viewing two satellites simultaneously, in contrast to viewing only one.

(c) The increase in gyro drift rates results in a modest increase in position errors, but the overall pattern of these errors is similar since there was no change in the measurement geometry.

2. Satellite configuration B (medium-altitude rings)

The satellites were assumed to be placed at an altitude of 1456 nautical miles in five polar rings and one equatorial ring with five satellites per ring giving a total of 30 satellites.[1] The position of the i^{th} satellite in the j^{th} ring is then given by

$$q_{ij} = 2\pi(i-1)/5 + (-1)^j\pi/10$$

$$a_j = \pi(j-1)/5$$

$$b_j = \pi/2$$

where i = 1,2,...,5 and j = 1,2,...,5 and

$$q_{ij} = 2\pi(i-1)/5$$

$$a_j = 0$$

$$b_j = 0$$

---

[1]This configuration was suggested for study by representatives of The Johns Hopkins University Applied Physics Laboratory.

where i = 1,2,...,5 and j = 6.

Five simulated flights were processed for this satellite configuration. Flights B-1, B-2 and B-3 were identical to A-1, A-2 and A-3 except for the changed satellite geometry. The resulting level position errors are plotted in Figures 4.8, 4.9 and 4.10 and resemble the results of the A series except the level of errors is greater due to the increased satellite altitudes.

Flight B-4 employed only one satellite measurement from a polar ring throughout the entire flight and the level position are plotted in Figure 4.11. In contrast to flight A-4, longitude errors are the cross-track errors during the entire flight and dominate the level position errors. During the equatorial portion of the flight (last 2 1/2 hours), an oscillatory nature in the errors is noted as the aircraft passes under the polar rings and the measurements from the nearly overhead satellite provide little information on longitude. Again, this demonstrates the advantage of viewing two satellites.

The fifth flight, B-5, of this series was identical to B-2 except the measurement noise in the filter model was reduced from 10 counts RMS to 3 counts RMS. This was done to test the mean square sensitivity of the filter to measurement noise. A significant reduction in the level position errors was noted as evidenced by the plot in Figure 4.12.

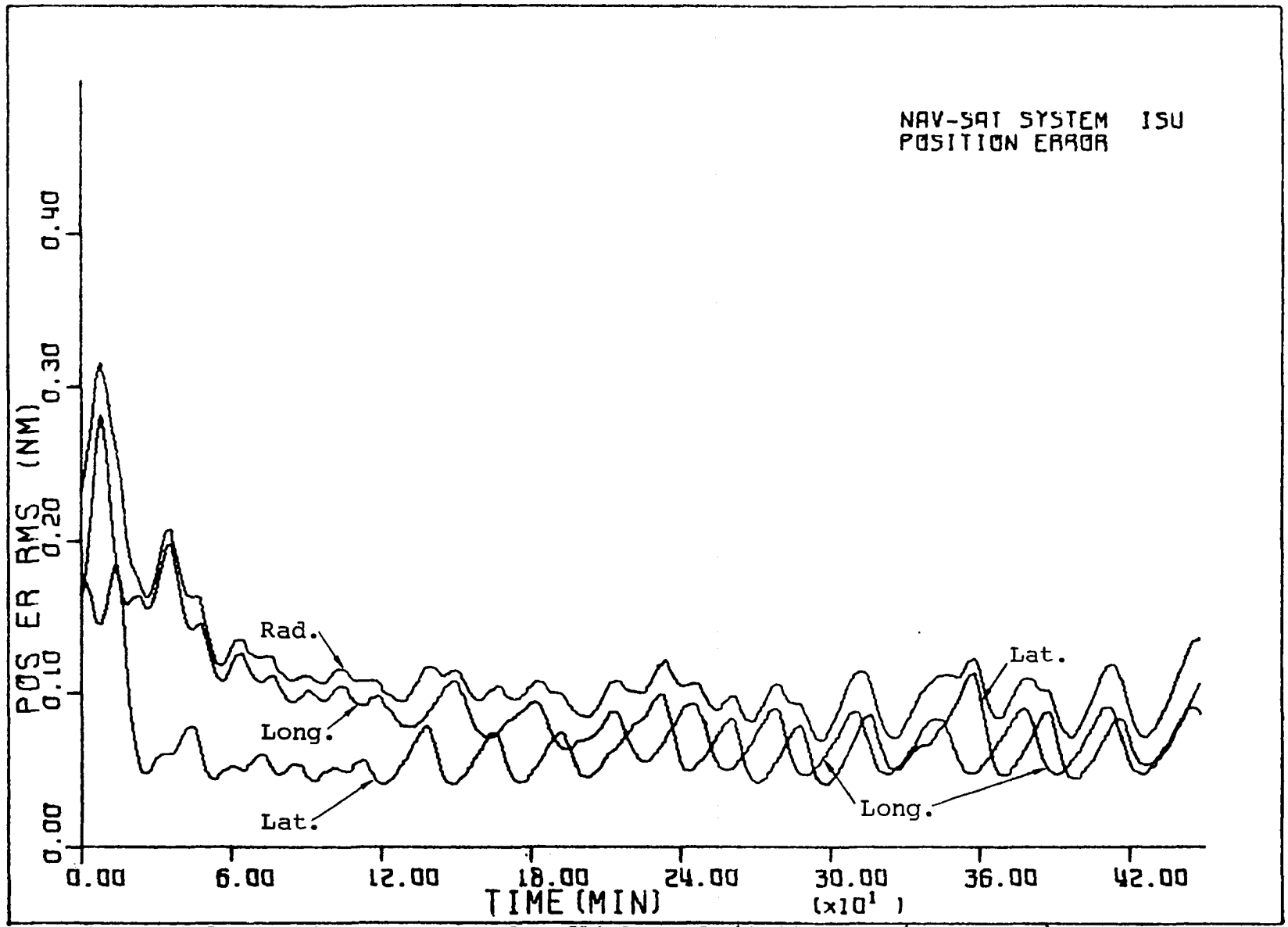

Figure 4.8. Position errors for flight B-1 (0.005 deg./hr. gyros)

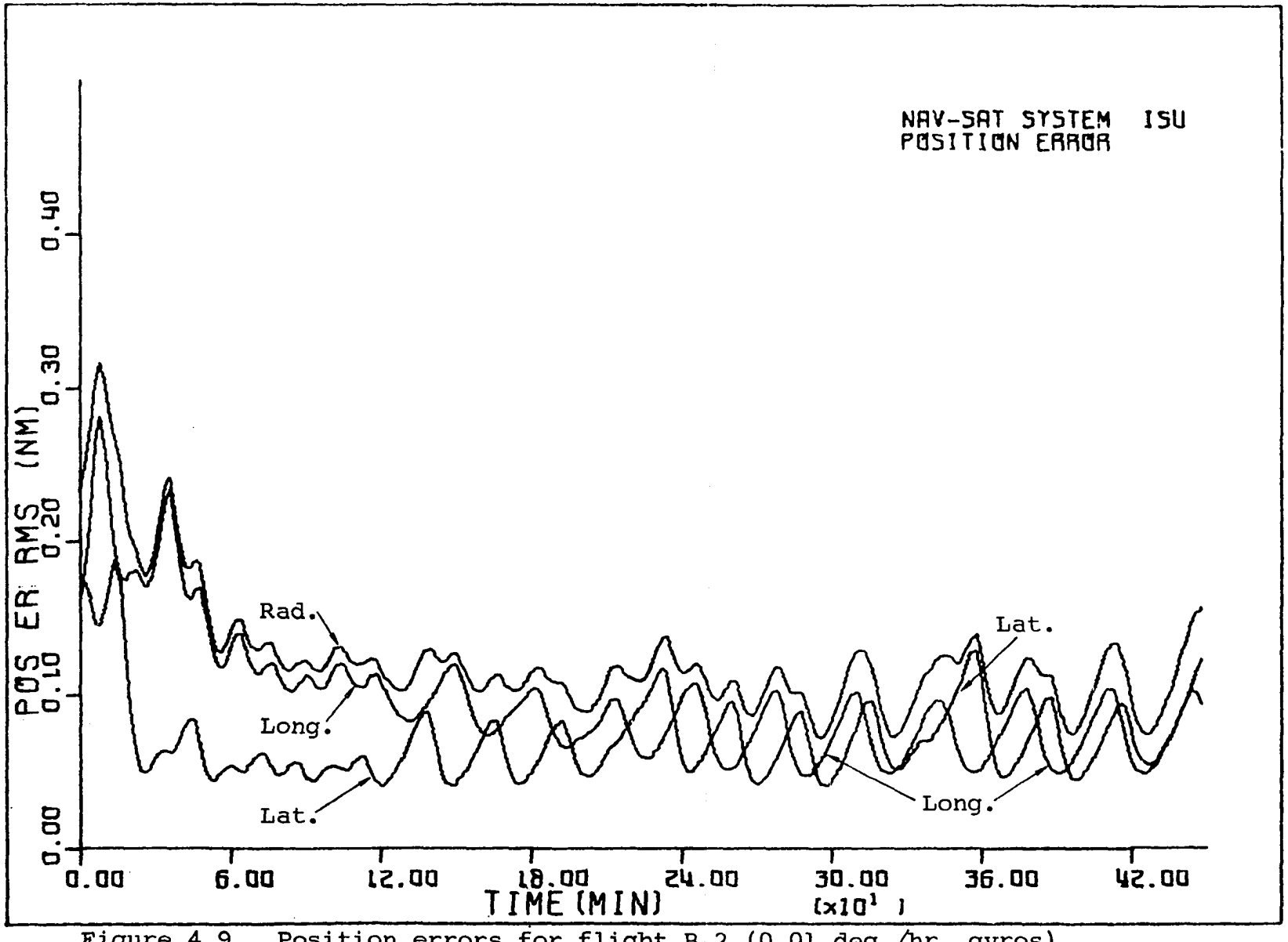

Figure 4.9. Position errors for flight B-2 (0.01 deg./hr. gyros)

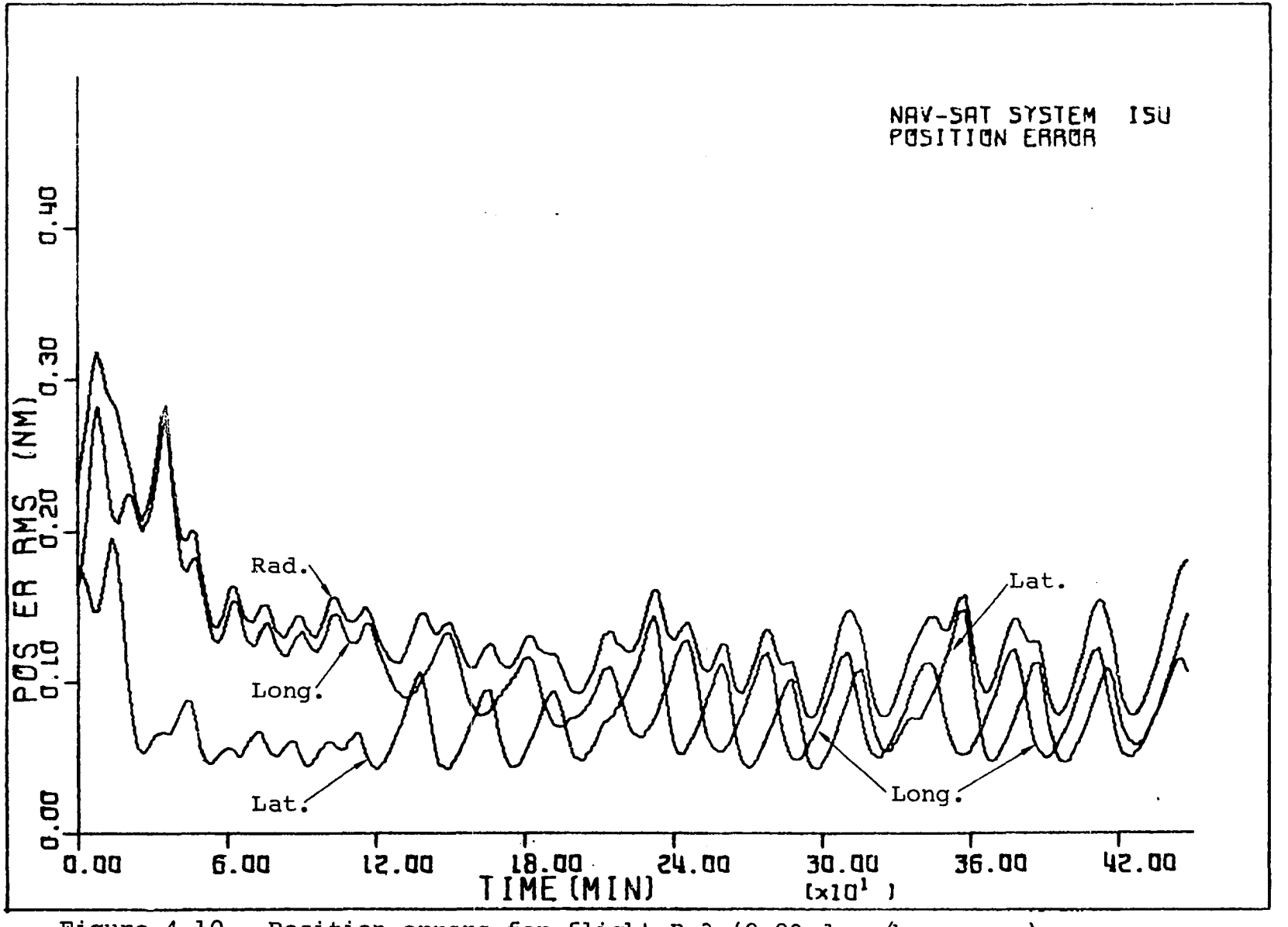

Figure 4.10. Position errors for flight B-3 (0.02 deg./hr. gyros)

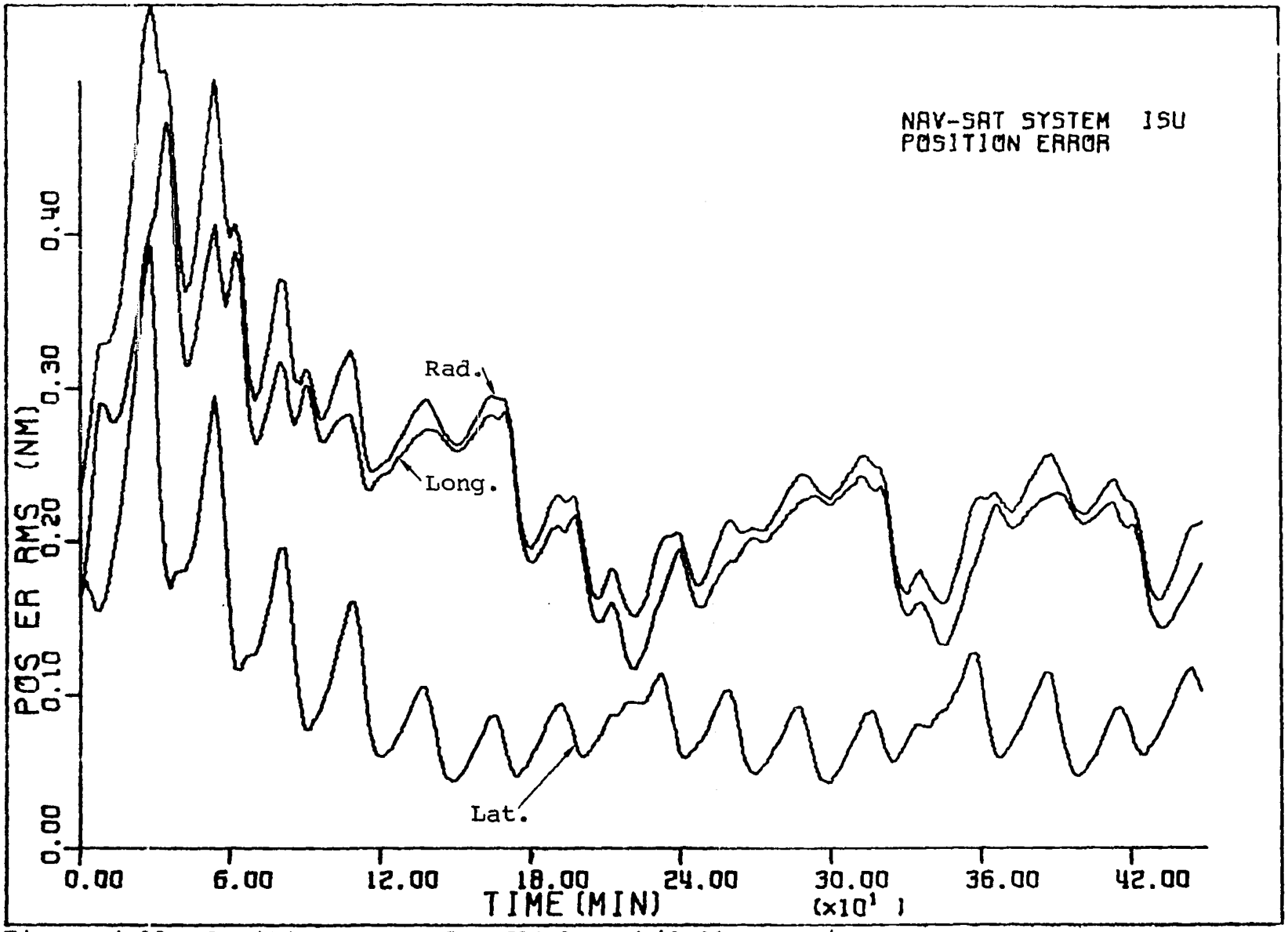

Figure 4.11. Position errors for flight B-4 (0.005 deg./hr. gyros using one satellite)

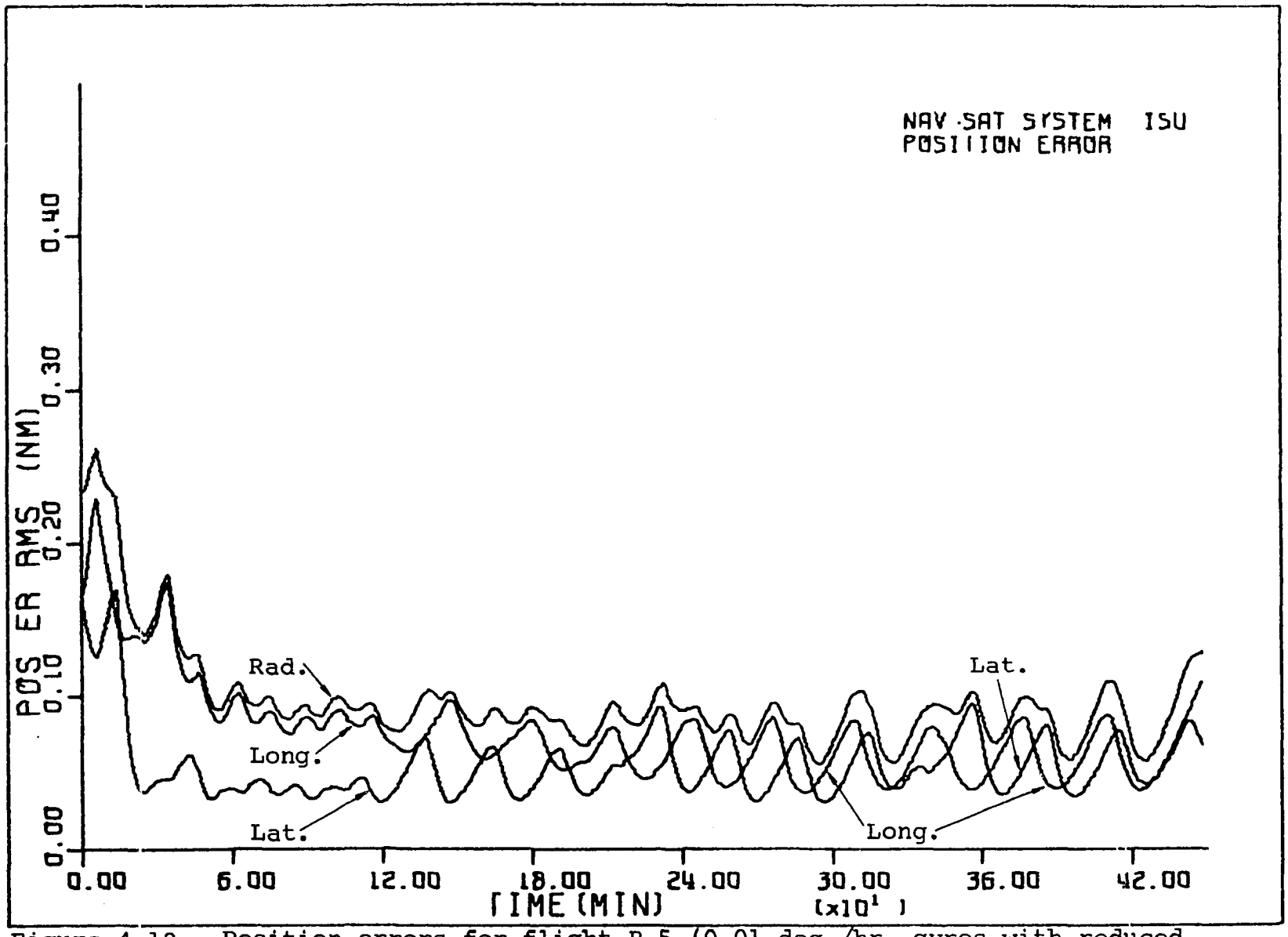

Figure 4.12. Position errors for flight B-5 (0.01 deg./hr. gyros with reduced measurement noise)

Although the results show considerable improvement in the filter's performance with this reduced measurement noise, the value of 3 counts RMS is unrealistically low for the measurement noise in this model. If one wished to expand the model, the orbital parameter errors of the satellites could be included as additional state variables; however, these errors were compensated for, at least to a degree, by increasing the uncorrelated measurement noise in this model. The results of this study suggest that an expanded model with the orbital errors appropriately modeled is worthy of additional investigation.

3. Satellite configuration C (high-altitude rings)

In this series of flights the satellites were placed in four high-altitude inclined rings. The altitude was 2243 nautical miles and the rings are inclined at 54.8 degrees (0.956 radians) with the equatorial plane and symmetrically spaced around the earth.[1] There are five satellites per ring and the position of the i^{th} satellite in the j^{th} ring is given by

---

[1]This configuration was suggested by Dr. R. G. Brown. The inclination angle is chosen such that the "worst case" satellite coverage occurs at points located at the poles and on the equator. At each of these points, the distance to the nearest satellite subtrack is the same.

$$q_{ij} = 2\pi(i-1)/5$$

$$a_j = \pi(j-1)/4$$

$$b_j = 0.956$$

where $i = 1,2,\ldots,5$ and $j = 1,2,3,4$.

This configuration of satellites has the attractive property that ring intersections are more widely distributed over the earth's surface than in the case with polar and equatorial rings. Polar rings for example all converge at the poles and give excellent coverage in that region. However, relatively few aircraft flights occur near the poles.

Although the use of inclined rings distributes satellite coverage more equitably, there is a fundamental problem involved which makes their use practically questionable. The earth's equatorial bulge will cause a precession of the inclined orbits about the earth's polar axis. The amount of precession increases with decreasing altitude and decreasing inclination angle. This is the reason that a higher altitude was chosen for this configuration. The precession rate of the satellites rings in configuration C is about 1.58 degrees per day (10). If all the rings precess at the same rate there would be few problems but this would require precise orbital correction capabilities which may be impractical. If it were not for the precession problem, a combination of

polar and inclined rings would also be very attractive. More information on the precession of inclined orbital satellites is available in Macko (10).

Three flights, C-1, C-2 and C-3, were identical to A-1, A-2 and A-3 except for the new satellite configuration. The plots of the level position errors in Figures 4.13, 4.14 and 4.15 show one outstanding difference from the A and B series. Satellite measurements from these inclined rings couple into the latitude and longitude channels about evenly during the early portion of the flight in contrast to the stronger coupling into the latitude channel in the A and B series.

The RMS errors in this series are considerably greater than when using the lower satellite configurations. This is understandable since the information contained in the Doppler profile of a satellite pass is distributed over a much longer time. The typical satellite pass requires about twice as long in configuration C as in configuration A. The measurement information is then being fed into the filter at a much slower rate, whereas the noise fed into the filter via the H matrix is coming in at the same rate. Thus, one would expect a degradation of performance.

One of the many trade-offs, other than accuracy, that would be involved in the selection of an actual satellite configuration would be the number of satellites which have to be maintained. For example, configuration C requires

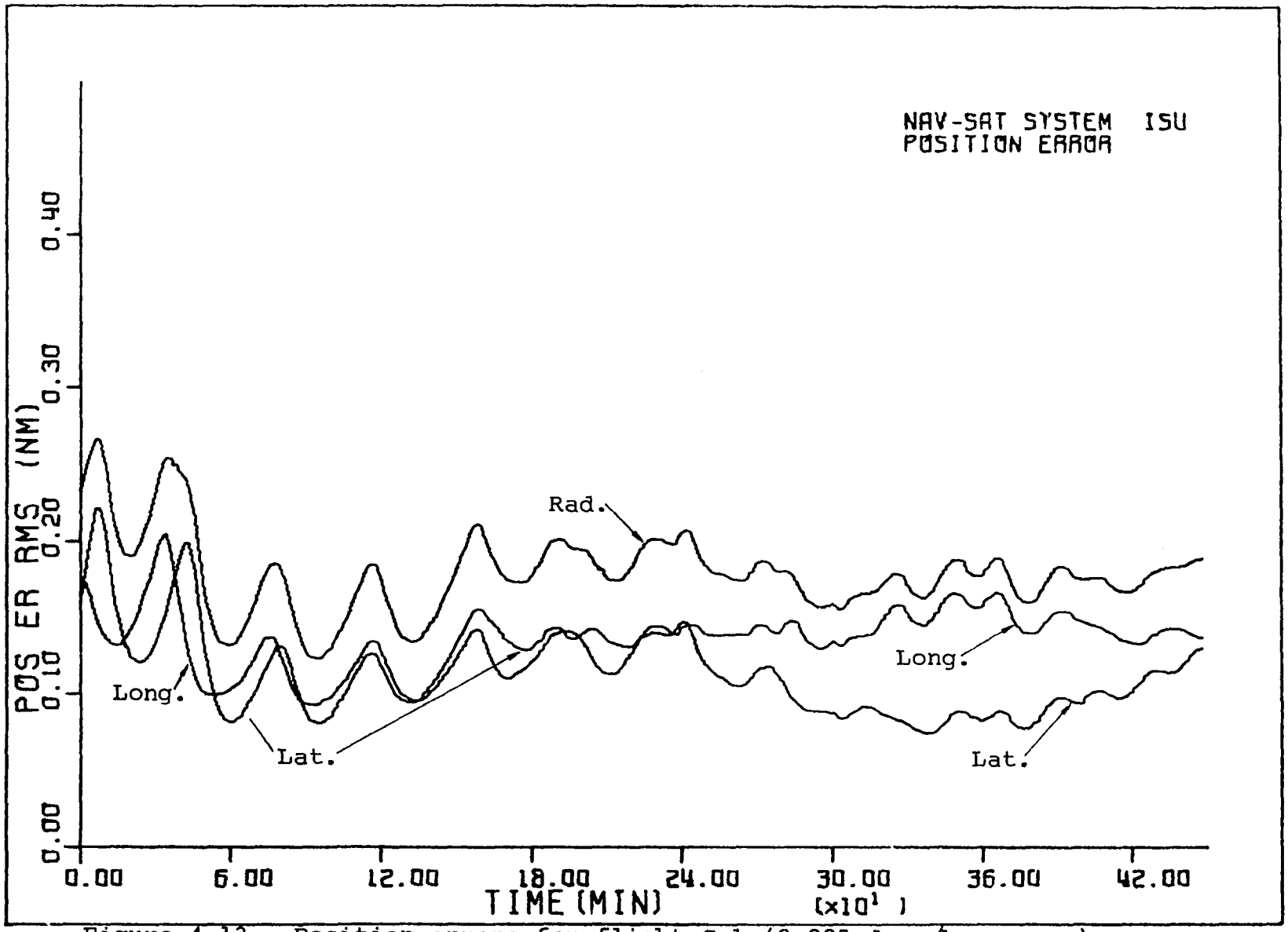

Figure 4.13. Position errors for flight C-1 (0.005 deg./hr. gyros)

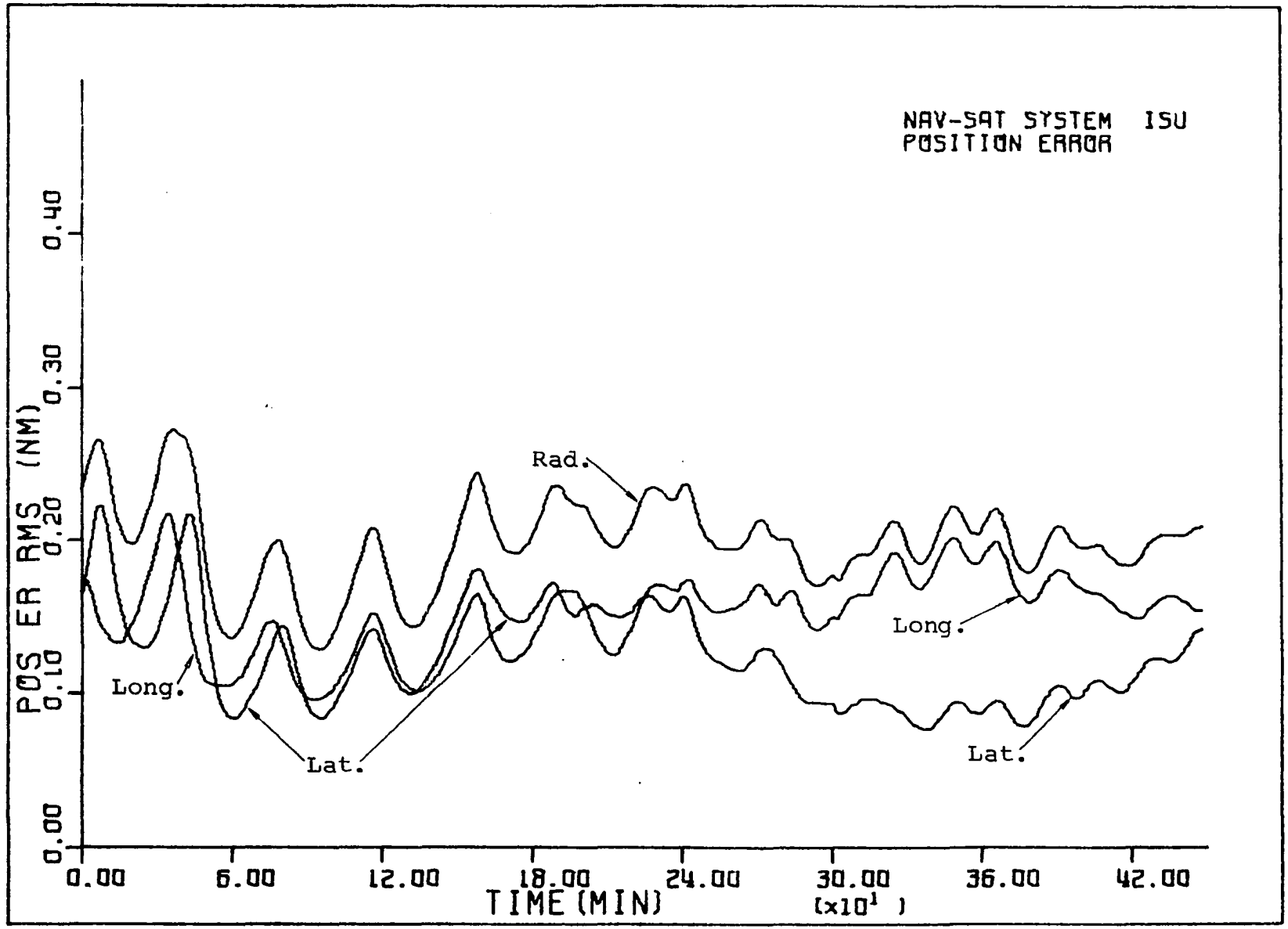

Figure 4.14. Position errors for flight C-2 (0.01 deg./hr. gyros)

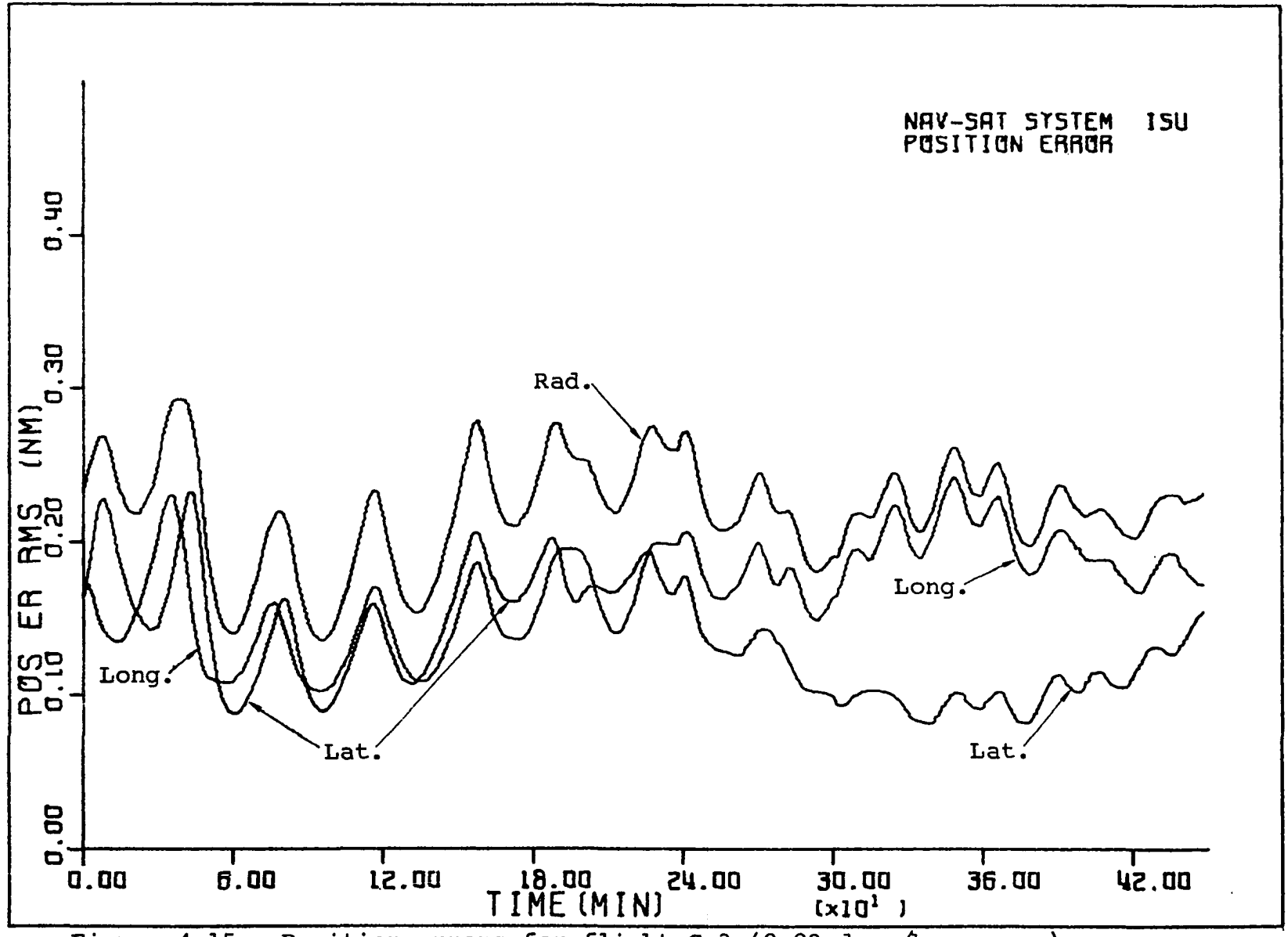

Figure 4.15. Position errors for flight C-3 (0.02 deg./hr. gyros)

only 20 whereas configuration A requires 42. This study does not attempt to investigate any of these other trade-offs.

E. Comparative Overall Results

The plots in the previous section give a good basis for comparing the fine structure performance of this integrated navigation system for the level position errors; however, these plots do not yield an overall measure of performance. It should be realized that the results of the simulation studies only constitute an ensemble of one in terms of starting times and flight trajectories. However, it is felt that the flights were of sufficiently long duration and covered a wide enough region of satellite coverage so that the results have meaning in terms of time averages.

A summary of the overall average performance is given in Table 4.4 in which the average errors for all the variables over the last 6 1/2 hours of the flight are tabulated. The first hour of flight was not included since it is somewhat of a transient period that depends on the initial conditions.

An informative plot is shown in Figure 4.16 which illustrates the increase in the radial position error as the altitude of the satellite rings increase. This is plotted for the three gyro qualities and the trade-off between

satellite altitude and gyro quality is clear from the plots.

The three inertial systems in the model could be considered to be of moderately good quality. It was decided to limit these studies to modest accuracy systems because one should also include the effects of satellite geodesy errors in the model if a very high quality inertial system is studied. The level errors for the "middle quality" pure inertial system used in this study are shown in Figure 4.17. This shows that with 0.01 degree/hour gyros, the system is about a 1 nautical mile per hour system in terms of radial error growth.

Since the level errors of the integrated system are several orders of magnitude less than the unaided inertial errors they could not be conveniently plotted together. However, the estimates of the vertical position error can conveniently be compared to those of the unaided inertial system. Recall that the vertical position error was modeled as approximately a random walk with an initial uncertainty of 200 feet RMS. Figure 4.18 shows the unaided inertial vertical error "walking off" in approximately a linear fashion.

Initially, the vertical position error is relatively small compared to some of the other errors in the system and the filter does not get an estimate of it until these larger errors have been reduced. The use of single satellite

measurements (flight B-4) and dual satellite measurements (flight B-1) bound the error. However, it can be seen in Figure 4.18 that it takes the single satellite system at least an hour longer than the two satellite system to begin to get an estimate of this error and bring it down to some steady-state value. Clearly, the two satellite system is significantly superior and does a respectable job in holding the RMS error under 130 feet after the first 1 1/2 hours of the flight.

Table 4.4. Average errors RMS of all state variables over last 6 1/2 hours of flight

Flight	Position in n.m. x 10^{1}				Velocity in knots			Gyro drift in deg./hr. x 10^{+2}		
	Rad.	Long.	Lat.	Vert.	Long.	Lat.	Vert.	x	y	z
A-1	0.704	0.522	0.452	0.195	0.221	0.201	0.296	0.263	0.382	0.407
A-2	0.755	0.562	0.480	0.196	0.260	0.233	0.296	0.468	0.723	0.783
A-3	0.822	0.616	0.513	0.198	0.325	0.285	0.296	0.865	1.346	1.525
A-4	2.344	2.165	0.854	0.325	0.495	0.316	0.296	0.310	0.394	0.421
B-1	1.016	0.773	0.628	0.250	0.256	0.233	0.295	0.271	0.382	0.411
B-2	1.111	0.847	0.680	0.247	0.306	0.277	0.296	0.481	0.723	0.789
B-3	1.235	0.943	0.743	0.253	0.387	0.344	0.296	0.882	1.346	1.540
B-4	2.125	0.769	1.879	0.423	0.309	0.405	0.296	0.279	0.394	0.423
B-5	0.862	0.664	0.518	0.221	0.253	0.228	0.291	0.466	0.668	0.782
C-1	1.742	1.340	1.093	0.369	0.292	0.275	0.296	0.292	0.394	0.415
C-2	1.951	1.520	1.193	0.376	0.359	0.329	0.296	0.517	0.755	0.793
C-3	2.182	1.719	1.303	0.381	0.466	0.414	0.296	0.936	1.437	1.535

Table 4.4 (Continued)

Flight	Accelerometer bias in g's x 10^{+4}		Psi in $\overset{\frown}{\text{sec.}}$ x 10^{-2}			Oscillator bias in counts	
	x	y	x	y	z	sat. A	sat. B
A-1	0.444	0.449	0.102	0.099	0.518	4.6	5.0
A-2	0.447	0.451	0.107	0.104	0.956	4.8	5.1
A-3	0.448	0.455	0.116	0.111	1.770	5.0	5.3
A-4	0.448	0.451	0.148	0.108	0.555	5.8	---
B-1	0.445	0.449	0.107	0.102	0.524	4.7	4.6
B-2	0.448	0.452	0.113	0.108	0.959	4.9	4.8
B-3	0.450	0.455	0.126	0.119	1.770	5.2	5.1
B-4	0.446	0.452	0.108	0.142	0.563	5.9	---
B-5	0.447	0.451	0.108	0.104	0.889	3.7	3.7
C-1	0.448	0.449	0.123	0.115	0.542	5.5	5.2
C-2	0.451	0.451	0.135	0.124	1.001	5.9	5.6
C-3	0.454	0.453	0.152	0.137	1.879	6.4	6.0

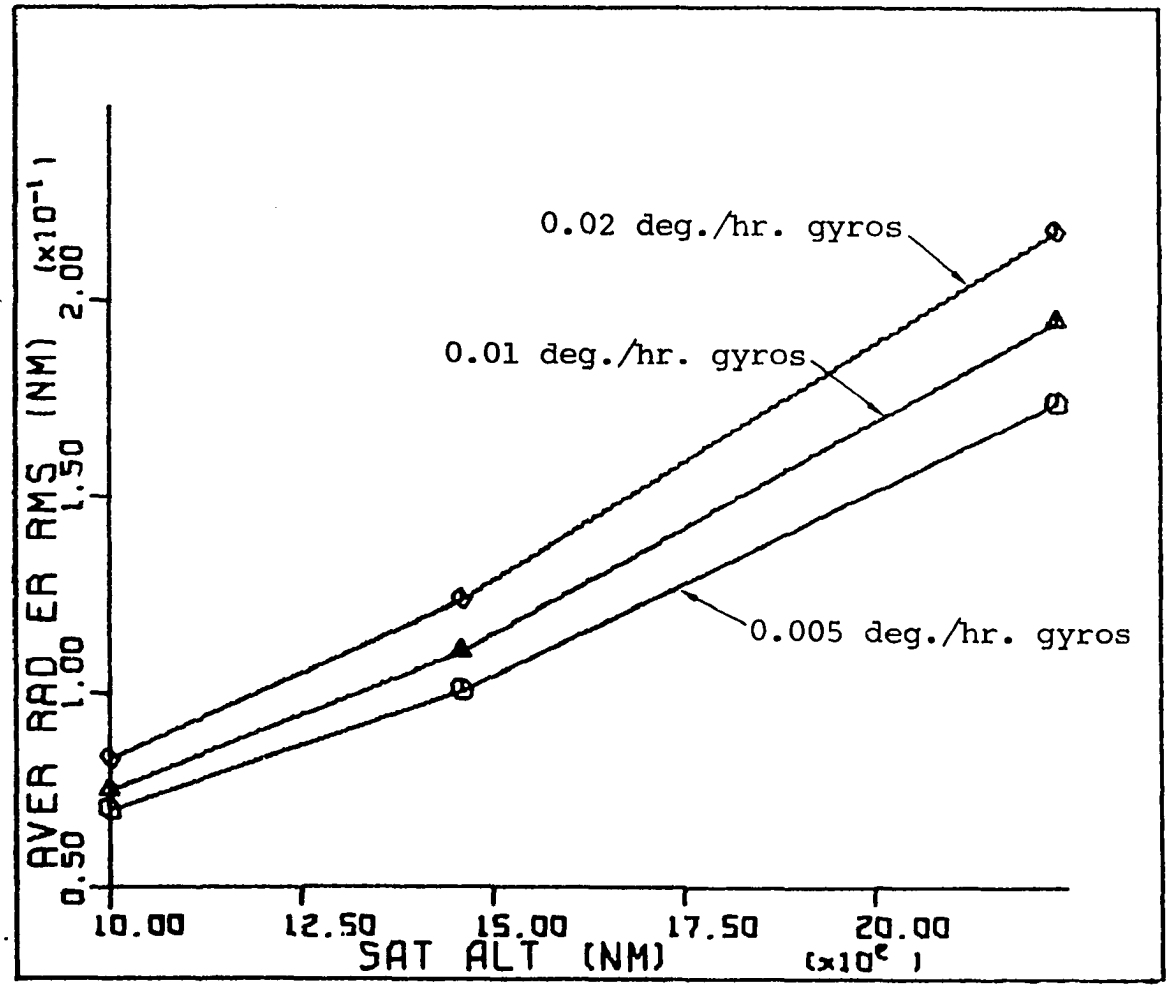

Figure 4.16. Average radial error for satellite configurations for three different satellite altitudes (linear interpolation)

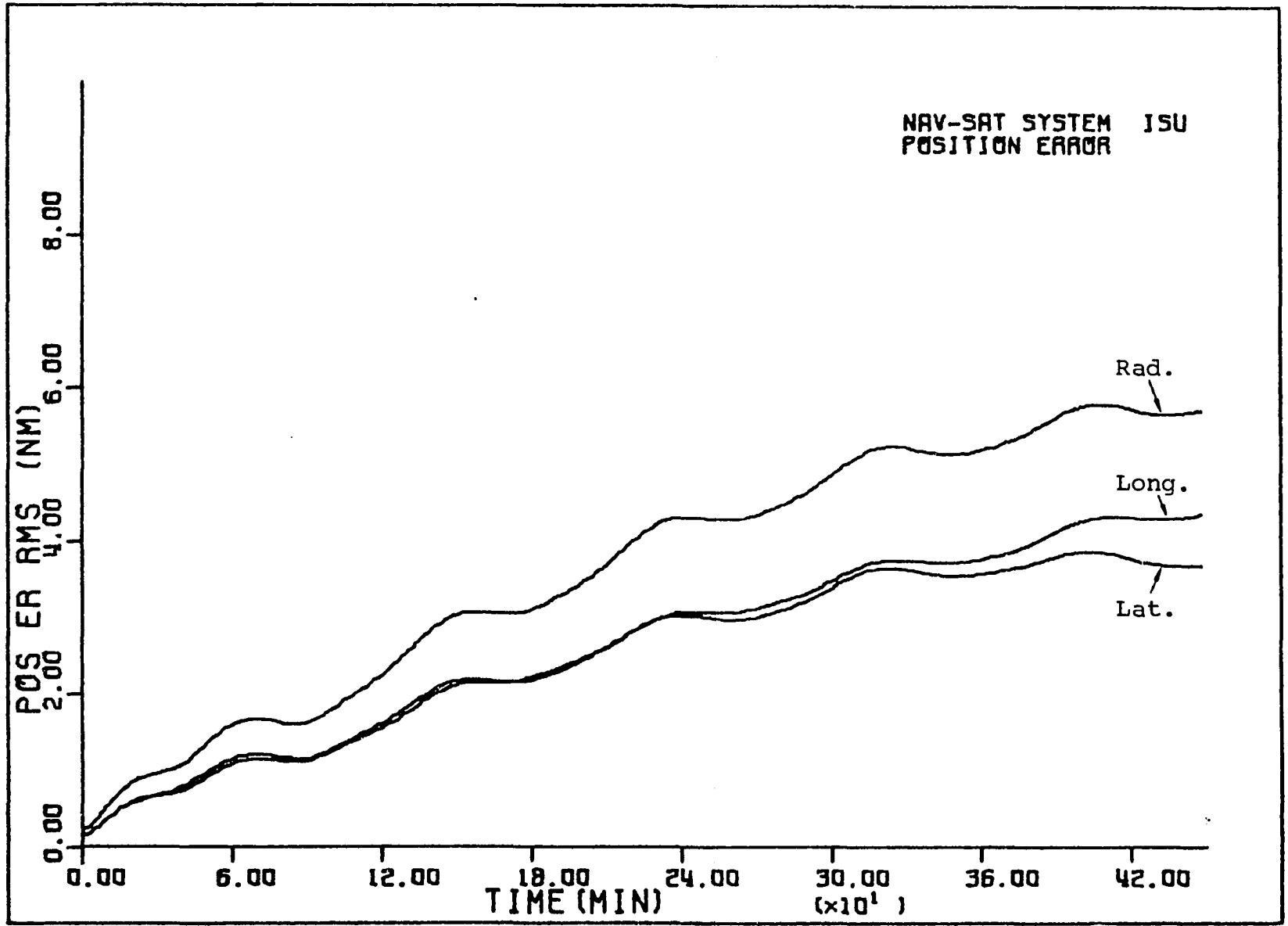

Figure 4.17. Position errors for unaided inertial navigation system (0.01 deg./hr. gyros)

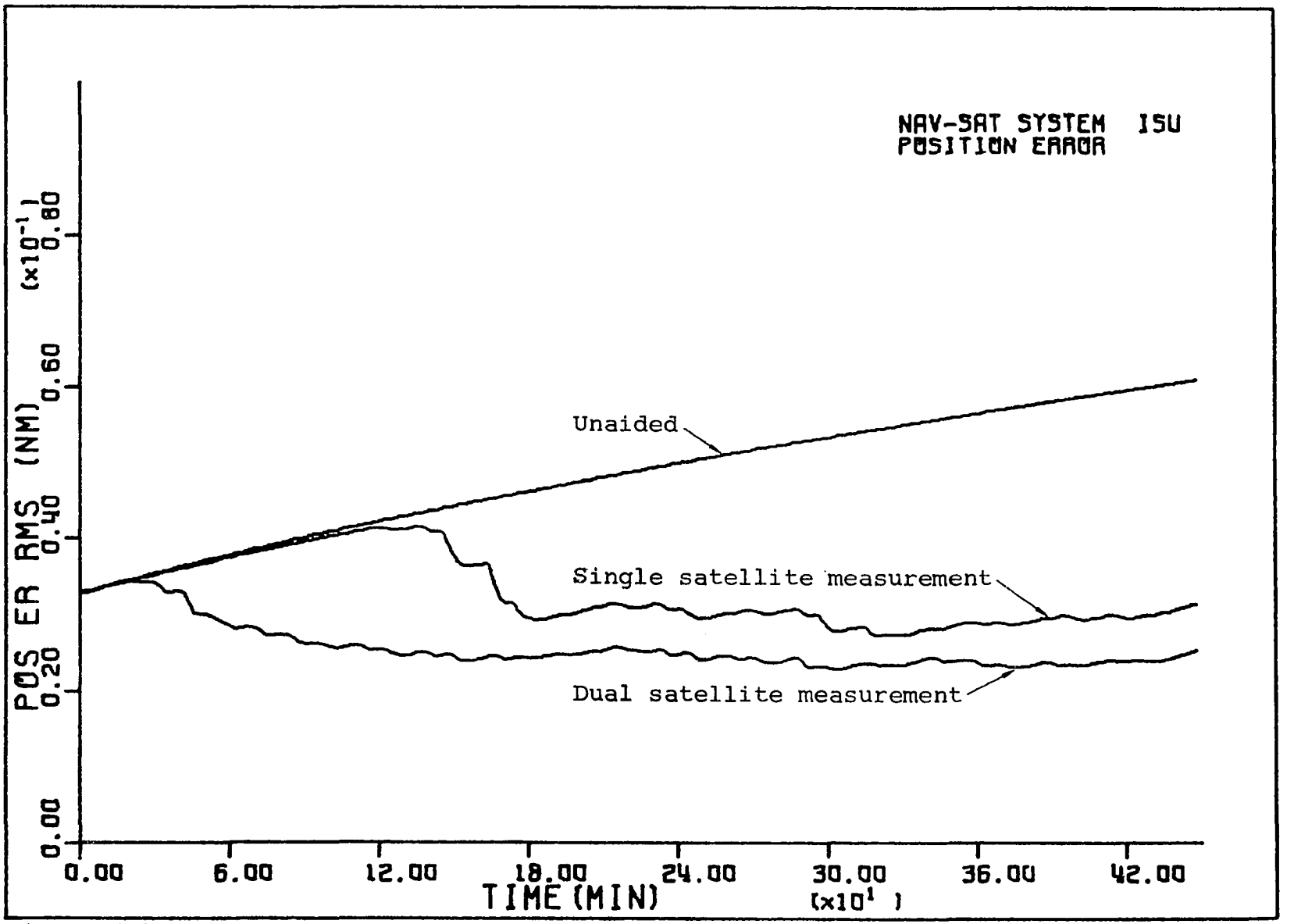

Figure 4.18. Vertical position errors for satellite configuration B (0.005 deg./hr. gyros)

V. CONCLUSIONS

The following results were revealed by this error analysis study for an integrated inertial/Doppler-satellite navigation system.

(a) The addition of a second satellite measurement resulted in a reduction of average RMS radial position errors by about a factor of two for the "two-in-view" system over that of the "one-in-view" system.

(b) The degree of improvement which can be obtained with the "two-in-view" system depends on the orbital geometry of the two satellites. The inherent imbalance of qualities in the along-track and cross-track estimates from a Doppler-satellite is minimized by choosing two satellites whose subtrack velocities are orthogonal. The RMS radial position error for a system with orthogonal satellites is only about two-thirds of the error for an identical system with two nearly parallel satellites.

(c) As the altitude of the satellites is increased, the Doppler information is coming into the filter at a slower rate and the quality of the estimates is reduced. The three satellite altitudes studied showed that the RMS radial error increases almost

linearly with increasing satellite altitude. This degradation is the price one pays for the privilege of providing continuous dual satellite coverage with a fewer number of satellites in higher orbits.

(d) Results of parametric studies showed the accuracy trade-off which is possible between the inertial system quality and the satellite altitude.

The numerical results for all the simulated systems studied are presented in the text. The level position errors are shown in detail in graphical form and the time averages of the RMS errors for all the state variables are presented in tabulated form.

The measurement model used for the filter processed both satellite measurements simultaneously assuming that the counting intervals of the two satellites were synchronized and time-coincident. These measurements may also be processed in a sequential manner. Sequential processing has several advantages over simultaneous processing in that the effect of each individual measurement on the filter's estimates can be assessed and the measurement noise matrix, which is inverted in the Kalman filter recursive equations, is simply a scaler. The primary disadvantage of sequential processing of the measurements for the delayed-state filter is that the dimensionality of the recursive equations is doubled and this poses a computational problem for a system with a large

number of state variables. For this reason, sequential processing was not used for the simulation studies. However, a treatment of this theoretical problem is presented in Appendix B. Another theoretical problem arises if one does not assume coincidence of the counting interval, and a treatment of this problem is also presented in Appendix B.

There appear to be several aspects of the integrated inertial/Doppler-satellite problem which bear future investigation. One of these aspects is the effect of the addition of satellite geodesy errors to the model, and another is the inclusion of range measurements from the satellites in addition to the Doppler-count measurements. One is always interested in improving the performance of the system. However, whether the improvement would be worth the increase in model complexity remains to be seen.

VI. LITERATURE CITED

1. Bona, B. E. and Hutchinson, C. E. Optimum reset of an inertial navigator from satellite observations. National Electronics Conference Proceedings 21: 569-574. 1965.

2. Brown, R. G. Analysis of an integrated inertial/Doppler-satellite navigation system. Part 1. Iowa State University, Engineering Research Institute Technical Report ERI -- 62600. 1969.

3. Brown, R. G. and Hagerman, L. L. An optimum inertial/Doppler-satellite navigation system. J. of the Institute of Navigation 16, No. 3: 260-269. 1969.

4. Brown, R. G. and Hartman, G. L. Kalman filter with delayed states as observables. National Electronics Conference Proceedings 24: 67-72. 1968.

5. Brown, R. G. and Winger, D. J. Analysis of an integrated inertial/Doppler-satellite navigation system. Part 2. Iowa State University, Engineering Research Institute Technical Report ERI -- 78400. 1970.

6. Guier, W. H. and Weiffenbach, G. C. A satellite navigation system. Institute of Radio Engineering Proceedings 48: 507-516. 1960.

7. Hagerman, L. L. An optimum Doppler-satellite inertial navigation system. Unpublished Ph.D. thesis. Ames, Iowa, Library, Iowa State University. 1963.

8. Kalman, R. E. A new approach to linear filtering and prediction problems. Trans. ASME, J. Basic Engineering 82: 35-95. 1960.

9. King-Hele, D. Theory of satellite orbits in an atmosphere. London, England, Butterworth and Co., Ltd. 1964.

10. Macko, S. J. Satellite Tracking. New York, John F. Rider Publisher, Inc. 1962.

11. Meditch, J. S. Stochastic optimal linear estimation and control. New York, McGraw-Hill Book Co., Inc. 1969.

12. O'Donnell, C. F. Inertial navigation analysis and design. New York, McGraw-Hill Book Co., Inc. 1964.

13. Pitman, G. R., Jr., ed. Inertial guidance. New York, John Wiley and Sons, Inc. 1962.

14. Shchigolev, B. M. Mathematical analysis of observations. New York, American Elsevier Publishing Co., Inc. 1965. (Originally published in the U.S.S.R. in 1960.)

15. Sorenson, H. W. Kalman filtering techniques. In Leondes, C. T., ed. Advances in Control Systems. Vol. 3. Pp. 219-292. New York, Academic Press, Inc. 1966.

16. Stansell, T. A. The Navy navigation satellite system: description and status. J. of the Institute of Navigation 15, No. 3: 229-243. 1968.

17. Watson, G. A. An algorithm for geodetic navigation for the TRANSIT satellite system. Unpublished Ph.D. thesis. Ames, Iowa, Library, Iowa State University. 1963.

VII. ACKNOWLEDGMENTS

The author wishes to thank his major professor, Dr. R. G. Brown, for the suggestion of this topic and for his valuable help and patience throughout the course of the study.

The author is also indebted to the Engineering Research Institute at Iowa State University for providing financial support through Project Themis under the Office of Naval Research Contract No. N00014-68-A-0162.

VIII. APPENDIX A

A. Analysis of Unequally Precise Measurements

The following is similar to a treatment of this topic by Shchigolev (14). Let some hypothesis be made regarding an unknown quantity, a, which is to be estimated based on n independent but unequally precise measurements. The measurements $x_1, x_2, \ldots, x_n$ have known mean square errors $\sigma_1^2, \sigma_2^2, \ldots, \sigma_n^2$ and each error, $e = x - a$, is normally distributed with a distribution

$$f_k(e) = \frac{1}{\sigma_k (2\pi)^{1/2}} \exp\left[-\frac{e^2}{2\sigma_k^2}\right] = \left[\frac{p_k}{2\pi}\right]^{1/2} \exp\left[-\frac{p_k e^2}{2}\right] \tag{A.1}$$

where

$$p_k = \frac{1}{\sigma_k^2} \quad .$$

The probability of obtaining an error close to e_k, denoted by $P(e_k < e < e_k + \varepsilon)$ or $P(e \tilde{\sim} e_k)$, is then

$$P(e \tilde{\sim} e_k | a) = \left[\frac{\varepsilon^2 p_k}{2\pi}\right]^{1/2} \exp\left[-\frac{p_k e_k^2}{2}\right] \quad . \tag{A.2}$$

Since the results of the measurements are mutually independent random variables,

$$P(e \tilde{=} e_1, e_2, \ldots, e_n | a)$$

$$= \left[\frac{\varepsilon^2}{2\pi}\right]^{n/2} (p_1\ p_2\ \cdots\ p_n)^{1/2}\ \exp\left[-\frac{\sum_{k=1}^{n} p_k e_k^2}{2}\right] . \quad (A.3)$$

Under the hypothesis chosen, the errors $e_1, e_2, \ldots, e_n$ are uniquely determined by $x_1, x_2, \ldots, x_n$ so

$$P(e \tilde{=} e_1, e_2, \ldots, e_n) = P(x \tilde{=} x_1, x_2, \ldots, x_n | a) \quad . \quad (A.4)$$

If no a priori information concerning a exists and assuming all the hypotheses regarding a are equally likely, Bayes' theorem leads to the result that the probabilities of the hypotheses after the measurements were taken are proportional to the conditional probabilities of the measurements under those hypotheses or

$$P(a | x_1, x_2, \ldots, x_n) = K \exp\left[-\frac{\sum_{k=1}^{n} p_k e_k^2}{2}\right] \quad (A.5)$$

where K is a constant.

The most probable hypothesis will be that which gives

$$S(a) = \sum_{k=1}^{n} p_k e_k^2 = \sum_{k=1}^{n} p_k (x_k - a)^2 \quad (A.6)$$

its minimum value. This most probable value of a is a weighted mean, and can be expressed as

$$\bar{x}_p = \frac{\sum_{k=1}^{n} p_k x_k}{\sum_{k=1}^{n} p_k} \quad . \quad (A.7)$$

IX. APPENDIX B

A. The Delayed-State Kalman Filter

Let the state equation of a random process be expressed as

$$\underline{x}(k) = \emptyset(k,k-1)\underline{x}(k-1) + \underline{g}(k-1) \qquad (B.1)$$

where

$\underline{x}(k)$ is the state vector at time t_k,

$\emptyset(k,k-1)$ is the state transition matrix from time t_{k-1} to t_k, and

$\underline{g}(k-1)$ is the system response to white noise input driving functions.

Let the measurement equation which linearly relates the measurement and the state be expressed as

$$\underline{y}(k) = M(k)\underline{x}(k) + \underline{v}(k) \qquad (B.2)$$

where

$\underline{y}(k)$ is the discrete measurement vector at t_k,

$M(k)$ is the matrix linearly relating the present state to the measurement, and

$\underline{v}(k)$ is the uncorrelated measurement error.

Assume the following statistical properties hold for Equations B.1 and B.2

(a) The initial state $\underline{x}(0)$ is gaussian with zero mean.

(b) The sequence $\underline{g}(k)$ is gaussian with zero mean. $E[\underline{g}(j)\underline{g}'(i)] = H\delta_{ji}$ where H is the positive semi-definite and symmetric covariance matrix of the process noise, and δ_{ji} is the kronecker delta function.

(c) The sequence $\underline{v}(k)$ is gaussian with zero mean. $E[\underline{v}(j)\underline{v}'(i)] = V\delta_{ji}$ where V is the positive semi-definite and symmetric covariance matrix of the measurement noise.

(d) The process and measurement noise are uncorrelated or $E[\underline{g}(k)\underline{v}'(k)] = 0$.

(e) The initial state estimate is uncorrelated with the process and measurement noise or $E[\underline{x}(0)\underline{g}'(k)] = 0$ and $E[\underline{x}(0)v'(k)] = 0$.

An estimate of the state at t_k based on all measurements through $\underline{y}(k)$ is denoted by $\hat{\underline{x}}(k|k)$ and the error associated with this estimate is $\underline{e} = [\underline{x}(k) - \hat{\underline{x}}(k|k)]$. Kalman (8) has shown that the minimum mean square error is given by the estimate

$$\hat{\underline{x}}(k|k) = E[\underline{x}(k)|\underline{y}(1),\underline{y}(2),\ldots,\underline{y}(k)] \quad . \tag{B.3}$$

If the gaussian assumptions above are dropped, this estimate is the minimum mean square error linear estimate.

The set of recursive equations which are used to implement the estimator or Kalman filter is derived in detail in

several references (11, 15) and can be expressed as

$$P(k|k-1) = \emptyset(k,k-1)P(k-1|k-1)\emptyset'(k,k-1) + H(k-1) \quad (B.4)$$

$$\hat{\underline{x}}(k|k-1) = \emptyset(k,k-1)\hat{\underline{x}}(k-1|k-1) \quad (B.5)$$

$$B(k) = P(k|k-1)M'(k)[M(k)P(k|k-1)M'(k) + V(k)]^{-1} \quad (B.6)$$

$$P(k|k) = P(k|k-1) - B(k)[M(k)P(k|k-1)M'(k) + V(k)]B'(k) \quad (B.7)$$

$$\hat{\underline{x}}(k|k) = \hat{\underline{x}}(k|k-1) + B(k)[\underline{y}(k) - M(k)\hat{\underline{x}}(k|k-1)] \quad (B.8)$$

where

$\hat{\underline{x}}(k-1|k-1)$ is the optimal estimate of $\underline{x}(k-1)$ given all measurements through t_{k-1},

$P(k-1|k-1)$ is the covariance matrix of the estimation error $[x(k-1) - \hat{\underline{x}}(k-1|k-1)]$,

$\hat{\underline{x}}(k|k-1)$ is the optimal estimate of $\underline{x}(k)$ given all measurements through t_{k-1},

$P(k|k-1)$ is the covariance matrix of the estimation error $[\underline{x}(k) - \hat{\underline{x}}(k|k-1)]$,

$B(k)$ is the gain matrix which optimally "weights" the measurements at t_k into the estimate,

$\hat{\underline{x}}(k|k)$ is the optimal estimate of $\underline{x}(k)$ given all measurements through t_k,

$P(k|k)$ is the covariance matrix of the estimation error $[\underline{x}(k) - \hat{\underline{x}}(k|k)]$,

H(k-1) is the covariance matrix of the state response to the white noise inputs in the time interval (t_{k-1}, t_k), and

V(k) is the covariance matrix of the uncorrelated measurement error at t_k.

There are a number of cases where the measurement is a linear function of the previous state as well as the present state. The measurement equation is then not of the form of Equation B.2 but can be expressed as

$$\underline{y}(k) = M(k)\underline{x}(k) + N(k)\underline{x}(k-1) + \underline{v}(k) \quad . \tag{B.9}$$

A simple approach to this problem was presented by Brown and Hartman (4) in which a new state vector is formed by augmenting the present state vector with the previous state, or

$$\begin{bmatrix} \underline{x}(k) \\ \underline{x}(k-1) \end{bmatrix} = \begin{bmatrix} \Phi(k,k-1) & 0 \\ I & 0 \end{bmatrix} \begin{bmatrix} \underline{x}(k-1) \\ \underline{x}(k-2) \end{bmatrix} + \begin{bmatrix} \underline{g}(k) \\ 0 \end{bmatrix} \quad . \tag{B.10}$$

The measurement equation can now be expressed as

$$\underline{y}(k) = [M(k)N(k)] \begin{bmatrix} \underline{x}(k) \\ \underline{x}(k-1) \end{bmatrix} + \underline{v}(k) \quad . \tag{B.11}$$

Let the augmented model be denoted by a starred notation so Equations B.10 and B.11 can be written as

$$\underline{x}^*(k) = \Phi^*(k,k-1)\underline{x}^*(k-1) + \underline{g}^*(k-1) \tag{B.12}$$

$$\underline{y}^*(k) = M^*(k)\underline{x}^*(k) + \underline{v}^*(k) \quad . \tag{B.13}$$

These equations are of the same forms as Equations B.1 and B.2 and the set of recursive filter Equations B.4 through B.8 are valid when reinterpreted in terms of this delayed state model.

It should be pointed out that $\underline{x}^*(k)$ is not truly a state vector at time t_k since it has been augmented by the delayed state. Also, $\phi^*(k,k-1)$ is not truly a transition matrix since it does not have all the properties of a transition matrix. However, all the necessary conditions for the derivation of the conventional Kalman filter equations still hold so the recursive equations are valid.

At this point one might comment that it appears that it will be necessary to work with vectors and matrices with double the dimensionality of the state vector. This is not necessarily true as will be shown below.

Let the covariance matrix of the augmented system be written as

$$P^*(k-1|k-1) = \begin{bmatrix} P(k-1|k-1) & P(k-1,k-2|k-1) \\ P(k-1,k-2|k-1) & P(k-2|k-1) \end{bmatrix} \quad \text{(B.14)}$$

Applying Equation B.4 to the augmented system,

$$P^*(k|k-1) = \begin{bmatrix} \phi(k,k-1) & 0 \\ I & 0 \end{bmatrix} P^*(k-1|k-1) \begin{bmatrix} \phi'(k,k-1) & I \\ 0 & 0 \end{bmatrix} + \begin{bmatrix} H(k-1) & 0 \\ 0 & 0 \end{bmatrix}$$

$$= \begin{bmatrix} \phi(k,k-1)P(k-1|k-1)\phi'(k,k-1)+H(k-1) & \phi(k,k-1)P(k-1|k-1) \\ P(k-1|k-1)\phi'(k,k-1) & P(k-1|k-1) \end{bmatrix} \quad \text{(B.15)}$$

Note that the upper left hand term in $P^*(k|k-1)$ is nothing more than $P(k|k-1)$ in the conventional filter.

The most important point is that in the projection of $P^*(k-1|k-1)$ through the "transition" matrix $\emptyset^*(k,k-1)$, only $P(k-1|k-1)$ appears in $P^*(k|k-1)$. That is, the covariance of the smoothed estimate, $P(k-2|k-1)$, and the cross-covariance terms, $P(k-1,k-2|k-1)$, do not appear. This means that it is not necessary to compute these terms in the recursive equations since they disappear in the projection. As far as the estimate of the state vector is concerned, the a priori estimate of the delayed portion of state vector, $\hat{\underline{x}}(k-1|k-1)$, is simply the a posteriori estimate from the previous step of the recursive process.

It is then possible to derive a set of recursive equations for the delayed-state filter which does not require increasing the dimensionally of the matrices. The derivation can be obtained by direct substitution of the starred quantities (in partitioned form) into the conventional recursive Equations B.4 through B.8. The delayed-state recursive Equations 3.4 through 3.9 result from retaining only those terms which relate to the upper half of the augmented state vector.

B. Delayed-State Sequential Processing

The argument in the preceding section treated the measurement as a vector quantity with all the measurements at t_k being included in $\underline{y}(k)$ and these measurements were used simultaneously in revising the estimate of the state vector. There are sometimes advantages in using the measurements one at a time to revise the estimates. This is usually termed sequential processing of the measurements.

The advantage of sequential processing is that it allows an inspection of benefits obtained from each measurement. For example, if the measurement is a two tuple, one of these measurements may be providing very little information to the filter and perhaps could be eliminated as not being practically justifiable. However, when the two measurements are processed simultaneously one does not get any assessment as to which measurement is providing the most information. One other practical advantage in sequential processing is that the dimensionality of the inverted term in Equation B.6 is that of the measurement. This will always be a scaler for sequential processing in the conventional Kalman filter.

Consider that the measurement vector is an n tuple of independent component measurements. Under the condition of independence, Sorenson (15) has shown that the data may be processed sequentially using the conventional recursive equations where the time interval is considered to be zero

between the measurement components.

One must be careful when applying this concept to the delayed-state filter because $\emptyset^*(k,k-1)$ does not represent a true transition matrix as was previously noted. The problem does not arise until one considers the a priori covariance matrix for the second measurement component. Assume that the covariance matrix after the first measurement component is

$$P^{(1)*}(k|k) = \begin{bmatrix} P^{(1)}(k|k) & P^{(1)}(k,k-1|k) \\ P^{(1)}(k,k-1|k) & P^{(1)}(k-1|k) \end{bmatrix} . \quad (B.16)$$

where the superscript (1) refers to the covariance after processing the first measurement at t_k. The a priori covariance matrix for the second measurement component will then be simply $P^{(1)*}(k|k)$ projected through a unity transition matrix. This then requires that the smoothed estimate covariance $P^{(1)}(k-1|k)$, as well as the cross covariance terms $P^{(1)}(k,k-1|k)$ be computed. Essentially, this means that the full delayed-state model must be processed and the recursive equations developed by Brown and Hartman are only applicable to the last component of the measurement vector.

Sequential processing using a delayed-state filter would be preferable from a computational standpoint only when the dimension of the state vector is small and the dimension of the measurement vector is large. In the

simulation studies of this paper, the state vector was large and the measurement vector was only a two tuple, so simultaneous processing was used.

C. The Delayed-State Filter Using Non-Time-Coincident Measurements

The delayed-state filter can be used when the observation is linearly related to the state vector at both the beginning and end of the time interval. If there are several observables of this nature and their time intervals are coincident, then the measurement will be a vector and the recursive equations of Chapter III are valid.

In some situations, it is conceivable that one would not have the liberty to make all measurements or observations over coincident time intervals. Consider the case in which two measurements, a and b, are made over time intervals which are of equal duration but are not coincident. This situation can be handled by augmenting the state vector with two delayed states. The state and measurement equations would then be of the form

$$\underline{x}^*(k) = \begin{bmatrix} \underline{x}(k) \\ \underline{x}(k-1) \\ \underline{x}(k-2) \end{bmatrix} = \begin{bmatrix} \phi(k,k-1) & 0 & 0 \\ I & 0 & 0 \\ 0 & I & 0 \end{bmatrix} \underline{x}^*(k-1) + \begin{bmatrix} \underline{g}(k-1) \\ 0 \\ 0 \end{bmatrix} \tag{B.17}$$

$$y^*(k) = [M(k) \quad 0 \quad N(k)]\underline{x}^*(k) + v(k) \qquad (B.18)$$

where $y^*(k)$ is a scaler. Equations B.17 and B.18 are of the form of Equations B.1 and B.2 so the recursive Equations B.4 through B.8 apply when reinterpreted in terms of this "double-delayed-state" formulation.

It appears that the dimensionality of the recursive filter equations for this model is triple that of the conventional nondelayed-state model. However, when one projects the covariance matrix of the estimates ahead in time using Equation B.4, the covariance and cross-covariance terms involving the estimate of $\underline{x}(k-2)$ do not appear, and it is therefore not necessary to process the smoothed estimate of $\underline{x}(k-2)$ and its associated covariance terms. In effect, the dimensionality of the recursive equations is reduced to double that of the conventional filter.

X. APPENDIX C

A. The Basic Inertial Mechanization Equation

The acceleration sensed by the accelerometers of an inertial navigation system is given by

$$\underline{a} = (\ddot{\underline{R}})_I - \underline{g}_m \qquad (C.1)$$

where

$\underline{a}$ is the acceleration sensed by ideal accelerometers,

$\underline{R}$ is the radius vector from center of earth to true position,

$\underline{g}_m$ is the gravitational mass attraction vector, and

$(\ )_I$ is the derivative in inertial reference frame.

The solution of Equation C.1 is carried out by a computer whose coordinate frame is usually rotating in inertial space at some angular rate, $\underline{\omega}_c$, so Equation C.1 can be rewritten in this rotating system as

$$(\ddot{\underline{R}})_c + 2\underline{\omega}_c \times \dot{\underline{R}} + \dot{\underline{\omega}}_c \times \underline{R} + \underline{\omega}_c \times (\underline{\omega}_c \times R) = \underline{a} + \underline{g}_m \quad . \qquad (C.2)$$

It should be realized that with perfect instrumentation, the solution of Equation C.2 would be perfectly mechanized with no error in the velocity and position readouts.

B. The Inertial System Error Equations

An approach to the derivation of the inertial system error equations is given by Pitman (13). Consider three x,y,z coordinate systems which are nearly coincident. They are the computer, platform and true coordinate systems. Let the incremental angle required to rotate the true coordinates into the platform coordinates be $\underline{\phi}$ and the incremental angle required to rotate the true coordinates into the computer coordinates be $\delta\underline{\theta}$. In other words, $\underline{\phi}$ is the tilt of the platform and $\delta\underline{\theta}$ is related to position error in the computer readout. A new variable, $\underline{\psi}$, is then defined as

$$\underline{\psi} \triangleq \underline{\phi} - \delta\underline{\theta} \quad . \tag{C.3}$$

It can be shown that

$$\dot{\underline{\psi}} + \underline{\omega} \times \underline{\psi} = \underline{\varepsilon} \tag{C.4}$$

where

$\underline{\omega}$ is the platform angular rate with respect to inertial reference, and

$\underline{\varepsilon}$ is the gyro drift rate error.

In the mechanization Equation C.2, a $\delta\underline{R}$ error in the position vector will also cause the mass attraction vector to be reduced by an amount $\omega_0^2\ \delta\underline{R}_{tan}$ where $\delta\underline{R}_{tan}$ is the tangential component of $\delta\underline{R}$ and ω_0^2 is g_m/R. The measured acceleration will be in error due to accelerometer error,

$\delta\underline{a}$, and since $\underline{a}$ is sensed in the platform coordinate system rather than the computer coordinates, $\underline{a}$ is reduced by the amount $\underline{\psi} \times \underline{a}$. Inclusion of the preceding error terms into Equation C.2 results in the position error equation

$$\delta\ddot{\underline{R}} + 2\underline{\omega} \times \delta\dot{\underline{R}} + \dot{\underline{\omega}} \times \delta\underline{R} + \underline{\omega} \times (\underline{\omega} \times \delta\underline{R}) = \delta\underline{a} - \underline{\psi} \times \underline{a} \quad \omega_0^2 \, \delta\underline{R}_{tan} \quad . \tag{C.5}$$

Equations C.4 and C.5 are the two basic error equations that describe the inertial system errors. Equation C.4 describe what are termed the 24 hour error dynamics, and its three components are

$$\dot{\psi}_x + \omega_y\psi_z - \omega_z\psi_y = \varepsilon_x \tag{C.6}$$

$$\dot{\psi}_y + \omega_z\psi_x - \omega_x\psi_z = \varepsilon_y \tag{C.7}$$

$$\dot{\psi}_z + \omega_x\psi_y - \omega_y\psi_x = \varepsilon_z \quad . \tag{C.8}$$

Equation C.5 describes what are termed the Schuler error dynamics. In the geocentric navigation coordinate frame of Figure 3.2, $\delta R_x = R\delta\theta_y$ and $\delta R_y = -R\delta\theta_y$ and the two components of Equation C.5 can be written as

$$\begin{aligned} &R\delta\ddot{\theta}_y + 2\dot{R}\delta\dot{\theta}_y + (\ddot{R}/R - \omega_y^2 - \omega_z^2 - \omega_0^2)R\delta\theta_y + 2\omega_z R\delta\dot{\theta}_x \\ &+ (2\omega_z\dot{R}/R + \dot{\omega}_z - \omega_y\omega_x)R\delta\theta_x + 2\omega_y\delta\dot{R}_z + (\dot{\omega}_y + \omega_z\omega_x)\delta R_z \\ &= \delta a_x - \psi_y a_z + \psi_z a_y \end{aligned} \tag{C.9}$$

and

$$-R\delta\ddot{\theta}_x - 2\dot{R}\delta\theta_x + (-\ddot{R}/R + \omega_x^2 + \omega_z^2 - \omega_0^2)R\delta\theta_x + 2\omega_z\delta\dot{\theta}_y$$

$$+ (2\omega_z\dot{R}/R + \dot{\omega}_z + \omega_x\omega_y)R\delta\theta_y - 2\omega_x\delta\dot{R}_z + (-\dot{\omega}_x + \omega_z\omega_y)\delta R_z$$

$$= \delta a_y - \psi_z a_x + \psi_x a_z \qquad \text{(C.10)}$$

where

$$a_x = 2\omega_y\dot{R} + \dot{\omega}_y R + \omega_x\omega_z R \qquad \text{(C.11)}$$

$$a_y = -2\omega_x\dot{R} - \dot{\omega}_x R + \omega_y\omega_z R \qquad \text{(C.12)}$$

and

$$a_z = \ddot{R} - (\omega_x^2 + \omega_y^2)R + g_m \quad . \qquad \text{(C.13)}$$

The vertical channel is assumed to be implemented by a means independent of the level inertial errors.

XI. APPENDIX D

A. The Computer Program

A sample printout of the computer program which was used to conduct the simulation studies follows this page. Specifically, this is the program which was used in simulated flight C-2. The programs used for the other simulated flights are similar to this program, the major differences being the satellite orbital configurations and the inertial system gyro qualities.

```
C  INTEGRATED INERTIAL/DOPPLER-SATELLITE NAVIGATION SYSTEM EMPLOYING
C  MULTIPLE SATELLITE COVERAGE                D. WINGER
      DOUBLE PRECISION A(16,16),PHI(16,16),PN(16,16),PO(16,16),
     1DUM(16,16),H(16,16) ,ZM(2,16),ZN(2,16)
      DOUBLE PRECISION RS,RV,AA,BB,CC,ANA,BNA,CNA,AOA,BOA,COA,
     1 CZZS,V1,V2, ANB,BNB,CNB,AOB,BOB,COB
      DOUBLE PRECISION DABS,DSIN,DCOS
      DIMENSION ISA(320),ISB(320)
      COMMON A,PHI,PO,PN,DUM,ZM,ZN,AA,BB,CC,V1,V2,CZZS,   RS,RV,VV,RTS,
     1 CMTNM,CMSTK,R,GM,WO,WE,PI,T,DT,WS,ISAT,IT,K,ISAO,ISBO,M,ISAN,ISBN
      DT=20.0
      ITAPEW=9
      ITAPER=8
      ITAPEP=10
      ITPM=11
      M=0
C  CONVERSION FACTORS
      RTM=1.0/2.908882E-4
      FTM=0.304800
      CMTNM=5.3996E-4
      CMSTK=1.0/5.144444E-1
      RTS=1.0/4.848137E-6
C  CONSTANTS
      RO=20.92574E6
      GME=1.407654E16
      PI=3.141592
C  ENTER VEHICLE AND SATELLITE ALTITUDES IN NM
      ALTV=4.0
C  ENTER VEHICLE VELOCITY IN KNOTS
      VV= 500.0/3600./CMTNM
      RE=RO*FTM*CMTNM
      ELM =20.*PI/180.
      C2E=COS(ELM)*COS(ELM)
      RAT=(SQRT(8./3.)+SQRT(8./3.-4.*(1.-1./3./C2E)))/2./(1.-1./3./C2E)
      ALTS=(RAT-1.)*RE
      RS=(RE+ALTS)/CMTNM
      RV=(RE+ALTV)/CMTNM
```

```
      R=RV
      RSF=RS/FTM
      RVF=RV/FTM
      WO= SQRT(GME/RVF/RVF/RVF)
      WS= SQRT(GME/RSF/RSF/RSF)
      GM=GME/RVF/RVF*FTM
      WE=15.04107*PI/180./3600.
      V1=0.D0
      V2=0.D0
C  INITIALIZE ALL MATRICES TO ZERO
      DO 1 I=1,16
      DO 1 J=1,16
      PO(I,J)=0.0D0
      PN(I,J)=0.0D0
      A(I,J)=0.0D0
      H(I,J)=0.0D0
      PHI(I,J)=0.0D0
    1 DUM(I,J)=0.0D0
      DO 670 I=1,2
      DO 670 J=1,16
      ZM(I,J)=0.0D0
      ZN(I,J)=0.0D0
  670 CONTINUE
C  ENTER VARIANCES OF MARKOV PROCESSES
      V9=(0.01/RTS/WO)**2
      V10=V9
      V11=V9
      V12=(10.0/RTS)**2
      V13=V12
      V14=(0.50*FTM/R/WO)**2
      V15=1.00E6
      V16=1.00E6
      V8=V14
C  ENTER BETAS OF MARKOV PROCESSES     IN PER SEC
      B9=1./ 10.00/3600.
      B10=B9
      B11=B9
```

```
      B12=1./ 10.00/3600.
      B13=B12
      B14=0.18
      B15=1.0E-8
      B16=1.0E-8
      B8=B14
C   ENTER CONSTANT A TERMS
      A(1,9)=WO
      A(2,10)=WO
      A(3,11)=WO
      A(7,12)=WO
      A(5,13)=-WO
      A(9,9)=-B9
      A(10,10)=-B10
      A(11,11)=-B11
      A(12,12)=-B12
      A(13,13)=-B13
      A(14,14)=-B14
      A(15,15)=-B15
      A(16,16)=-B16
      A(8,14)=WO
      A(4,5)=WO
      A(6,7)=WO
C   ENTER INITIAL COVARIANCE MATRIX
      PO(1,1)=(14.1/RTS)**2
      PO(2,2)=PO(1,1)
      PO(3,3)=( 3.0/RTM)**2
      PO(4,4)=(1000.0*FTM/R)**2
      PO(5,5)=( 4.0*FTM/WO/R)**2
      PO(6,6)=PO(4,4)
      PO(7,7)=PO(5,5)
      PO(8,8)=(200.0*FTM/R)**2
      PO(9,9)=(0.010/WO/RTS)**2
      PO(10,10)=PO(9,9)
      PO(11,11)=PO(9,9)
      PO(12,12)=(10.0/RTS)**2
      PO(13,13)=PO(12,12)
```

```
      PO(14,14)=(0.50*FTM/R/WO)**2
      PO(15,15)=1.0D6
      PO(16,16)=1.0D6
C  ENTER COVARIANCE H MATRIX OF STATE RESPONSES DUE TO UNCORRELATED
C  WHITE NOISE INPUT
      H(8,8)=WO*WO*2.0*V8/B8*(DT-2.0/B8*(1.0-EXP(-38*DT))
     1+0.5/B8*(1.0-EXP(-2.0*B8*DT)))
      H(14,14)=V14*(1.0-EXP(-2.0*B8*DT))
      H(8,14)=2.0*WO*V14*((1.0-EXP(-B8*DT))/B8
     1-(1.0-EXP(-2.0*B8*DT))/2.0/B8)
      H(14,8)=H(8,14)
      H(9,9)=V9*(1.0-EXP(-2.0*B9 *DT))
      H(10,10)=H(9,9)
      H(11,11)=H(9,9)
      H(12,12)=V12*(1.0-EXP(-2.0*B12*DT))
      H(13,13)=V13*(1.0-EXP(-2.0*B13*DT))
      H(15,15)=V15*(1.0-EXP(-2.0*B15*DT))
      H(16,16)=V16*(1.0-EXP(-2.0*B15*DT))
C  READ IN SATELLITE NUMBERS
      READ (1,170) (ISA(N),N=1,320)
      READ (1,170) (ISB(N),N=1,320)
  170 FORMAT (40I2)
      DO 3 N=2,320
      IF (ISA(N))3,2,3
    2 ISA(N)=ISA(N-1)
    3 CONTINUE
      DO 5 N=2,320
      IF (ISB(N))5,4,5
    4 ISB(N)=ISB(N-1)
    5 CONTINUE
  175 FORMAT(20I3)
      WRITE(3,175) (ISA(N),N=1,320)
      WRITE(3,175) (ISB(N),N=1,320)
      T=0.0
      ISAO=21
      ISBO=21
      K=0
```

```
      DO 8 I=1,16
    8 PN(I,I)=PO(I,I)
      CALL SCALE
C   MAIN LOOP
      DO 500 K=1,1350
      T=T+DT
C   COMPUTE TIME VARYING A TERMS
      IF(T-18020.) 110,111,112
  110 CONTINUE
      WX=WE* COS(PI/4.0-VV*T/R)
      WY=-VV/R
      WZ=WE* SIN(PI/4.0-VV*T/R)
      WXD=-WY*WZ
      WYD=0.0
      WZD=WX*WY
      GO TO 120
  111 CONTINUE
      WX=WE* COS(PI/4.0-VV*18000./R) +VV/R
      WY=0.0
      WZ= VV*TAN(PI/4.0-VV*18000./R)/R+WE*SIN(PI/4.0-VV*1800./R
      WXD=VV/R/DT
      WYD=VV/R/DT
      WZD=(    WZ                        -WE*SIN(PI/4.-VV*18000./R))/DT
      GO TO 120
  112 CONTINUE
      IF(T-18040.) 113,113,130
  113 CONTINUE
      WXD=0.0
      WYD=0.0
      WZD=0.0
  120 CONTINUE
      A(1,3)=-WY
      A(1,2)=WZ
      A(2,1)=-WZ
      A(2,3)=WX
      A(3,1)=WY
      A(3,2)=-WX
```

```
      A(7,5)=-2.0*WZ
      A(7,6)=(WY*WY+WZ*WZ-WO*WO)/WO
      A(7,8)= (-WYD-WZ*WX)/WO
      A(7,2)=(WX*WX+WY*WY-WO*WO)/WO
      A(7,3) =(-WXD+WY*WZ)/WO
      A(7,14)=-2.0*WY
      A(7,4)= (WY*WX-WZD)/WO
      A(5,14)=-2.0*WX
      A(5,7)= 2.0*WZ
      A(5,8)= (-WXD+WY*WZ)/WO
      A(5,6)=(WZD+WX*WY)/WO
      A(5,4)=(WX*WX+WZ*WZ-WO*WO)/WO
      A(5,1)=(WX*WX+WY*WY-WO*WO)/WO
      A(5,3)= (WYD+WX*WZ)/WO
C  COMPUTE PHI
      CALL MTEXP
      PHI(14,14)=EXP(-B8*DT)
  130 CONTINUE
C  COMPUTE APRIORI COVARIANCE MATRIX
      DO 22 I=1,8
      DO 22 J=1,16
      SUM=0.0D0
      DO 21 N=1,16
   21 SUM=SUM+PHI(I,N)*PO(N,J)
   22 DUM(I,J)=SUM
      DO 24 I=1,16
      DUM(9,I)=PHI(9,9)*PO(9,I)
      DUM(10,I)=PHI(10,10)*PO(10,I)
      DUM(11,I)=PHI(11,11)*PO(11,I)
      DUM(12,I)=PHI(12,12)*PO(12,I)
      DUM(13,I)=PHI(13,13)*PO(13,I)
      DUM(14,I)=PHI(14,14)*PO(14,I)
      DUM(15,I)=PHI(15,15)*PO(15,I)
   24 DUM(16,I)=PHI(16,16)*PO(16,I)
      DO 26 I=1,16
      DO 26 J=1,8
      SUM=0.0D0
```

```
      DO 25 N=1,16
   25 SUM=SUM+DUM(I,N)*PHI(J,N)
   26 PN(I,J)=SUM
      DO 28 I=1,16
      PN(I,9)=DUM(I,9)*PHI(9,9)
      PN(I,10)=DUM(I,10)*PHI(10,10)
      PN(I,11)=DUM(I,11)*PHI(11,11)
      PN(I,12)=DUM(I,12)*PHI(12,12)
      PN(I,13)=DUM(I,13)*PHI(13,13)
      PN(I,14)=DUM(I,14)*PHI(14,14)
      PN(I,15)=DUM(I,15)*PHI(15,15)
   28 PN(I,16)=DUM(I,16)*PHI(16,16)
      DO 29 I=1,16
      DO 29 J=1,16
   29 PN(I,J)=PN(I,J)+H(I,J)
      DO 31 I=1,16
      DO 31 J=1,16
      PN(I,J)=(PN(I,J)+PN(J,I))/2.0D0
   31 PN(J,I)=PN(I,J)
      DO 32 I=1,16
      DO 32 J=1,16
      IF(DABS(PN(J,I))-1.0D-25) 30,30,32
   30 PN(J,I)=0.0D0
   32 CONTINUE
      N=1+(K-1)/6
   50 ISAT=ISA(N)
C  COMPUTE TERMS FOR MEASUREMENT MATRIX
      CALL ABC
      ANA=AA
      BNA=BB
      CNA=CC
      IF(CZZS-0.65) 51,52,52
   51 V1=10.0D10
      GO TO 53
   52 V1=100.0
   53 CONTINUE
C  DETERMINE IF PREVIOUS SATELLITE IS THE SAME AS THE CURRENT SATELLITE
```

```
      IF(ISAO-ISA(N))55,60,55
C  RESET COVARIANCE
   55 DO 56 I=1,16
      PN(I,15)=0.0D0
   56 PN(15,I)=0.0D0
      PN(15,15)=1.0D6
C  RECOMPUTE OLD ABC BY STEPPING BACK DT
      T=T-DT
      CALL ABC
      T=T+DT
      AOA=AA
      BOA=BB
      COA=CC
   60 CONTINUE
   71 ISAT=ISB(N)
C  COMPUTE TERMS FOR MEASUREMENT MATRIX
      CALL ABC
      ANB=AA
      BNB=BB
      CNB=CC
      IF(CZZS-0.65) 65,66,66
   65 V2=10.0D10
      GO TO 67
   66 V2=100.0
   67 CONTINUE
C  DETERMINE IF PREVIOUS SATELLITE IS THE SAME AS THE CURRENT SATELLITE
      IF(ISBO-ISB(N)) 73,77,73
C  RESET COVARIANCE
   73 DO 75 I=1,16
      PN(I,16)=0.0D0
   75 PN(16,I)=0.0D0
      PN(16,16)=1.0D6
C  RECOMPUTE OLD ABC BY STEPPING BACK DT
      T=T-DT
      CALL ABC
      T=T+DT
      AOB=AA
```

```
      BOB=BB
      COB=CC
   77 CONTINUE
      WRITE (ITPM)     ((PHI(I,J),I=1,16),J=1,16),ANA,BNA,CNA,AOA,BOA,
     1COA,ANB,BNB,CNB,AOB,BOB,COB,V1,V2,ISAO,ISA(N),ISBO,ISB(N),K
      ZM(1,4)=BNA
      ZM(1,6)=CNA
      ZM(1,8)=R*ANA
      ZM(1,15)=1.0D0
      ZM(2,4)=BNB
      ZM(2,6)=CNB
      ZM(2,8)=R*ANB
      ZM(2,16)=1.0D0
C  FORM N MEAS MATRIX
      ZN(1,4)=-BOA
      ZN(1,6)=-COA
      ZN(1,8)=-R*AOA
      ZN(2,4)=-BOB
      ZN(2,6)=-COB
      ZN(2,8)=-R*AOB
C  COMPUTE GAINS
      CALL GAIN
C  COMPUTE APOSTERIORI COVARIANCE
C  COMPUTE STANDARD DEVIATION OF ESTIMATES AND RECORD
      ISBO=ISB(N)
      AOB=ANB
      BOB=BNB
      COB=CNB
      ISAO=ISA(N)
      AOA=ANA
      BOA=BNA
      COA=CNA
      CALL SCALE
   89 CONTINUE
      DO 100 I=1,16
      DO 100 J=1,16
  100 PO(I,J)=PN(I,J)
```

```
500 CONTINUE
    WRITE(ITAPEW)  K, ((PO(I,J),I=1,16),J=1,16)
    STOP
    END



    SUBROUTINE MTEXP
    DOUBLE PRECISION A(16,16),B(16,16),W(16,16),Y(16,16),SUM
    DOUBLE PRECISION       AA,BB,CC,V1,V2,CZZS,          RS,RV
    DOUBLE PRECISION PN(16,16), PO(16,16), DUM(16,16),ZM(2,16),
   1 ZN(2,16)
    DOUBLE PRECISION DABS
    COMMON A,  B,PO,PN,DUM,ZM,ZN,AA,BB,CC,V1,V2,CZZS,   RS,RV,VV,RTS,
   1 CMTNM,CMSTK,R,GM,WO,WE,PI,T, C,WS,ISAT,IT,K,ISAO,ISBO,M,ISAN,ISBN
    IP=8
    MP=8
    N=16
    NT=8
    IIP=IP+1
    DO 50     J=1,N
    DO 50     I=1,N
    A(I,J)=A(I,J)*C
    W(I,J)=A(I,J)
 50 Y(I,J)=0.0D0
    DO 53     J=1,N
    DO 53     I=1,N
    IF(I-J)  52,51,52
 51 B(I,J)=1.0D0
    GO TO 53
 52 B(I,J)=0.0D0
 53 CONTINUE
    DO 75     KD=2,NT
    XD=KD
    DO 54     J=1,N
    DO 54     I=1,N
 54 B(I,J)=B(I,J)+W(I,J)
```

```
      DO 56     J=1,IP
      DO 56     I=1,IP
      SUM=0.0D0
      DO 55     L=1,IP
   55 SUM=SUM+W(I,L)*A(L,J)
   56 Y(I,J)=SUM/XD
      DO 57     J=IIP,N
   57 Y(J,J)=W(J,J)*A(J,J)/XD
      DO 62     J=IIP,N
      DO 62     I=1,IP
   62 Y(I,J)=W(I,J)*A(J,J)
      DO 59     J=IIP,N
      DO 59     I=1,IP
      SUM=0.0D0
      DO 60     L=1,IP
   60 SUM=SUM+W(I,L)*A(L,J)
   59 Y(I,J)=(Y(I,J)+SUM)/XD
      DO 58     J=1,N
      DO 58     I=1,N
   58 W(I,J)=Y(I,J)
      DO 80 I=1,N
      DO 80 J=1,N
      SCRW= DABS(W(I,J))-1.0D-25
      IF(SCRW) 504,504,80
  504 W(I,J)=0.0D0
   80 CONTINUE
   75 CONTINUE
      DO 90 J=1,N
      DO 90 I=1,N
   90 A(I,J)=A(I,J)/C
      RETURN
      END


      SUBROUTINE ABC
      DOUBLE PRECISION A(16,16),PHI(16,16),PN(16,16),PO(16,16),
```

```
     1DUM(16,16),          ZM(2,16),ZN(2,16)
      DOUBLE PRECISION       AA,BB,CC,V1,V2,              RS,RV
      DOUBLE PRECISION VCLAT,VLONG,CXXC,CXYC,CXZC,CYXC,CYYC,CYZC,
     1CZXC,CZYC,CZZC,AJ,APH,CAPH,SAPH,BET,CBET,SBET,XSI,YSI,ZSI,
     2XS,YS,ZS,CXZS,CYZS,CZZS,RHO,XLAM,ZETA,GAM,ETA,CZ,SZ,CG,SG,CE,SE
      DOUBLE PRECISION DSIN,DCOS,DSQRT
      COMMON A,PHI,PO,PN,DUM,ZM,ZN,AA,BB,CC,V1,V2,CZZS,   RS,RV,VV,RTS,
     1 CMTNM,CMSTK,R,GM,WO,WE,PI,T,DT,WS,ISAT,IT,K,ISAO,ISBO,M,ISAN,ISBN
      XLAM=2.997925/4.0
C  COMPUTE VEHICLE LAT AND LONG
      IF(T-18000.) 264,264,265
  264 CONTINUE
      VCLAT=PI/4.0-VV*T/RV
      VLONG=0.0
      GO TO 270
  265 VLONG = VV*(T-18000.)/RV/DCOS(VCLAT)
  270 CONTINUE
      CXXC=-DSIN(VCLAT)*DCOS(VLONG)
      CXYC=-DSIN(VCLAT)*DSIN(VLONG)
      CXZC=DCOS(VCLAT)
      CYXC=DSIN(VLONG)
      CYYC=-DCOS(VLONG)
      CYZC=0.0D0
      CZXC=DCOS(VCLAT)*DCOS(VLONG)
      CZYC=DCOS(VCLAT)*DSIN(VLONG)
      CZZC=DSIN(VCLAT)
      GAM=54.8*PI/180.
      I=(ISAT  -1)/5+1
      J=ISAT  -(I-1)*5
      AJ=J
      AI=I
  348 ZETA=                  (WS*T+2.0D0*PI*(AJ-1.0D0)/5.0D0)
      CZ=DCOS(ZETA)
      SZ=DSIN(ZETA)
      CG=DCOS(GAM)
      SG=DSIN(GAM)
      ETA=(AI-1.)*PI/2.0D0
```

```
      CE=DCOS(ETA)
      SE=DSIN(ETA)
      XSI=RS*CZ*CE-RS*SZ*CG*SE
      YSI=RS*CZ*SE+RS*SZ*CG*CE
      ZSI=RS*SZ*SG
  358 CONTINUE
      XS=XSI* COS(WE*T)+YSI* SIN(WE*T)
      YS=-XSI* SIN(WE*T)+YSI* COS(WE*T)
      ZS=ZSI
C  COMPUTE DIRECTION COSINES BETWEEN THE NAV COORDINATES AND THE
C  SAT RADIUS VECTOR
      CXZS=(XS*CXXC+YS*CXYC+ZS*CXZC)/RS
      CYZS=(XS*CYXC+YS*CYYC+ZS*CYZC)/RS
      CZZS=(XS*CZXC+YS*CZYC+ZS*CZZC)/RS
      RHO=DSQRT(RV*RV+RS*RS-2.0D0*RS*RV*CZZS)
      AA=  (RV-RS*CZZS)/RHO/XLAM
      BB=  (RV*RS*CYZS)/RHO/XLAM
      CC= -(RV*RS*CXZS)/RHO/XLAM
      RETURN
      END



      SUBROUTINE GAIN
      DOUBLE PRECISION A(16,16),PHI(16,16),PN(16,16),PO(16,16),
     1 DUM(16,16),     ZM(2,16),ZN(2,16),D2(16,2),D3(16,2),D4(16,2),
     2B(16,2),T1(2,2),T2(2,2),T3(2,2),T4(2,2),Q(2,2),QI(2,2),V(2,2)
      DOUBLE PRECISION       AA,BB,CC,V1,V2,CZZS,          RS,RV,SUM
      DOUBLE PRECISION DABS
      COMMON A,PHI,PO,PN,DUM,ZM,ZN,AA,BB,CC,V1,V2,CZZS,   RS,RV,VV,RTS,
     1 CMTNM,CMSTK,R,GM,WO,WE,PI,T,DT,WS,ISAT,IT,K,ISAO,ISBO,M,ISAN,ISBN
C  FORM PN*ZMT AND STORE AS D2
      DO 100 I=1,16
      DO 100 J=1,2
      SUM=0.0D0
      DO 99 N=1,16
   99 SUM=SUM+PN(I,N)*ZM(J,N)
```

```
  100 D2(I,J)=SUM
C   FORM PHI*PO*ZNT AND STORE AS D3
      DO 105 I=1,16
      DO 105 J=1,2
      SUM=0.0D0
      DO 104 N=1,16
  104 SUM=SUM+DUM(I,N)*ZN(J,N)
  105 D3(I,J)=SUM
C   FORM ZM*D3 AND STORE AS T4
      DO 108 I=1,2
      DO 108 J=1,2
      SUM=0.0D0
      DO 107 N=1,16
  107 SUM=SUM+ZM(I,N)*D3(N,J)
  108 T4(I,J)=SUM
C   FORM ZN*PO*PHIT*ZMT FROM TRANSPOSE OF T4
      DO 109 I=1,2
      DO 109 J=1,2
  109 T3(I,J)=T4(J,I)
C   FORM SUM OF D2 AND D3 AND STORE AS D4
      DO 106 I=1,16
      DO 106 J=1,2
  106 D4(I,J)=D2(I,J)+D3(I,J)
C   FORM PO*ZNT AND STORE AS D3
      DO 114 I=1,16
      DO 114 J=1,2
      SUM=0.0D0
      DO 113 N=1,16
  113 SUM=SUM+PO(I,N)*ZN(J,N)
  114 D3(I,J)=SUM
C   FORM ZN*D3 AND STORE AS T2
      DO 118 I=1,2
      DO 118 J=1,2
      SUM=0.0D0
      DO 117 N=1,16
  117 SUM=SUM+ZN(I,N)*D3(N,J)
  118 T2(I,J)=SUM
```

```
C  FORM ZM*D2 AND STORE AS T1
      DO 120 I=1,2
      DO 120 J=1,2
      SUM=0.0D0
      DO119 N=1,16
  119 SUM=SUM+ZM(I,N)*D2(N,J)
  120 T1(I,J)=SUM
      V(1,1)=V1
      V(1,2)=0.0D0
      V(2,1)=0.0D0
      V(2,2)=V2
C  FORM Q
      DO 122 I=1,2
      DO 122 J=1,2
  122 Q(I,J)=T1(I,J)+T2(I,J)+T3(I,J)+T4(I,J)+V(I,J)
C  FORM INVERSE OF Q
      DENOM=Q(1,1)*Q(2,2)-Q(1,2)*Q(2,1)
      QI(1,1)=Q(2,2)/DENOM
      QI(2,2)=Q(1,1)/DENOM
      QI(2,1)=-Q(2,1)/DENOM
      QI(1,2)=-Q(1,2)/DENOM
C  FORM B FROM D4*QI
      DO 130 I=1,16
      DO 130 J=1,2
      SUM=0.0D0
      DO 129 N=1,2
  129 SUM=SUM+D4(I,N)*QI(N,J)
  130 B(I,J)=SUM
C  FORM D4*BT AND SUBTRACT FROM PN FOR REVISED PN
      DO 135 I=1,16
      DO 135 J=1,16
      SUM=0.0D0
      DO 134 N=1,2
  134 SUM=SUM+D4(I,N)*B(J,N)
  135 PN(I,J)=PN(I,J)-SUM
C     SYMMETRIZE PN MATRIX
      DO 66 I=1,16
```

```
      DO 66 J=1,16
      PN(I,J)=(PN(I,J)+PN(J,I))/2.0D0
   66 PN(J,I)=PN(I,J)
      DO 69 I=1,16
      DO 69 J=1,16
      IF(DABS(PN(J,I))-1.0D-25) 68,68,69
   68 PN(I,J)=0.0D0
   69 CONTINUE
      RETURN
      END



      SUBROUTINE SCALE
      DOUBLE PRECISION A(16,16),PHI(16,16),PN(16,16),PO(16,16),
     1DUM(16,16),          ZM(2,16),ZN(2,16)
      DOUBLE PRECISION       AA,BB,CC,V1,V2,CZZS,          RS,RV
      DOUBLE PRECISION DSQRT
      COMMON A,PHI,PO,PN,DUM,ZM,ZN,AA,BB,CC,V1,V2,CZZS,   RS,RV,VV,RTS,
     1 CMTNM,CMSTK,R,GM,WO,WE,PI,T,DT,WS,ISAT,IT,K,ISAO,ISBO,M,ISAN,ISBN
      ITAPEW=9
C     COMPUTATION OF STANDARD DEVIATION OF ESTIMATES AND INVERSE SCALING
      DPSIX=DSQRT(PN(1,1))*RTS
      DPSIY=DSQRT(PN(2,2))*RTS
      DPSIZ=DSQRT(PN(3,3))*RTS
      DPOSX=DSQRT(PN(4,4))*R*CMTNM
      DVELX=DSQRT(PN(5,5))*WO*R*CMSTK
      DPOSY=DSQRT(PN(6,6))*R*CMTNM
      DVELY=DSQRT(PN(7,7))*WO*R*CMSTK
      DPOSZ=DSQRT(PN(8,8))*R*CMTNM
      DGYDXP=DSQRT(PN(9,9))*WO*RTS
      DGYDYP=DSQRT(PN(10,10))*WO*RTS
      DGYDZP=DSQRT(PN(11,11))*WO*RTS
      DACCLX=DSQRT(PN(12,12))*WO*WO*R/GM
      DACCLY=DSQRT(PN(13,13))*WO*WO*R/GM
      DVELZ=DSQRT(PN(14,14))*WO*R*CMSTK
      DSCNTA=DSQRT(PN(15,15))
```

```
      DSCNTB=DSQRT(PN(16,16))
      ERR=DSQRT(PN(4,4)+PO(6,6)) *R*CMTNM
      TH=T/60.
      M=M+1
      WRITE(3,189)
  189 FORMAT( 1X/'     N      TIME     POS SD(NM)     VEL SD(KN)'4X,
     1'PSI SD(SEC)   GYR SD(D/H)   ACCL SD(GS)',3X,
     2'SAT A    COUNT SD    SATB    COUNT SD')
      WRITE(3,190) M,TH,DPOSX,DVELX,DPSIX,DGYDXP,DACCLX,ISAO,DSCNTA,
     1ISBO,DSCNTB
  190 FORMAT(1X,I4,3X,F6.2,3X,5(E11.4,3X),2X,2(I3,3X,E11.4,4X))
      WRITE(3,191)  DPOSY,DVELY,DPSIY,DGYDYP,DACCLY,V1,V2
  191 FORMAT(1X,'  RAD ERR(NM)   ',5(E11.4,3X),   D9.2,11X,D9.2)
      WRITE(3,192)ERR,DPOSZ,DVELZ,DPSIZ,DGYDZP
  192 FORMAT(2X,E11.4,4X,4( E11.4,3X))
      WRITE(ITAPEW)  M, K,TH,DPOSX,DPOSY,DPOSZ,DVELX,DVELY,DVELZ,DGYDXP,
     1DGYDYP,DGYDZP,DACCLX,DACCLY,DPSIX,DPSIY,DPSIZ,DSCNTA,DSCNTB,
     2 ERR,ISAO,ISBO
      RETURN
      END
```